

Spectrum access in white spaces using spectrum sensing and geolocation databases

Konstantinos Koufos

Spectrum access in white spaces using spectrum sensing and geolocation databases

Konstantinos Koufos

A doctoral dissertation completed for the degree of Doctor of Science in Technology to be defended, with the permission of the Aalto University School of Electrical Engineering, at a public examination held at the lecture hall S1 of the school on 4 December 2013 at 12 noon.

Aalto University
School of Electrical Engineering
Department of Communications and Networking

Supervising professor

Professor Riku Jäntti

Thesis advisor

Dr Kalle Ruttik

Preliminary examiners

Professor Mikko Valkama, Tampere University of Technology, Finland

Dr Maziar Nekovee, Samsung R&D Institute, UK

Opponents

Professor Behnaam Aazhang, Rice University, US

Professor Mikko Valkama, Tampere University of Technology, Finland

Aalto University publication series

DOCTORAL DISSERTATIONS 195/2013

© Konstantinos Koufos

ISBN 978-952-60-5454-4

ISBN 978-952-60-5455-1 (pdf)

ISSN-L 1799-4934

ISSN 1799-4934 (printed)

ISSN 1799-4942 (pdf)

<http://urn.fi/URN:ISBN:978-952-60-5455-1>

Unigrafia Oy

Helsinki 2013

Finland



Author

Konstantinos Koufos

Name of the doctoral dissertation

Spectrum access in white spaces using spectrum sensing and geolocation databases

Publisher School of Electrical Engineering

Unit Department of Communications and Networking

Series Aalto University publication series DOCTORAL DISSERTATIONS 195/2013

Field of research Communications Engineering

Manuscript submitted 4 June 2013

Date of the defence 4 December 2013

Permission to publish granted (date) 5 November 2013

Language English

Monograph

Article dissertation (summary + original articles)

Abstract

A spectrum license grants users the right to transmit on a particular piece of spectrum. Historically, a spectrum license has been allocated for a particular technology. While this strategy facilitates interference control, it also results in spectrum scarcity as more spectrum-efficient technologies are invented. In order to meet the increasing data traffic demands in a timely manner, a shared use of the spectrum seems to be the only viable solution. According to this line of thinking, different technologies with possibly different deployment densities can share the same spectrum under certain conditions. While shared spectrum access improves spectral efficiency, it also increases the risk for harmful interference among the different systems. This calls for a change in the traditional way of issuing spectrum licenses: instead of specifying transmit power levels, the spectrum usage rights specify the generated interference that is permitted.

Spectrum access to white spaces would enhance spectrum utilisation, while also testing the approach of controlling the interference between different systems directly rather than through the transmission power. The amount of interference generated to the license holder can be controlled by spectrum sensing and/or geolocation database access.

Interference control using spectrum sensing usually boils down to a signal detection problem. In this thesis, we show that the traditional signal detection framework is not appropriate for recovering transmission opportunities in the spatial domain and propose an alternative model. Also, sensing strategies for energy efficient wideband spectrum sensing and trade-off analysis between the service requirement and the demand in the measured spectrum are demonstrated.

At this moment, spectrum access to white spaces is mostly possible via geolocation databases. The database is responsible for handling spectrum access requests while complying with certain regulatory conditions. In this thesis, we suggest some interference control and power allocation algorithms that may govern the operation of the database. The algorithms have a low complexity to enable a real-time operation in the database. They involve simple models to capture the impact of the non-uniform demand density, terrain-based propagation and fading correlations on the generated interference. Also, we propose a joint rate and power allocation algorithm that protects the license holder in all cases.

Keywords Aggregate interference models, flexible spectrum use, spectrum sensing strategy

ISBN (printed) 978-952-60-5454-4

ISBN (pdf) 978-952-60-5455-1

ISSN-L 1799-4934

ISSN (printed) 1799-4934

ISSN (pdf) 1799-4942

Location of publisher Helsinki

Location of printing Helsinki

Year 2013

Pages 211

urn <http://urn.fi/URN:ISBN:978-952-60-5455-1>

Preface

This doctoral thesis has been carried out at the Department of Communications and Networking at Aalto University during the years 2008-2012. The work has been funded by the Graduate School of Electrical and Communications Engineering and the EU FP7 project QUASAR.

This thesis could never have been completed without the support from many other people. First and foremost, I would like to express my sincere gratitude to my supervisor, Professor Riku Jäntti, for his guidance, constructive criticism and encouragement during these years. His suggestions have helped generalizing our findings thereby opening new directions to our research work. I would also like to thank him for generating a pleasant and secure working environment.

I would like to extend my gratitude to my instructor, Dr Kalle Ruttik, for showing me how to conduct research and how to document it. Daily interactions with Kalle have been a unique learning experience and also an enjoyable experience as his way of thinking is very much different than mine.

I am thankful to my co-author Mr Byungjin Cho for his hard work while preparing Publication III and to co-worker in QUASAR project Mr Jussi Kerttula for helpful discussions both on technical and personal matters. Thank you for the support Cho and Jussi. I would also like to thank the thesis pre-examiners, Professor Mikko Valkama and Dr Maziar Nekovee for their constructive comments that helped improving the clarity and the presentation quality of the thesis.

Evening coffee breaks with colleagues Mr Aamir Mahmood and Mr Aftab Hossain have always been motivating due to their willingness to listen to the ups and downs of my research progress and also to share their own. My warmest thanks for your time and support. My thanks also to Dr Lu Wei. Support from the department's support personnel, particularly

from Sari Kiveliö and Sanna Patana for travel and study arrangements is greatly appreciated and acknowledged.

Finally, the least I can do is to acknowledge the discrete help of my friends Dinos, Leena, Aamir and Umar, my parents Theodoros and Anastasia and my brother Dimitris.

Helsinki, November 11, 2013,

Konstantinos Koufos

Contents

Preface	iii
Contents	v
List of Publications	vii
Author's Contribution	ix
1. Introduction	1
1.1 Motivation	1
1.2 Organisation and contribution of the thesis	5
1.3 Publication summary	7
2. Sensing-based spectrum access	11
2.1 Distributed detection in sensor networks	13
2.1.1 Classification of distributed detection schemes	13
2.1.2 Combination rules in the centralized scheme	15
2.2 Cooperative sensing in secondary spectrum access networks	18
2.3 Recovering spatial spectrum sharing opportunities	20
2.4 Discussion	25
3. MAC layer sensing	27
3.1 Sensing time optimization	28
3.1.1 Sensing-throughput trade-off	28
3.1.2 Sensing-outage trade-off	31
3.2 Optimizing the number of users involved in sensing	31
3.3 Optimizing the number of measured bands	35
3.4 Resource allocation for a known primary traffic model	38
3.4.1 Sensing time and time slot optimization	40
3.4.2 Exploration-exploitation trade-off	40

3.5 Discussion	42
4. Database-based spectrum access	45
4.1 Information provided to the database and returned to the secondary device	45
4.2 Regulatory rules for secondary access in TVWS in Europe	47
4.2.1 Power allocation in the co-channel	48
4.2.2 Power allocation in the adjacent channel	49
4.3 Discussion	50
5. Secondary interference models	53
5.1 Interferers with fixed locations	54
5.2 Interferers with random locations	57
5.2.1 Interferers with contention control	59
5.3 Impact of terrain morphology on generated interference	60
5.3.1 Impact of user density on generated interference	62
5.4 Impact of shadowing correlation on generated interference	64
5.5 Discussion	66
6. Secondary power allocation	69
6.1 Interference margin	70
6.1.1 Hierarchical interference control	71
6.2 Optimization of secondary transmit power	72
6.3 Optimization of secondary rate	75
6.3.1 Multiple secondary transmission pairs	77
6.4 Joint power and channel allocation	79
6.5 Discussion	81
7. Summary and future work	83
7.1 Summary and conclusions	83
7.2 Future work	85
Bibliography	87
Publications	109

List of Publications

This thesis consists of an overview and of the following publications which are referred to in the text by their Roman numerals.

- I** Konstantinos Koufos, Kalle Ruttik and Riku Jäntti. Controlling the interference from multiple secondary systems at the TV cell border. In *Proc. IEEE Personal Indoor and Mobile Radio Communications (PIMRC)*, Toronto, Canada, pages 645-649, September 2011.
- II** Konstantinos Koufos and Riku Jäntti. Proportional fair power allocation for secondary transmitters in the TV white space. *Journal of Electrical and Computer Engineering*, 2013.
- III** Byungjin Cho, Konstantinos Koufos, Kalle Ruttik and Riku Jäntti. Power allocation in the TV white space under constraint on secondary system self-interference. *Journal of Electrical and Computer Engineering*, 2012.
- IV** Kalle Ruttik, Konstantinos Koufos and Riku Jäntti. Model for computing aggregate interference from secondary cellular network in presence of correlated shadow fading. In *Proc. IEEE Personal Indoor and Mobile Radio Communications (PIMRC)*, Toronto, Canada, pages 433-437, September 2011.
- V** Konstantinos Koufos, Kalle Ruttik and Riku Jäntti. Aggregate interference from WLAN in the TVWS by using terrain-based channel model. In *Proc. IEEE International Conference on Cognitive Radio Oriented Wireless Networks (CROWNCOM)*, Stockholm, Sweden, pages 185-189, June 2012.
- VI** Konstantinos Koufos, Kalle Ruttik and Riku Jäntti. Signal model for dynamic spectrum allocation close to the cell border of a primary

transmitter. In *Proc. IEEE International Symposium on New Frontiers in Dynamic Spectrum Access Networks (DySPAN)*, Chicago, US, pages 1-5, October 2008.

VII Konstantinos Koufos, Kalle Ruttik and Riku Jäntti. Distributed Sensing in Multiband Cognitive Networks. *IEEE Transactions on Wireless Communications*, Volume 10, issue 5, pages 1667-1677, May 2011.

VIII Konstantinos Koufos, Kalle Ruttik and Riku Jäntti. Voice Service in Cognitive Networks over the TV Spectrum. *IET Communications*, Volume 6, issue 8, pages 991-1003, May 2012.

Author's Contribution

Publication I: “Controlling the interference from multiple secondary systems at the TV cell border”

The author formulated the optimization problem and generated the results. The author wrote the paper under the guidance of Dr Kalle Ruttik and Professor Riku Jäntti.

Publication II: “Proportional fair power allocation for secondary transmitters in the TV white space”

Professor Riku Jäntti proposed the power allocation scheme and the author extended it to incorporate mobile users. The author generated the results and wrote the paper under the guidance of Professor Riku Jäntti.

Publication III: “Power allocation in the TV white space under constraint on secondary system self-interference”

The author formulated the problem and proposed the power allocation scheme. Together with Mr Byungjin Cho the author wrote the paper under the guidance of Dr Kalle Ruttik and Professor Riku Jäntti.

Publication IV: “Model for computing aggregate interference from secondary cellular network in presence of correlated shadow fading”

The author proposed a model for incorporating slow fading correlation into the calculation of the moments of aggregate interference. In this pub-

lication, Dr Kalle Ruttik proposed an integral-based model to describe interference without fading correlation. The author, together with Dr Kalle Ruttik, validated the suitability of the proposed models and wrote the paper under the supervision of Professor Riku Jäntti.

Publication V: “Aggregate interference from WLAN in the TVWS by using terrain-based channel model”

The author was responsible for Section II-2 and Section III, while Dr Kalle Ruttik was responsible for Section I, Section II-1 and Section IV. Professor Riku Jäntti supervised the work.

Publication VI: “Signal model for dynamic spectrum allocation close to the cell border of a primary transmitter”

The author carried out the theoretical analysis and generated the results. In this publication, Dr Kalle Ruttik proposed a model for the signal level distribution in the TV white space. The author wrote the paper under the guidance of Dr Kalle Ruttik and Professor Riku Jäntti.

Publication VII: “Distributed Sensing in Multiband Cognitive Networks”

The author formulated the problem, carried out the theoretical analysis and generated the results. In this publication, Professor Riku Jäntti proposed utilising knapsack packing problem algorithms while the author generated the proofs. The author wrote the paper under the guidance of Dr Kalle Ruttik and Professor Riku Jäntti.

Publication VIII: “Voice Service in Cognitive Networks over the TV Spectrum”

The author formulated the problem, proposed the optimization algorithm and generated the results. Dr Kalle Ruttik and Professor Riku Jäntti proposed studying the trade-off between service requirement and spectrum demand. The author wrote the paper under the guidance of the other authors.

List of Abbreviations

ASA	Authorised shared access
BPP	Binomial point process
CDF	Cummulative distribution function
CF	Characteristic function
CSMA/CA	Carrier sensing multiple access with collision avoidance
DCA	Dynamic channel assignment
DTT	Digital terrestrial television
DVB-T	Digital Video Broadcasting-Terrestrial
ECC	Electronic Communications Committee
EGC	Equal gain combining
F-W	Fenton-Wilkinson
FC	Fusion centre
FCC	Federal Communication Committee
HDC	Hard decision combining
i.i.d.	Independent and identically distributed
ITM	Irregular terrain channel model
ITU	International Telecommunication Union
LRT	Likelihood ratio test
LSA	Licensed shared access
MAC	Medium access control

List of Abbreviations

MCKP	Multiple-choice knapsack problem
MGF	Moment-generating function
MRC	Maximum ratio combining
OFCOM	Office of Communications
OFDM	Orthogonal frequency division multiplexing
PDF	Probability distribution function
PF	Proportional fair
PHY	Physical layer
PMSE	Programme Making and Special Events
PPP	Poisson point process
QoS	Quality of service
RSPG	Radio Spectrum Policy Group
RV	Random variable
S-Y	Schwartz-Yeh
SDC	Soft decision combining
SINR	Signal-to-interference-and-noise ratio
SNR	Signal-to-noise ratio
SPF	Simplified proportional fair
TPC	Transmit power control
TV	Television
TVWS	TV white spaces
WLAN	Wireless local area network
WSD	White space device
WSN	Wireless sensor networks

List of Symbols

Greek Symbols

α	Weights for Chair-Varshney test
$\gamma(\cdot, \cdot)$	Lower incomplete Gamma function
Γ_i	SINR at the i -th secondary test point
γ_i	TV SINR at the i -th TV test point
Γ_t	Secondary system SINR target
γ_t	TV SINR target
Δt	Time elapsed since last transition
δ	Hardcore distance
η, η'	Decision thresholds at a sensor
Λ	Likelihood ratio
λ_m	Intensity of Matern point process
λ_p	Intensity of Poisson point process
μ_g	Distance-based pathloss for secondary signal
μ_{off}	Death rate of two-state Markov process
μ_{on}	Birth rate of two-state Markov process
μ_{TV}	Distance-based pathloss for TV signal
ν	Activity factor
ξ	Scaling constant equal to $10/\log(10)$
ρ	Correlation coefficient
σ	Slow fading standard deviation
σ_{SU}	Slow fading standard deviation for secondary signal
σ_{TV}	Slow fading standard deviation for TV signal
τ	Measurement time
ω	Belief vector

Latin Symbols

\mathcal{D}	Set of dominating TV test points
\mathcal{G}	Propagation pathloss using ITM
\mathcal{J}	Subset of secondary transmitters
\mathcal{MI}	Multiple interference margin
\mathcal{M}	Number of measured spectrum bands
\mathcal{K}	Number of collected samples at the detector
\mathcal{SM}	Safety margin
A	Secondary deployment area
a	Weight coefficient
A_f	Transmitter's footprint
c	Pathloss attenuation constant
$C(n, k)$	Number of k combinations in n -element set
d	Secondary cell radius
$f_u(\cdot)$	Utility function
G	Propagation pathloss including fading
g	Distance-based propagation pathloss
h	Reporting channel between sensor and fusion
H_1	Hypothesis 1
H_0	Hypothesis 0
I_Δ	Interference margin
I_B	Interference from a BPP
I_C	Interference due to a cellular system downlink
I_P	Interference from a PPP
I_t	Aggregate interference level
$I_{\Delta l}$	Lower bound of interference margin
$I_{\Delta l}^{(SU)}$	Interference margin at secondary test points
J	Function in multi-objective optimization
L	Decision test statistic
L_P	Number of test points for modelling slow fading
M	Number of candidate spectrum bands
N	Number of secondary users
n	Pathloss attenuation exponent
N_P	Number of primary test points
N_S	Number of secondary systems
N_{min}	Minimum number of users allocated to a band
O_t	Outage probability target
$O_t^{(SU)}$	Outage probability target for the secondary system
P	Power spent for sensing at a user

p	Transition probabilities in two-state Markov model
p_0	Mean generated interference from a secondary user
P_ϵ	Primary signal detection level
P_d	Power density
P_N	Noise power level
P_S	Primary signal level
P_t	Secondary transmit power level
$Q^{-1}(\cdot)$	Inverse of the Gaussian $Q(\cdot)$ function
q_1	Location probability with TV signal only
q_2	Location probability with secondary interference
R	TV service area radius
R_n	TV protection area radius
s	Transmitted signal sample
T	Duration of the detection cycle
t, t'	Decision thresholds at the fusion centre
u	Output of signal processing at the sensor
u_0	Decision at the fusion centre
w	Noise sample
x	Random variable modelling slow fading
x_q	Gaussian confidence factor
y	Measurement at the sensor
z	Received data at the fusion centre
\mathcal{R}_{max}	An upper bound to \mathcal{R}
\mathcal{R}	Expected secondary data rate
\mathcal{R}_0	Secondary data rate over available bands
\mathcal{R}_1	Secondary data rate over occupied bands
Pr_0	Prior probability for hypothesis H_0
Pr_1	Prior probability for hypothesis H_1
Pr_b	Blocking probability
Pr_{false}	False alarm rate
$\text{Pr}_{false}^{(F)}$	False alarm rate at the fusion centre
Pr_{miss}	Misdetection probability
$\text{Pr}_{miss}^{(F)}$	Misdetection probability at the fusion centre
Pr_{out}	Constraint on the misdetection probability
Pr_{und}	Constraint on the false alarm rate

1. Introduction

1.1 Motivation

In the early days of radio regulations, a specific radiocommunication service was mapped onto a specific technology. Spectrum licenses were either linked to a particular technology or else they directly determined the transmission/reception characteristics of the radio devices (e.g. the spectrum mask). Interference between devices operating with different services on the same or on neighbouring spectrum bands was controlled by allocating spectrum licenses that were compatible with one another [1]. Due to a lack of harmonised spectrum usage for most of the services, cross-border compatibility studies must also be carried out.

With the advances in technology, a single radio device now offers applications that can be grouped under multiple services. As a result, the traditional approach linking a particular spectrum band, or spectrum license, to a particular service has turned out to be inefficient [2]. At the same time, world-wide spectrum measurements indicate that the exclusive use of a spectrum band by a particular service results in spectrum underutilisation in space and/or time [3, 4]. This phenomenon is usually referred to as spectrum scarcity.

According to predictions made by Cisco, global mobile data traffic will increase 13-fold between 2012 and 2017 [5]. More spectrum would be needed to accommodate the high traffic demands. One way to find more spectrum is to rearrange the existing spectrum allocations, usually referred to as spectrum refarming. For example, the transition from analog to digital television (TV) freed up spectrum because digital TV transmission is more spectrum efficient. At the World Radio Conference 2007 (WRC-07), the frequency band 790-862 MHz which formerly had been used

mainly for analog TV broadcasting, were allocated for mobile broadband services. In Finland, 2×30 MHz in this spectrum band would be auctioned off in 2013. During the WRC-12, the International Telecommunication Union (ITU) announced that the frequency band 694-790 MHz would also be licensed for mobile services in Europe starting from January 2015 [6].

Spectrum refarming is a demanding process in terms of time and cost. Also, while spectrum allocation on an exclusive basis facilitates interference control, it also results in spectrum scarcity. An alternative method for meeting the increasing traffic demand in a timely manner is to minimise spectrum scarcity through a shared use of spectrum. *Shared use of spectrum refers to situations in which a number of independent users and/or devices are allowed to access the same range of frequencies under certain conditions* [7].

The concept of shared use of spectrum has been around for a while. For example, the frequency band 3400-3700 MHz is currently shared worldwide on a co-primary basis between earth stations in the fixed-satellite service and radio relays in the fixed service [8]. In the future, it is envisioned that mobile network operators will share their spectrum in space and/or time to maximise their revenue [9]. For example, an operator may agree to let other operators use their spectrum to provide high-speed wireless access inside a crowded shopping mall. Different operators can offer wireless access inside different buildings, thereby eliminating inter-operator interference and making it possible to enjoy higher available bandwidths.

Shared spectrum access can also be achieved in a scenario in which users have different access priorities. A user may possess exclusive license rights on a spectrum band, but due to the fact that the band receives limited use, the same band can also be accessed in an unlicensed manner by other users. The spots in time and/or space not utilised by the primary spectrum owner are known under the term white space: *White space is a label indicating a part of the spectrum, which is available on a non-interfering / non-protected basis with regard to primary services and other services with a higher priority on a national basis* [10]. As a result, there are no performance guarantees for unlicensed (or secondary) users accessing the white spaces. At the same time, *no individual authorisation or coordination is required and no fee payable for using the spectrum. Access is regulated solely by adherence to pre-defined regulatory conditions* [11].

A popular candidate for secondary spectrum access has been the TV broadcasting spectrum. The TV spectrum is characterised by good propagation conditions and sparse frequency reuse, resulting in attractive white spaces in the spatial domain. In the UK, it is expected that TV white spaces (TVWS) will first be used to provide wireless broadband access to rural communities due to the low cost and long-range propagation of these frequencies [12]. Other use cases may involve future home networks for enhancing wireless multimedia streaming and indoor-to-outdoor wireless broadband access [13]. In Europe, the regulatory conditions for secondary spectrum access have been set in terms of location-specific TV channel availability and the maximum permitted transmit power level.

There are three different types of spectrum sharing in secondary spectrum access, which can be distinguished based on the level of cooperation between the primary and the secondary users [14]. In *overlay spectrum sharing*, the primary user is willing to communicate some of its operational parameters to the secondary user. For example, if the secondary user is aware of the primary signal structure, it can transmit a combined version of primary and secondary signals. The amplification of the primary signal generates additional interference headroom at the primary receivers, which can be filled in by the secondary signal transmissions. Signal processing methods (e.g. successive interference cancellation, dirty paper coding, etc.) can be used to eliminate the primary signal and enhance the performance on the secondary system side. A popular application of overlay spectrum sharing is co-channel secondary transmission inside the TV service area, usually referred to as TV black space transmission [15].

Interweave spectrum sharing does not involve any sort of cooperation between the different types of users. The secondary user cannot access the spectrum unless the transmissions of the primary and secondary users are orthogonal to each other. For example, if interweave spectrum sharing is employed in the time domain, the secondary user must vacate the spectrum as soon as the primary user returns. Interweave secondary spectrum access is also referred to as opportunistic spectrum access [14, 16].

Finally, in *underlay spectrum sharing* the primary user is willing to tolerate some amount of additional disturbance. The secondary user is allowed to utilise the primary spectrum provided that the generated aggregate secondary interference to the primary users is maintained un-

der specific protection margins. This approach resembles ultra-wideband transmission where the available power is spread over a wide range of spectrum so, the generated interference level over any narrow primary spectrum band becomes negligible [14, 16].

Underlay spectrum sharing resembles interweave spectrum sharing in the spatial domain in the sense that primary and secondary users can be simultaneously active while the generated secondary interference should be controlled under some threshold. Secondary spectrum access in the TVWS is a form of underlay/spatial-interweave secondary spectrum sharing. Also, note that the primary spectrum can become available for secondary spectrum access using a combination of spectrum sharing types. For example, secondary users can interweave their transmissions in time when the primary user is silent and use the principle of underlay spectrum sharing (i.e. control of generated interference) when the primary user returns.

In underlay spectrum sharing, the secondary user must adjust its transmission parameters in order to cope with the interference that can be tolerated by the primary user. Instead of restricting the secondary user to a particular spectrum mask, the system designer can take as input the interference limits of the primary user and adjust any other parameter, e.g. secondary deployment density, to cope with the primary demand. As a result, secondary spectrum access can also be viewed as a test trial for changing the traditional way of issuing spectrum licenses. Specifying the limits on the amount of interference that a system can tolerate is more flexible compared to the traditional approach of setting spectrum masks [1]. Any technology and deployment density can be selected provided that it satisfies the interference constraints.

Even though the topic of this thesis is secondary spectrum access, the proposed algorithms are also applicable for a recently proposed method of shared spectrum access: the authorized shared access (ASA) method [17]. The Radio Spectrum Policy Group (RSPG) adopted the term licensed shared access (LSA) for ASA and defined it as follows: *An individual licensed regime of a limited number of licensees in a frequency band, already allocated to one or more incumbent users, for which the additional users are allowed to use the spectrum (or part of the spectrum) in accordance with sharing rules included in the rights of use of spectrum granted to the licensees, thereby allowing all the licensees to provide a certain level of QoS* [18]. Due to the limited number of new licenses in ASA/LSA, the

quality of service (QoS) for the new users can be predicted. This makes a clear difference compared to secondary spectrum access. ASA/LSA is expected to make use of recent progress in secondary spectrum access methods.

1.2 Organisation and contribution of the thesis

In this thesis, we present methods that can be used to detect transmission opportunities for secondary spectrum users under the requirement to protect the primary spectrum owner. The presented methods make use of either spectrum sensing or access to a geolocation database. In the database-based scheme, the database possesses all the information needed to estimate the amount of interference generated to the primary system. As a result, secondary spectrum access is reduced to interference control problem. In the sensing-based scheme, the generated interference is estimated by using signal level measurements. As we will discuss in Chapter 2, sensing-based spectrum access usually boils down to a signal detection problem.

Single-user detection is problematic when the primary transmitter is hidden to the secondary user while the primary receivers are not. Sensing can be still valuable for secondary spectrum access in the case of distributed detection [19]. In a distributed setup, it is highly improbable that the primary transmitter will be hidden from all secondary users. Distributed signal detection algorithms and their performance in the fading channel are discussed in Chapter 2. In Section 2.3, we show that the traditional detection framework is not appropriate for recovering the spectrum in the spatial domain. We propose an alternative detection model that recovers more available spectrum without violating the protection constraints of the primary system.

A medium access control (MAC) layer sensing protocol optimizes the allocation of sensing resources while taking into account the secondary performance targets. In Chapter 3, we classify the MAC layer protocols for secondary spectrum sensing based on whether the secondary system has some sort of knowledge about the primary traffic pattern or not. In this thesis, the contributions of MAC layer sensing are related to unaware secondary systems. In Chapter 3.2 we propose a MAC scheme for energy efficient wideband spectrum sensing. In Section 3.3, we show how to design a sensing strategy based on the capacity requirement of the secondary

service.

At this moment, the regulation trends for secondary spectrum access interlink geolocation databases and TVWS [20]. The regulator must determine the nature of the information registered in the database and returned to the device as well as the set of rules governing the operation of the database. Note that the regulatory rules can be different in different parts of the world. Without any doubt, they must be implemented in the database by using low-complexity algorithms that enable a real-time operation.

In this thesis, we suggest some secondary interference models and power allocation algorithms for geolocation-controlled secondary spectrum access. The system model assumptions adopted in Publication I through Publication V are closely related to the regulatory rules adopted by the Electronic Communications Committee (ECC). The models and algorithms proposed in this thesis have also been communicated to the ECC [21, 22, 23]. Currently, the ECC is making an attempt to harmonise secondary spectrum access in TVWS in a pan-European level. The ECC rules are shortly discussed in Chapter 4.

In Chapter 5, we present interference models for secondary networks with a cellular, random access and contention type of MAC. We argue that the interference from different types of networks can be controlled by adjusting different parameters. In Section 5.3, we propose a low-complex method for modelling the interference from random access secondary networks with a non-uniform user density. The impact of terrain-based propagation on the interference level is captured by fitting terrain-based pathloss values to a power law model. For large protection areas around the primary receivers, the interference levels generated from different secondary transmitters at the primary receiver start being correlated with one another. In order to capture the fading correlation without doing an excessive amount of computations in the database, we propose a constant correlation coefficient model in Section 5.4.

Given the maximum amount of generated interference that is permitted by the primary system, the secondary transmit power allocation becomes a resource sharing problem. In Chapter 6, we cast the secondary power allocation algorithms as constrained optimization problems. We maximise different secondary utilities, including the secondary transmit power level and secondary transmission rate, in Section 6.2 and Section 6.3, respectively. Unlike existing regulatory rules in Europe and the US, the pro-

posed rules protect the primary system in all cases. The issue of fairness in resource allocation is also highlighted in Chapter 6. Finally, the thesis results are summarised in Chapter 7.

1.3 Publication summary

The thesis is an overview of eight publications. The first five deal with the database-controlled secondary spectrum access and the rest with the sensing-based secondary spectrum access.

In Publication I, we suggest a method for allocating the transmission power levels in the downlink of cellular systems that operate in the TVWS. The challenge is to control the generated interference at multiple TV receivers. In order to meet the challenge, we selected a bound for the aggregate interference level that was independent of the locations of the cellular base stations and that resulted in relatively simple expressions for the interference control. Since the exact locations of the base stations are not required for bounding the interference level, the proposed scheme allows for multiple cellular systems, possibly belonging to different operators, to cooperate for purposes of interference control with a small communication signalling overhead.

Different secondary utility functions can be optimized under a constraint for the maximum generated interference that is permitted by the primary system. In Publication II, the sum of the transmit power levels is maximised in the logarithmic domain. For reducing implementation complexity in the case of large-scale problem instances, we propose a simplified proportional fair power allocation algorithm. The modified algorithm performs at a nearly optimal level and it can also be applied to make decentralized power allocation possible for mobile secondary transmitters.

The existing power allocation rules adopted by the ECC and Federal Communication Committee (FCC) in the US do not take into account self-interference in the secondary system when identifying the transmission power levels. In Publication III, we extend the results of Publication I and Publication II to incorporate the cellular network self-interference into the power allocation scheme. We presented power allocation as an optimization problem. The results of this publication are useful for cellular network planning in the TVWS and also for designing the protection distance separation between the cellular and TV systems.

In Publication IV, we compute the distribution of the aggregate interfer-

ence in an environment with correlated shadowing. Estimating the shadowing cross-correlation between all transmission pairs is a complex task. In order to avoid it, we propose to estimate the interference distribution by using a constant correlation coefficient model. Also, the uncorrelated and the fully correlated secondary transmissions can easily be evaluated and provide useful bounds for the aggregate interference level.

In Publication I-Publication IV, we model the interference from multiple transmitters that are deployed in a cellular layout. In Publication V, we model the interference from randomly located transmitters, such as, for instance, in cellular uplink or wireless local area networks (WLAN). We compute the distribution of the aggregate interference in a realistic environment, incorporating spatially non-uniform service demand and terrain-based radio propagation. In order to estimate the distribution of the aggregate interference, we proposed two modifications to the well-known Poisson point process (PPP) model. The proposed model has a low complexity and makes it possible to estimate the aggregate interference under a massive use of spectrum, which is ultimately the decisive factor for the commercial feasibility of secondary services.

Traditional sensing-based spectrum allocation schemes degenerate the interference control process into a signal detection problem. Usually, the signal detection algorithms utilise a binary hypothesis test, assuming that the signal is either present at a fixed level or absent. In Publication VI, we model the signal level under both hypotheses. The proposed model makes it possible to discover more opportunities for secondary spectrum access in comparison with the traditional hypothesis framework. Also, the analytical predictions of the model provide a better match for the way in which the signal detector performs in a realistic environment.

In Publication VI, the secondary system measures a single spectrum band. The secondary system can benefit from distributing the spectrum measurements across multiple spectrum bands. In Publication VII, we identify how many bands need to be measured in different fading environments. It is shown that for energy efficient tracking, it is not always optimal to measure the complete candidate bandwidth and involve all secondary users in spectrum measurements.

In Publication VII, the performance of the secondary network is described in terms of throughput. In Publication VIII, we consider a constant bit rate service and measure the secondary performance in terms of its service blocking probability. The objective is to design a sensing strat-

egy based on a certain blocking probability target. Publication VIII examines the fundamental relationship between the capacity requirement of a particular service and the demand placed on the measured spectrum.

2. Sensing-based spectrum access

Spectrum sensing can be used to detect secondary transmission opportunities either in time and/or in space. When the primary system employs bursty transmission, the secondary user can detect the empty time slots and multiplex its signal over them without causing any performance degradation at the primary receivers. On the other hand, when the primary system employs continuous transmission, the secondary user has to estimate the interference it generates at the primary receivers by using signal level measurements. This is difficult to do in practice because the locations of primary receivers are not known. In order to bypass the location uncertainty, one can consider that the secondary transmission must be harmless for the primary receivers if the secondary user is located far away from the primary transmitters.

The primary signal level at the location of the secondary user can be used as a proxy for its distance to the primary transmitter [24]. A target signal level, P_ϵ , can be defined to decide whether the secondary user is located far enough away from the primary transmitter or not. The secondary user is granted the primary system's spectrum provided that the signal level at its location is below the target level. Essentially, the interference estimation process for sensing-based spectrum access in the spatial domain can also be reduced to a signal detection problem and the results from classical detection theory can be used.

The traditional signal detection framework defines two hypotheses [25]. Hypothesis H_0 models the presence of pure noise, while hypothesis H_1 consists of a signal embedded in the noise. The detector measures the spectrum and has to decide which hypothesis is present.

$$H_1 : y(n) = \sqrt{P_S} \cdot s(n) + w(n) \quad (2.1i)$$

$$H_0 : y(n) = w(n) \quad (2.1ii)$$

where $y(n)$ and $s(n)$ are the n -th received and the transmitted signal sam-

ple, respectively, $w(n)$ is the noise sample and P_S denotes the signal level at the sensor's location. With sensing-based secondary spectrum access the signal level, P_S , should be replaced by the target level, P_e .

For binary hypothesis testing, the optimal decision test is a likelihood ratio test (LRT) both in a Bayesian and Neyman-Pearson sense [26, pp.9, 17]. Accordingly, the user constructs the likelihood ratio, $\Lambda(\mathbf{y})$, of the hypotheses and compares it with a threshold, η :

$$\Lambda(\mathbf{y}) = \frac{p(\mathbf{y}|H_1)}{p(\mathbf{y}|H_0)} \stackrel{H_1}{\geq} \eta, \quad (2.2)$$

where $p(\mathbf{y}|H_i)$, $i \in \{0, 1\}$ is the joint probability distribution function (PDF) of the measured samples, \mathbf{y} , conditioned on each hypothesis.

After replacing the PDFs $p(\mathbf{y}|H_i)$, $i \in \{0, 1\}$ in equation (2.2), the likelihood ratio can be written as a function of the measured samples $L(\mathbf{y})$. The function, $L(\mathbf{y})$, is called the test statistic. Upon receiving the measured samples, the detector evaluates the statistic, $L(\mathbf{y})$, and compares it with a threshold, η' :

$$L(\mathbf{y}) = \stackrel{H_1}{\geq} \eta'. \quad (2.3)$$

In threshold-based binary signal detection algorithms, there are four possible courses of action. Two of them correspond to erroneous decision: a misdetection describes a case where the signal is present but the detector favours hypothesis H_0 . A false alarm describes a case where the signal is absent but the detector votes for hypothesis H_1 . Within the context of secondary spectrum access, a misdetection generates interference at the primary receivers, while a false alarm is tantamount to a lost secondary transmission opportunity.

The reliability of spectrum sensing for a certain signal level is usually described in terms of the following two metrics: the misdetection probability \Pr_{miss} and the false alarm rate \Pr_{false} . These metrics can be evaluated provided that the PDF of the measured samples conditioned on each hypothesis is known and that the decision threshold at the detector is set.

Single sensor detection may suffer from poor performance due to multipath fading and shadowing. The sensor has to account for the rare possibility of a deep signal fade. In order not to miss the signal, the sensor has either to operate at a high false alarm rate or use excessive sensing times. Distributed detection makes it possible to average out the fading with multiple independent sensors. For the same misdetection probability and an equal number of measured samples, a lower false alarm rate is achieved in comparison with single sensor detection.

Distributed detection was originally developed to improve the performance and survivability of radar systems and it became quite popular with the development of wireless sensor networks (WSN). Since early 2000, it has been proposed as a means to uncover secondary spectrum sharing opportunities in licensed spectrum bands (see [27] and the references therein). First, we review the most fundamental results for distributed detection and data fusion. Then, we discuss how these results have been used and extended within the context of secondary spectrum access.

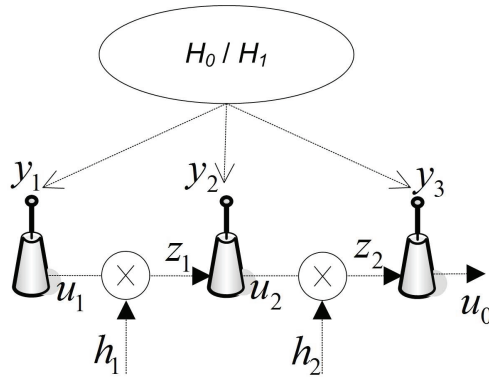
2.1 Distributed detection in sensor networks

Tenney and Sandell have extended the well-known Bayesian detection theory to include multiple distributed sensors [28]. In the distributed setup, it is assumed that multiple sensors observe the same phenomenon, either hypothesis H_0 or H_1 , and jointly decide on the presence of the true hypothesis. The distributed detection schemes can be classified in terms of their network configuration. For instance, it is possible to have a central node, also known as a fusion centre (FC), which can either decide on behalf of the sensors or not. Also, distributed detection algorithms may use a different amount of information exchange between the sensors and a different combination rule for the sensor measurements at the FC.

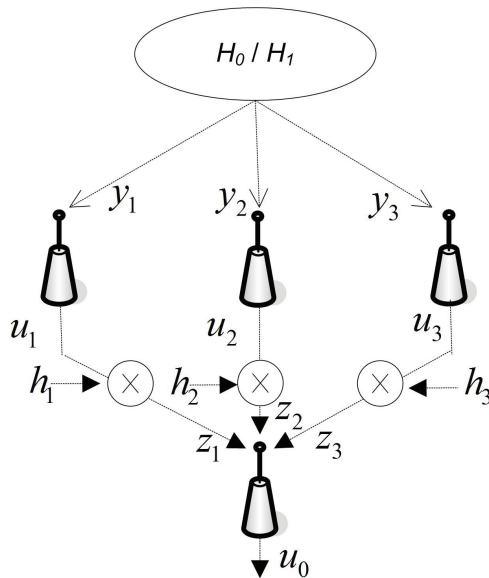
2.1.1 Classification of distributed detection schemes

The most common distributed sensor configurations are serial, decentralized and centralized configurations [29].

The configuration of sensors depicted in Fig 2.1a is known as a serial configuration. The first sensor in the sequence processes the collected measurement, y_1 , and communicates the result, u_1 , to the second sensor over the reporting channel, h_1 . The second sensor combines its own measurement with the data, z_1 , received from the first sensor and sends the outcome to the third sensor. The last sensor in the sequence is responsible for making the overall decision, u_0 . The sensors in the serial configuration should be ranked for optimal detection performance. Even if the reliability of the sensor's decisions is known a priori, this is a complex task and no general results exist so far [30]. Also, the serial configuration is very sensitive to link failures and suffers from a high delay.



(a) Serial configuration.



(b) Centralized configuration.

Figure 2.1. Distributed detection schemes.

In the centralized configuration (see Fig. 2.1b), the measurements, y_i , are processed at each sensor in parallel. The processed data, u_i , is communicated to the FC. The FC receives the data, z_i , sent over the reporting channel h_i and decides on behalf of the sensors whether the signal is present or not. Within the context of cooperative sensing for secondary spectrum sharing, the centralized scheme has become the most popular because it makes it possible to reach the final decision quickly. The detection performance in the centralized scheme depends on the local processing at the sensors, the link quality of the reporting channels and the decision rule employed by the FC.

Unlike (the serial and) the centralized scheme, the decentralized scheme

does not rely on a FC for making the overall decision. Each sensor processes the measurement locally and shares the result with all of the other sensors until a consensus is reached. The decentralized scheme needs lots of iterations to converge because the local decisions at the sensors are coupled.

Since the centralized scheme has been widely used in secondary spectrum sharing scenarios, we next review the most fundamental results for centralized detection and data fusion for WSN.

2.1.2 Combination rules in the centralized scheme

The detection performance of the centralized scheme is affected by the amount of information conveyed from the sensors to the fusion centre. There are two extreme cases: a scheme where the exact measurements are conveyed, known as soft decision combining (SDC), and a scheme where only a binary decision is communicated, known as hard decision combining (HDC). For the SDC scheme, the collected measurements at the i -th sensor are communicated to the FC, $u_i = y_i$, while for the HDC scheme the u_i is binary, $u_i = \text{sign}(L(y_i) - \eta')$.

The performance of the SDC depends on the decision threshold set at the FC. The performance of the HDC depends also on the decision rule employed by the FC. The two extremes provide useful bounds for the performance of any other centralized scheme. Independent and identically distributed (i.i.d.) sensors transmitting softened hard decisions at the FC (i.e. multi-bit information indicating also the quality of their decisions) achieve better detection performance than does HDC scheme [31]. Also, the detection performance of a two-bit quantizer is inferior, but close, to the performance of SDC with significantly less cooperation signalling overhead [32].

HDC has become more popular than SDC because it allows for a finite communication bandwidth over the reporting channel and also reduces the power budget requirement. While classic detection theory for a single sensor can be applied to an analysis of SDC, the HDC is more challenging to analyse because the local thresholds at the sensors and the fusion rule are coupled [33].

Optimal HDC: Since the decisions of the sensors can be treated as observations at the FC, the optimal fusion rule is an LRT:

$$\frac{p(u_1, \dots, u_N | H_1)}{p(u_1, \dots, u_N | H_0)} \stackrel{H_1}{\geq} t, \quad (2.4)$$

where N is the number of sensors and t the threshold at the FC.

If the sensor measurements conditioned on each hypothesis are independent and the local thresholds at the FC are known, then the LRT test, inequality (2.4), boils down to the weighted sum of the individual decisions compared with a threshold, t' [34]:

$$\sum_{i=1}^N \alpha_i \cdot u_i \geq t'. \quad (2.5)$$

This is known as the Chair-Varshney test. The optimal weights, α_i , are functions of the misdetection probability and the false alarm rate of an individual sensor's decision and are, therefore, dependent on the performance reliability of the sensors [34]:

$$\alpha_i = \begin{cases} \log \frac{1 - \Pr_{miss}^{(i)}}{\Pr_{false}^{(i)}}, & u_i = +1 \\ \log \frac{1 - \Pr_{false}^{(i)}}{\Pr_{miss}^{(i)}}, & u_i = -1. \end{cases} \quad (2.6)$$

For identical sensors, $\alpha_i = \alpha$, equation (2.5) degenerates to $\sum_{i=1}^N u_i \geq t'/\alpha$ and the optimal fusion rule becomes the K -out-of- N decision rule [31], also known as the voting rule: the fusion centre favours hypothesis H_1 if at least K sensors indicate that a signal is present.

Under hypothesis H_0 , the sensor votes for hypothesis H_1 with probability \Pr_{false} . As a result, the false alarm probability at the FC, $\Pr_{false}^{(F)}$, follows the binomial distribution; its parameters are the total number of sensors N and the probability of false alarm at the sensors:

$$\Pr_{false}^{(F)} = \sum_{i=K}^N C(N, i) \cdot \Pr_{false}^i \cdot (1 - \Pr_{false})^{N-i}, \quad (2.7)$$

where $C(N, i)$ is the number of i combinations in a set with N elements.

Under hypothesis H_1 , the detection probability at the FC follows the binomial distribution, too, with the parameters N and $(1 - \Pr_{miss})$. The misdetection probability at the FC is:

$$\Pr_{miss}^{(F)} = 1 - \sum_{i=K}^N C(N, i) \cdot (1 - \Pr_{miss})^i \cdot \Pr_{miss}^{N-i}. \quad (2.8)$$

The logical OR and the AND rule, widely used in distributed detection with fusion, are special cases of the K -out-of- N decision rule for $K = 1$ and $K = N$, respectively. For i.i.d. sensors collecting Gaussian-distributed measurements, the OR rule is superior at high false alarm rates while the AND rule is superior at low false alarm rates [35]. However, this claim does not hold for a general PDF of a sensor's observations [36].

Thus far, it has been assumed that the performance characteristics of the sensors are fixed and known [31, 34]. For a globally optimal performance, neither local thresholds nor the fusion rule are fixed a priori [33]. Due to the high number of computations involved, person-by-person optimization techniques are used to approximate the optimal solution [26, pp.75]. Also, when the sensor observations are i.i.d., it becomes asymptotically optimal to use the same local thresholds [37].

Correlated measurements: For correlated sensor observations, the optimal fusion rule requires the joint statistics of the sensor decisions on the left-hand-side of inequality (2.4), which are difficult to estimate in practice. One could, however, design identical local thresholds and model the correlated decisions between any pair of sensors with a common correlation coefficient, ρ , $0 \leq \rho \leq 1$. Based on this assumption, the detection performance deteriorates when the degree of correlation increases [38, 39]. For SDC, the detection performance with exponentially correlated log-normal shadowing is worse than that with uncorrelated fading [40, 41]. There is also one study claiming that a correlation among secondary users can improve the detection performance, provided that the fusion rule is convex [42].

Reporting errors: So far, it has been assumed that the local processing results are conveyed to the FC through error-free channels; with reference to Fig. 2.1b, $z_i = u_i$. However, the reporting data also suffers from pathloss, fading and noise. If the local thresholds are set by assuming ideal reporting channels, then the detection error probabilities at the FC will not meet the target detection constraints. Actually, even if the detectors at the sensors are flawless, the FC is not able to perform reliable detection in cases when the bit error probability over the reporting links is high [43].

Besides the local signal-to-noise ratio (SNR) at the sensors, the detection performance at the FC depends also on the error probability in the reporting channel [44]. The optimal K -out-of- N fusion rule can be different with ideal and non-ideal reporting channels [45]. In general, the SDC outperforms HDC in the presence of channel errors, while the majority rule is the most robust among the HDC schemes [46]. Counterintuitively, while the MRC is near optimal for a low SNR in the reporting channel, the EGC outperforms MRC at most SNR values [47].

Distributed detection and data fusion have essentially set the stage for the research on cooperative sensing for secondary spectrum sharing.

2.2 Cooperative sensing in secondary spectrum access networks

The results from distributed detection and data fusion are not directly applicable to cooperative sensing for secondary spectrum access. In the distributed detection setup, a common assumption is that all sensors are identical and that the signal level at their locations is known. In secondary spectrum sharing, the distances between users can be high, resulting in unequal primary signal levels [48]. Also, the users may not have enough resources to estimate the signal levels with sufficient accuracy. Instead, a target level, P_ϵ , is defined and spectrum access is granted only if the primary signal level is under the target level. Finally, a secondary user must comply to certain misdetection probability constraints.

Fading channel: When the measurement time is longer than the channel coherence time, the fast fading can be averaged out for a single user. On the other hand, the impact of shadow fading cannot be eliminated for a single user. In the worst case scenario, the primary transmitter is hidden from the user while the primary receivers are not. The hidden node problem can cause an unacceptable amount of generated interference for the primary system if it is not properly addressed. In order to account for the possibility of a deep signal fade, a margin should be added and the detection threshold must be reduced.

In a cooperative detection setup, it is highly improbable that the primary transmitter will be hidden from all secondary users. As a result, the detection threshold for each user can be set higher without violating the misdetection probability constraint at the FC. This is illustrated in Fig. 2.2. The decision threshold for single user with power detector and a 5% misdetection probability is set at -96.1 dBm. For a cooperative decision with the same misdetection probability at the FC, the decision threshold for each user can increase by 2.3 dB. On the other hand, increasing the individual measurement time does not bring considerable benefits.

Cooperative detection makes it possible to reduce the fading margin and to recover more available spectrum. This issue prompted researchers to study cooperative detection performance under different fading environments, that has not been carried out within the context of WSN.

Under Rayleigh fading and log-normal shadowing, the OR rule is not always optimal, so the K -out-of- N fusion rule should be used instead [40, 49, 50]. The majority rule, $K = (N + 1)/2$, is optimal for i.i.d. users if the

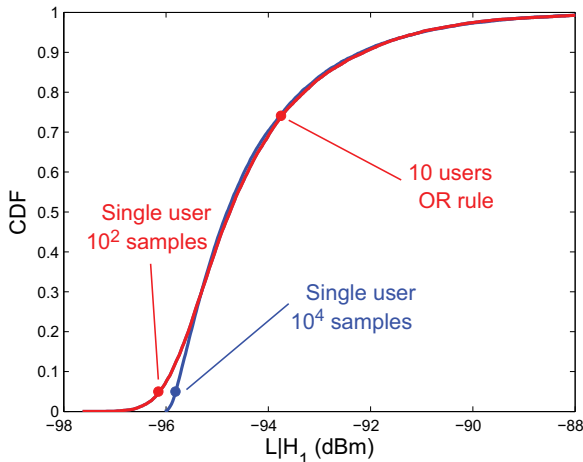


Figure 2.2. Simulated cumulative distribution function (CDF) of the test statistic L at the user under hypothesis H_1 and decision thresholds for power detection in log-normal shadow fading. The test statistic is $L = \frac{1}{\kappa/2} \sum_{i=1}^{\kappa/2} |y_i|^2$ where $\kappa/2$ is the number of collected complex samples. The slow fading standard deviation is $\sigma = 5$ dB, the primary signal level, P_ϵ , is -101 dBm and the noise level is -96 dBm.

optimality criterion is the total detection error rate without any explicit constraint on the misdetection probability [51]. Different SDC schemes, such as the MRC, EGC, square law combining and square law selection achieve different performance in the Rayleigh fading channel [32, 52]. In the low SNR regime, which is of practical interest for sensing-based spectrum sharing, the MRC becomes nearly optimal at the expense of requiring the instantaneous SNR.

SNR walls: Cooperative sensing has also been proposed as a means to overcome system-level uncertainties [53, 54]. For instance, the noise power level cannot be perfectly estimated and some uncertainty always exists. When the uncertainty is comparable to the level of the signal that we are trying to detect, the energy detection becomes unreliable no matter how many spectrum measurements are collected [55]. The minimum SNR that makes reliable energy detection possible is called the SNR wall [56]. In some cases, the impact of system-level uncertainties on signal detection can be overcome by cooperative user measurements. The cooperation of multiple independent users reduces the fading margin. The detection threshold for each user is set higher than it is for single user detection. Provided that the number of independent users is sufficient, the detection threshold may be set higher than the SNR wall, making reliable detection at the FC possible [54].

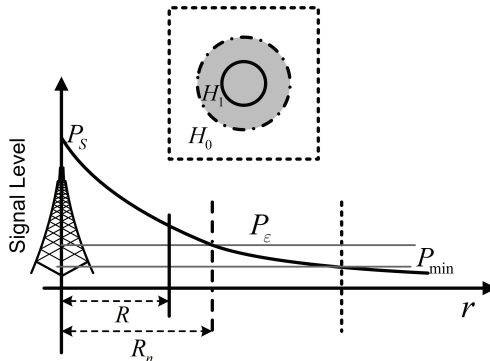
In Publication VI, we utilised the results for centralized detection with the HDC and K -out-of- N decision rule for recovering secondary transmission opportunities in the TV spectrum. As discussed in the next section, we have to modify the traditional signal detection model in equation (2.1) to better reflect the considered spectrum sharing scenario.

2.3 Recovering spatial spectrum sharing opportunities

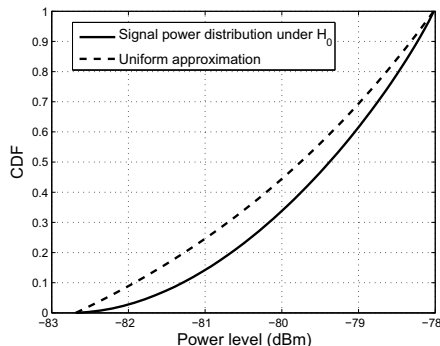
While studying the detection performance of cooperative schemes, it has been assumed that the primary user employs bursty transmission. An opportunity for secondary spectrum sharing exists during the time that the primary transmitter remains inactive. Within this context, the traditional signal detection framework in equation (2.1) has been used to distinguish between pure noise, H_0 , and the primary user signal embedded in the noise, H_1 .

The traditional signal detection framework is suitable for recovering spectrum sharing opportunities in the time domain. Wireless communication systems that use a continuous transmission also exist. TV broadcasters transmit almost continuously in their service area and so there is no opportunity for secondary spectrum access. However, it would be possible to use the TV spectrum provided that the amount of interference generated at the TV receivers is not harmful. To protect the TV receivers, a guard area can be defined around each receiver where the secondary transmission is not permitted. Fig. 2.3a shows the TV service area with radius R , the TV protection area with radius R_n and the TVWS (the area outside of the TV protection area) where the secondary operation is allowed.

The secondary user is not aware of its own location and it has to decide whether it is located outside of the TV protection area or not. In order to do that, the user can construct two hypotheses: hypothesis H_0/H_1 models the signal outside/inside of the TV protection area. In this setup, we propose in Publication VI to describe the detection performance in terms of the amount of area where the available spectrum is recovered. At the same time, the misdetection probability inside the TV protection area must be controlled. In Publication VI, we illustrate that the traditional spectrum sensing framework (2.1) is inappropriate for recovering spatial spectrum opportunities and, as a consequence, a great deal of available spectrum is lost. The reason for this is that hypothesis H_0 in equation (2.1) does not



(a) TV signal level and detection level.



(b) CDF of TV signal level outside of the TV protection area.

Figure 2.3. The system setup used for the modelling process.

incorporate the primary signal.

The TV transmitters should be mounted on high towers and their signal should be attenuated slowly. The TV signal may be at a low level outside the TV protection area but it still exists. To remedy the problem, in Publication VI, we modelled the primary signal not only under hypothesis H_1 , but also under hypothesis H_0 . The traditional hypothesis test can be modified to capture the primary signal under both hypotheses as:

$$H_1 : y(n) = \sqrt{P_S(R_n)} \cdot s(n) + w(n). \quad (2.9i)$$

$$H_0 : y(n) = \sqrt{P_S(r)} \cdot s(n) + w(n), r > R_n. \quad (2.9ii)$$

Unlike the traditional framework (2.1i), the primary signal level at the location of the secondary user is not known. Since the primary system does not trust the secondary deployment model, it has to protect the TV receivers even during the worst deployment scenario [57]. As a result, hypothesis H_1 in equation (2.9i) assumes that the secondary user is located

at the border of the TV protection area: $P_\epsilon = P_S(R_n)$. At the same time, hypothesis H_0 in equation (2.9ii) incorporates the primary signal level at the user location. The hypothesis test in equation (2.9) can be used to decide whether the primary signal level at the location of the user is equal to P_ϵ or lower. Provided that the noise power level at the user is known, the test essentially decides whether the primary SNR at the user location is lower than a target SNR level or not.

In Publication VI we consider energy detectors at the secondary users and model the primary user signal sample and the noise sample with complex Gaussian random variables with variances equal to P_S and P_N respectively. As a result, the distribution of the test statistic L for $\mathcal{K}/2$ collected complex samples, $L = \sum_{i=1}^{\mathcal{K}/2} |y_i|^2$, under hypothesis H_1 is Chi-square. Due to the fact that the primary signal level P_S varies in the amount of area covered by hypothesis H_0 , the distribution of the test statistic $p(L|H_0)$ becomes composite. The distribution $p(L|H_0)$ is found by integrating the distribution $p(L|P_S)$ for a fixed primary signal level, P_S , over the distribution $p(P_S|H_0)$ of all possible signal levels taken into account by hypothesis H_0 [25, pp. 86]:

$$p(L|H_0) = \int_{P_{min}}^{P_\epsilon} p(L|P_S) \cdot p(P_S|H_0) dP_S \quad (2.10)$$

where P_{min} is the signal level at the border of the secondary area.

The primary signal level distribution under hypothesis H_0 depends on the signal attenuation model and the user distribution. The solid line in Fig. 2.3b shows the distribution of the TV signal level outside of the TV protection area for the uniform distribution of secondary users and the power law attenuation model. In general, the signal level distribution has a complex form and it is difficult to use it for analytical derivations. In Publication VI, we propose to approximate the distribution of the TV signal level, $p(P_S|H_0)$, with the uniform distribution (see the dashed line in Fig. 2.3b).

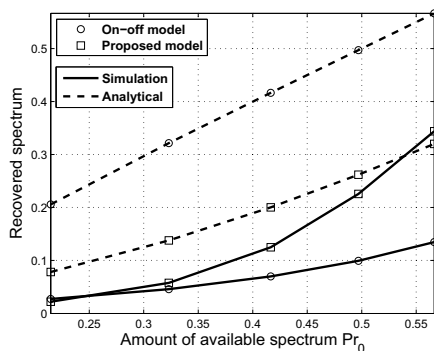
After replacing the uniform approximation, $p(P_S|H_0) \approx 1/(P_\epsilon - P_{min})$, in equation (2.10), the test statistic, $p(L|H_0)$, can be expressed in the form of the lower incomplete Gamma function, $\gamma(\cdot, \cdot)$. By using the series expansion of the $\gamma(\cdot, \cdot)$ function, the false alarm probability can be expressed as a finite series sum:

$$\Pr_{false} = 1 - \sum_{j=1}^{\mathcal{K}/2-1} \frac{(P_N + P_\epsilon) \cdot \gamma\left(j, \frac{\eta}{2 \cdot (P_N + P_\epsilon)}\right) - (P_N + P_{min}) \cdot \gamma\left(j, \frac{\eta}{2 \cdot (P_N + P_{min})}\right)}{(j-1)! \cdot P_\epsilon \cdot (\mathcal{K}/2 - 1)}. \quad (2.11)$$

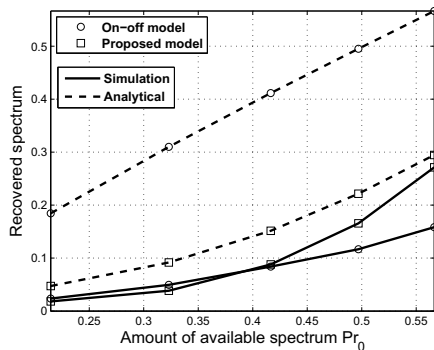
For comparison purposes, the false alarm probability under pure noise is:

$$\Pr_{false} = 1 - \frac{1}{\Gamma(\mathcal{K}/2)} \cdot \gamma\left(\frac{\mathcal{K}}{2}, \frac{\eta}{2 \cdot P_N}\right). \quad (2.12)$$

In Publication VI we propose to express the total amount of available spectrum as a ratio of the area covered by hypothesis H_0 divided by the full area. That can also be viewed as the prior probability, \Pr_0 , of hypothesis H_0 , and it corresponds to the amount of spectrum that is recovered in the absence of sensing errors. The quality of the signal detection models is assessed based on the amount of recovered available spectrum and also based on the similarities between the model prediction and simulation results.



(a) Soft combining.



(b) Hard decision combining.

Figure 2.4. Amount of TVWS recovered by spectrum sensing. $N = 5$ secondary users, $\mathcal{K}/2 = 5$ collected complex samples per user. Target SNR level P_e/P_N varies between 1 dB and 5 dB and the misdetection probability target is 1 %.

The comparison of the two models has been carried out both for single user detection and for distributed detection with SDC and HDC using the K -out-of- N decision rule [31] (see Fig. 2.4). The two models utilise differ-

ent decision thresholds because they evaluate the false alarm probability by using different expressions. For setting the decision thresholds, we minimised the total detection error probability under a constraint, Pr_{out} , in relation to the misdetection probability:

$$\text{Minimise : } \Pr_{\eta,t}^{miss} + \Pr_{false}. \quad (2.13i)$$

$$\text{Subject to: } \Pr_{miss} \leq \Pr_{out}. \quad (2.13ii)$$

Even though the proposed signal level approximation seems to be inaccurate (see Fig. 2.3b), it captures the system behaviour better than the pure noise hypothesis. Because of this, it makes it possible to derive an analytical performance prediction that matches up better with the simulation results in realistic environments. Also, the decision thresholds are in general larger compared with the thresholds calculated using the traditional model. As a result, there are cases where more available spectrum is recovered without violating the design constraint (2.13ii). One may further improve the prediction capability of the proposed model using a step-wise function to approximate the primary signal level distribution under hypothesis H_0 at the cost of higher implementation complexity.

The impact of using the noise-only hypothesis to recover spatial spectrum opportunities in the TVWS has also been pointed out in a number of studies [57, 58, 59, 60, 61]. In a study by Tandra, Mishra & Sahai [57], two new metrics are introduced to describe the trade-off between primary safety and secondary performance. The *Fear of Harmful Interference* metric is related to the protection of the TV system. It incorporates not only the uncertainty involved in secondary deployment, as in Publication VI, but also the uncertainty with respect to, for example, the fading distribution, the distance-based pathloss and the noise distribution. The *Weighted Probability of Area Recovered* metric is related to the secondary performance. An exponential distribution for user deployment is assumed and the false alarm probability is integrated with the user density. Unlike in Publication VI, a closed-form expression is not derived for the *Weighted Probability of Area Recovered*.

In two separate studies by Tandra, Sahai & Veeravalli [58, 59], the *Weighted Probability of Area Recovered* is extended to the *Weighted Probability of Space-Time Recovered* for recovering spectrum sharing opportunities jointly in space and time. In our own study [60], we utilise the uniform distribution to approximate the TV signal level outside, but close to, the TV protection area. For area farther outside the protection area,

we use the noise-only hypothesis. The simulations show that more available spectrum can be recovered. Finally, in another study [61] we integrate the uniform approximation into the autocorrelation-based detection of Orthogonal frequency division multiplexing (OFDM) signals and draw similar conclusions to the ones we drew in Publication VI.

2.4 Discussion

In this chapter, we reviewed the key results pertaining to distributed detection and data fusion for WSN and discussed how these results have been extended in the field of sensing-based secondary spectrum access. We focused on centralized distributed detection and outlined how the combination rule impacts detection performance at the FC. For improving detection performance and reducing the cooperation signalling overhead, one can find in the literature additional proposals, such as censoring of local measurements [62], clustering of sensors [63] and relaying [64]. A discussion of these methods is beyond the scope of this thesis.

Also, we argued that the traditional signal detection framework is not suitable for recovering spectrum sharing opportunities in the TVWS. TV signals exist practically everywhere. This calls for new performance metrics rather than the misdetection probability and false alarm rate. We proposed incorporating the primary signal level distribution into the signal detection framework and described the performance in terms of the percentage of TVWS where the available spectrum is recovered.

So far, it has been assumed that all users are involved in sensing and that they measure a single spectrum band. The distributed sensing problem becomes more realistic and challenging when there are multiple spectrum band candidates; then the users can distribute their measurements among any number of spectrum bands. A sensing strategy should be devised to determine, for instance, the order for measuring the different bands and allocating users for the bands. Also, cooperative spectrum measurements can be used to reduce the amount of sensing time required to achieve a target detection performance. That improves the spectrum usage efficiency because more time can be allocated for actual data transmission. Issues such as sensing-throughput trade-off, sensing scheduling and spectrum access can be grouped under the umbrella of MAC layer sensing. This is the topic of the next chapter.

3. MAC layer sensing

Physical layer (PHY) sensing captures the trade-off between primary system protection and secondary system performance by using the relationship between the misdetection probability and the false alarm rate. Unfortunately, the false alarm rate does not reveal much about the secondary system performance at higher network layers. A low false alarm probability does not guarantee high throughput or a low enough blocking probability.

Channel allocation schemes for cellular systems have been developed on the basis of meeting a target call blocking probability [65]. Due to the fact that the service demand varies in time and location, distributed channel assignment (DCA) schemes have become more popular than a fixed channel assignment since they are more spectrum efficient with non-uniform traffic loads. Within an autonomous DCA, the channel allocation is completely decentralized. The base stations learn about the interference originated from the neighbouring cells by assigning spectrum measurement tasks to the users. Then, they rank the channel candidates independent of one another and assign channels to the particular calls [66].

Similar to the self-organised DCA in cellular networks, the MAC layer in secondary spectrum access is responsible for coordinating both spectrum sensing and spectrum access. The difference lies in the fact that secondary spectrum sensing performance at the PHY should be integrated with the algorithms for allocating the sensing resources. For instance, a reliable detector that requires 'short' sensing times enables the MAC layer to request spectrum measurements over a wide channel bandwidth. If only a few channels are available for sensing, the MAC layer could request shortening the sensing time to increase the data transmission time. This close interaction between PHY sensing and the MAC layer is a unique feature of secondary spectrum access, giving rise to the term MAC layer sensing.

The sensing resources in secondary spectrum access are the spectrum measurement time, the users available for conducting spectrum measurements and the candidate spectrum bands. A careful review of MAC layer protocols reveals that the resource allocation depends on whether the secondary users are aware of the primary traffic model or not. In Section 3.1 through Section 3.3, we discuss MAC protocols for unaware secondary systems, whereas MAC protocols for aware systems are discussed in Section 3.4.

3.1 Sensing time optimization

In time-slotted secondary systems, some part of the time slot should be dedicated to spectrum sensing and the remaining part should be used for data transmission. If the secondary system is not aware of the primary traffic model, the time slot duration, T , must be smaller than the maximum permitted time the primary system can tolerate the secondary generated interference. Provided that the misdetection probability target is met, this strategy assures that the primary user is sufficiently protected.

For fixed time slot duration and misdetection probability, increasing the sensing time, τ , reduces the false alarm rate, but it also reduces the time, $T - \tau$, left for secondary data transmission. If the sensing time is reduced, an available band may be classified as occupied and the transmission opportunity will be lost. A sensing time that maximises the secondary throughput must exist. This is known as the sensing-throughput trade-off.

3.1.1 Sensing-throughput trade-off

Let us denote the secondary data rates over the available and occupied spectrum bands by \mathcal{R}_0 and \mathcal{R}_1 , respectively. Due to the impact of the primary generated interference to the secondary system, $\mathcal{R}_0 > \mathcal{R}_1$. The expected secondary data rate, \mathcal{R} , is the weighted sum of the data rates, \mathcal{R}_0 and \mathcal{R}_1 , with the probability of classifying a measured band as available:

$$\mathcal{R} = \mathcal{R}_0 \cdot \text{Pr}_0 \cdot (1 - \text{Pr}_{false}(\eta, \tau)) + \mathcal{R}_1 \cdot \text{Pr}_1 \cdot \text{Pr}_{miss}(\eta, \tau), \quad (3.1)$$

where Pr_0 and Pr_1 are the prior probabilities that a measured band is available and occupied, respectively.

The sensing-throughput trade-off for a single spectrum band can be for-

ulated as follows:

$$\text{Maximise}_{\eta, \tau} : \frac{T - \tau}{T} \cdot \mathcal{R}. \quad (3.2i)$$

$$\text{Subject to: } \Pr_{miss} \leq \Pr_{out} \quad (3.2ii)$$

$$\tau \leq T. \quad (3.2iii)$$

For fixed sensing time, the misdetection probability and the complementary false alarm rate both increase with increasing threshold. In order to maximise the expected data rate, the threshold must be set so that the optimization constraint (3.2ii) becomes tight. As a result, the threshold becomes a function of the sensing time and the misdetection probability target, \Pr_{out} . After replacing the threshold in equation (3.2i), a one-dimensional search within the time interval $(0, T]$ would be sufficient for identifying the optimal sensing time.

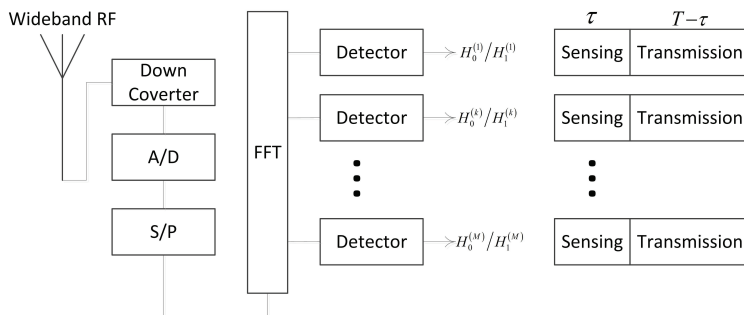


Figure 3.1. Multiband spectrum sensing detector and time slot structure.

In multiband spectrum sensing, the secondary user has either a wideband RF antenna or multiple narrowband RF front ends. It is assumed that the time slots over the different channels have equal durations and that they are perfectly aligned with each other (see Fig. 3.1). The extension of sensing-throughput trade-off over the M spectrum bands follows accordingly:

$$\text{Maximise}_{\eta, \tau} : \frac{T - \tau}{T} \cdot \sum_{k=1}^M \mathcal{R}^{(k)} \quad (3.3i)$$

$$\text{Subject to: } \Pr_{miss}^{(k)} \leq \Pr_{out} \forall k \quad (3.3ii)$$

$$\tau \leq T. \quad (3.3iii)$$

Impact of cooperative spectrum sensing: One way to increase the achievable throughput for the same misdetection probability target is to reduce the sensing time by introducing cooperative spectrum measurements. The sensing-throughput trade-off depends both on the fusion rule

and the local processing at the users [67]. There is already a number of studies investigating the sensing-throughput trade-off for the EGC, MRC, OR and AND fusion rules with energy detectors at the users [68, 69, 70]. The optimal sensing time and voting rule have been derived by Peh, Liang, Guan & Zeng [70]. The soft decision combining has a high overhead, which reduces the fraction of sensing time if the overall sensing-reporting time is fixed. For short sensing-reporting time and large number of users, the hard decision combining can perform better [71].

Impact of available power budget: The secondary transmission rate, \mathcal{R}_0 , depends on the secondary transmit power and the link quality. If the power budget is limited, the user may optimize the power allocation over the different channels to maximise the sum throughput. The transmit power allocated on each channel depends on the detection performance and the link quality of all the other channels. If the availability of a channel is low and the link quality is also poor, the user would rather save the available resource by allocating a limited power budget on that channel. On the other hand, if the availability of a channel is high and the link quality is good, the user should increase the measurement time to detect the transmission opportunity. At the same time, the user should allocate a high power level to exploit the favourable link conditions. Under transmit power constraints, the sensing time and the allocated power levels are coupled and they both contribute to sensing-throughput trade-off [72, 73].

Impact of RF front end: So far, it has been assumed that each user measures all the candidate channels (see Fig. 3.1). Due to the hardware and implementation costs, each user may have just a single narrowband antenna, which can scan one spectrum band at a time. In sequential spectrum sensing, the user has to divide the sensing time within a time slot among the channels available for sensing. The total sensing time and the sensing time dedicated to each band have been set by Fan & Jiang [74] to maximise the sum ergodic throughput. Spectrum bands with low primary SNR will dominate the sensing time.

Impact of channel sensing order: When the user is interested in accessing just a single channel within a time slot, the sensing-throughput trade-off in sequential spectrum sensing depends also on the channel sensing order. Let us consider a scenario in which all of the channels are identical except for their availabilities, $\Pr_0^{(k)}$. When it is determined that a channel is available, the user can either start transmitting or else keep on searching for a channel with better quality at that time slot. For a

given channel sensing order, this is an optimal stopping problem. A sensing order and a stopping rule exist that maximise the expected throughput [75]. Counterintuitively, it is not optimal to sense the channels in the order of decreasing availability. Also, it is in general not optimal to use the same sensing orders among different users due to channel contention [76]. When the channels are not identical, it is optimal to rank them in the order of their diminishing rates, $\mathcal{R}_0^{(k)}$, and access the first sensed-free channel [77]. Note that perfect sensing accuracy has been considered in the above-mentioned [75, 76, 77].

Even though much research has been devoted to analysing of the sensing-throughput trade-off, there is one method that promises to surpass it in a practical setting [78]. The secondary receiver may decode the useful signal, cancel it off from the received signal and perform primary signal detection on the remaining signal. If the primary signal is detected, the secondary transmission will be prohibited in the next time slot. In this way, the sensing and the transmission times become equal to the full time slot duration, enhancing both the detection reliability and throughput while the primary system is still protected.

3.1.2 Sensing-outage trade-off

The achievable secondary throughput has been widely used to characterise the secondary performance. Another performance metric that has received less attention is the secondary outage probability. While the outage probability analysis of cellular networks depends only on the channel link quality, with secondary spectrum access an outage can also occur due to excessive sensing time or, in the worst case, due to the inability to discover available spectrum bands. Similar to the sensing-throughput trade-off, there is an optimal spectrum sensing time that minimises the outage probability [79]. When the secondary link quality is good, the outage probability should converge to the probability of classifying the measured band as occupied.

3.2 Optimizing the number of users involved in sensing

Involving more users in spectrum measurements may marginally affect the detection performance at some point. If the energy consumption or cooperation signalling overhead is an issue, it may be more beneficial to

refrain some users from spectrum sensing. In Publication VII we consider identical users and discuss how many of them should be allocated for spectrum sensing in order to strike a balance between detection performance and an efficient utilisation of the available resource. For non-identical users, e.g. users experiencing different primary signal levels or employing different detectors, one can refer, for instance, to several recent studies [80, 81].

The trade-off between sensing performance and resource usage efficiency has been illustrated for a single spectrum band by Chen [82]. The trade-off is studied by using a cost function, which is the weighted sum of the detection probability and the efficiency of the resource usage. The number of users maximising the cost function is identified for different channel models (AWGN, log-normal and Rayleigh) using a numerical search. When the sensors are i.i.d. and the OR rule is employed, a closed-form expression for the optimal number of users can be derived [83].

In Publication VII we extend the results provided by Chen [82] to include multiple spectrum bands. The energy spent on sensing is used to assess the efficiency of the resource utilisation. The aim is to strike a balance between the expected secondary data rate and the energy consumption. The expected secondary data rate is a simple extension of (3.1) for M spectrum bands:

$$\mathcal{R} = \sum_{k=1}^M \mathcal{R}_0^{(k)} \cdot \text{Pr}_0^{(k)} \cdot (1 - \text{Pr}_{false}^{(k)}) + \mathcal{R}_1^{(k)} \cdot \text{Pr}_1^{(k)} \cdot \text{Pr}_{miss}^{(k)}. \quad (3.4)$$

We consider a fixed measurement time and assume that each user measures a single spectrum band within a particular time slot. If the energy spent per user is denoted by P , the total energy consumption increases linearly with the number of users involved in sensing $P \cdot \sum_{k=1}^M N_k$, where N_k denotes the number of users measuring the k -th spectrum band.

To analyse the trade-off, we combine in a single cost function J , the weighted sum of the objectives:

$$J = (1 - a) \cdot \frac{\mathcal{R}}{\mathcal{R}_{max}} - \frac{a}{N \cdot P} \cdot \sum_{k=1}^M N_k, \quad (3.5)$$

where $\mathcal{R}_{max} = \sum_{m=1}^M \mathcal{R}_0^{(k)} \text{Pr}_0^{(k)} + \mathcal{R}_1^{(k)} \text{Pr}_1^{(k)} \text{Pr}_{out}^{(k)}$ is a normalisation constant and $a, 0 \leq a \leq 1$ is the weighting coefficient.

We employ energy detectors at the users and EGC at the FC. We identify the number of users measuring each band, $\mathbf{N} = (N_1, \dots, N_M)^T$, and the decision thresholds at the FC, $\mathbf{t} = (t_1, \dots, t_M)^T$, so that the cost function J

is maximised. At the same time, we control the generated interference at the primary system through the probability of misdetection.

$$\text{Maximise : } J. \quad (3.6i)$$

$$\text{Subject to: } \sum_{k=1}^M N_k \leq N, \quad (3.6ii)$$

$$\Pr_{false}^{(k)} \leq \Pr_{und}^{(k)} \forall k, \quad (3.6iii)$$

$$\Pr_{miss}^{(k)} \leq \Pr_{out}^{(k)} \forall k, \quad (3.6iv)$$

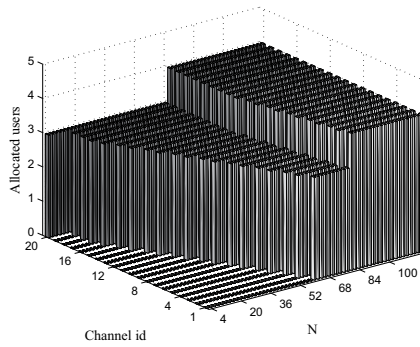
where the constraints (3.6iii) are optional and they can be used to guarantee a certain false alarm rate.

The optimization problem in equation (3.6) can also be formulated as a 0-1 multiple-choice knapsack packing (MCKP) problem. To solve it, we propose using the greedy MCKP algorithm [84, 85] along with an additional heuristic. The proposed algorithm provides near optimal solutions for small problem instances and we also use it to study energy efficient wideband spectrum sensing. We consider identical spectrum bands and investigate the impact of fading on the number of measured bands and the allocation of users.

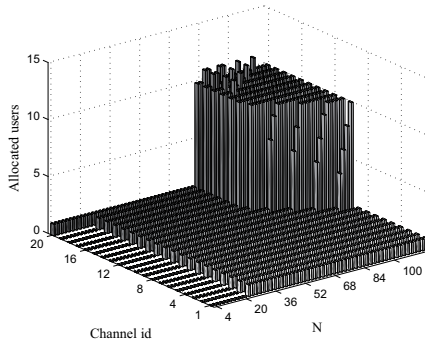
The following conclusions can be drawn based on Publication VII. If the fading can be averaged out at a single user, we will allocate the users to the spectrum bands in a round-robin fashion until the gain in detection accuracy becomes marginal (see Fig. 3.2a). When many users need to collect cooperative measurements to mitigate the fading effects, the sensing strategy is different. Initially, we will allocate one user per spectrum band to increase the chance of measuring enough available bands. We will start aggregating the users on the same band only if the cooperation gain outweighs the energy consumption in the cost function (see Fig. 3.2b).

In Publication VII, we did not consider the sensing-throughput trade-off. Actually, the sensing time and the amount of users engaged in spectrum sensing could be jointly set. For a fixed measurement time within a time slot, a greater degree of spatial diversity improves detection reliability but it also increases the communication reporting overhead. The time left for data transmission will be reduced. It turns out that it is beneficial to increase the number of cooperating users and reduce the individual measurement time for secondary throughput maximisation [86].

So far, the sensing resources have been allocated by considering the secondary throughput at the PHY as the optimization criterion. When there are multiple users competing for spectrum access, the throughput



(a) Fast fading.



(b) Slow fading.

Figure 3.2. User allocation over $M = 20$ candidate bands. The weighting parameter is $a = 0.15$. $\mathcal{K}/2 = 100$ complex samples per user, target detection SNR -12 dB, fading standard deviation 3 dB and misdetection probability target 5 %.

at the higher layers becomes a better performance measure. In a WLAN network with distributed coordination function, the saturation throughput decreases after a certain number of users compete for spectrum access [87]. The product of the saturation throughput multiplied by the probability of correctly detecting the available band has been defined as the effective secondary throughput by Chen, Yang & Zhao [88]. A single network size exists, which maximises the effective secondary throughput [88].

As a side-product of the analysis in Publication VII, we find that it may not be optimal to measure the complete bandwidth for energy efficient sensing. Similar conclusion is drawn when considering the overall energy consumption during sensing, probing and secondary transmission [89]. However, the required amount of measured bandwidth should primarily be associated with the capacity demand of the secondary service.

3.3 Optimizing the number of measured bands

Despite its importance, the relationship between the capacity requirement of the secondary service and the demand in measured spectrum has not received much attention in the existing literature. In Publication VIII, the relationship between the service demand and the sensing requirement is described as follows: if the users measure only a few spectrum bands, the sensing accuracy can be improved by using cooperative spectrum measurements, but the chance of detecting enough available bands for serving all the users will be low. On the other hand, if the measurements are distributed over many spectrum bands, then the chance of measuring enough available bands increases, but, due to the poor detection performance, the available bands can be classified as occupied and the secondary service opportunity in these bands will be lost.

The above trade-off can also be viewed from a different angle. Let us assume that a new secondary call arrives. The overall service demand increases, but the sensing performance can also be enhanced because there are more users available for sensing. In Publication VIII, we identify whether it is sufficient to rearrange the allocation of users into the existing bands and possibly decrease the measurement time, or whether we need to increase the number of measured bands to also serve the new user. The aim is to identify the rate at which the demand in measured spectrum increases with respect to the number of users requiring the service.

The optimization parameters are the user allocation over the measured bands and the measurement time. The required number of measured bands, \mathcal{M} , is minimised by placing constraints on the service blocking probability, Pr_b , the available resources (measurement time, number of users, candidate bands) and the target misdetection probability.

$$\underset{N_k, \tau}{\text{Minimise:}} \mathcal{M}. \quad (3.7\text{i})$$

$$\text{Subject to: } \text{Pr}_{un} \leq \text{Pr}_b, \quad (3.7\text{ii})$$

$$\tau \leq T, \quad (3.7\text{iii})$$

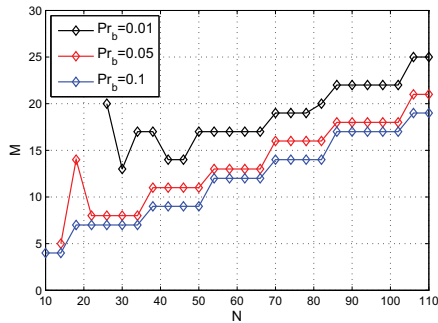
$$\sum_{k=1}^{\mathcal{M}} N_k = N, \quad (3.7\text{iv})$$

$$\mathcal{M} \leq M, \quad (3.7\text{v})$$

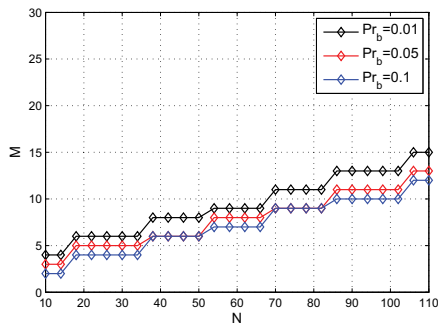
$$\text{Pr}_{miss}^{(k)} \leq \text{Pr}_{out} \forall k. \quad (3.7\text{vi})$$

For a fixed measurement time and number of measured spectrum bands, the complexity of the user allocation problem is $\mathcal{O}[C(N-1, \mathcal{M}-1)]$; this

means that it is not possible to conduct an exhaustive search at large problem instances. For a fixed number of measured bands, we use a greedy algorithm to approximate the optimal user allocation. In each iteration, the user is allocated to the band so that the blocking probability is minimised. The greedy algorithm is used to study the feasibility of low rate secondary services in the TVWS.



(a) Fraction of available spectrum bands, $Pr_0 = 50\%$.

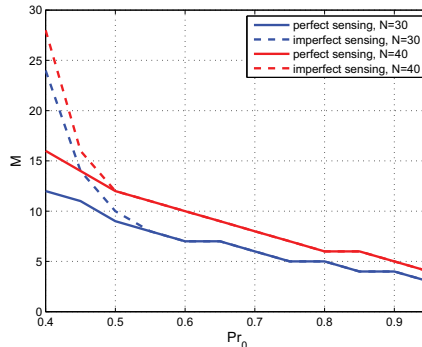


(b) Fraction of available spectrum bands, $Pr_0 = 75\%$.

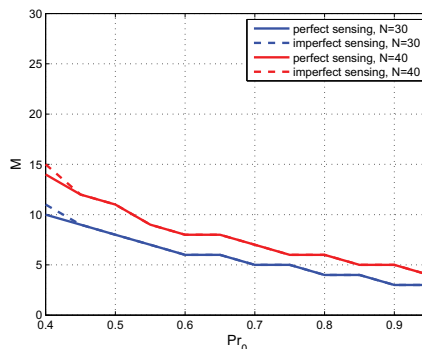
Figure 3.3. Minimum number of required measured bands, M , with respect to the number of secondary users for different secondary service blocking probability. Detection parameters are similar to the ones reported in the caption of Fig. 3.2.

In Fig. 3.3, we show the minimum required number of measured TV bands with respect to the number of users for a different service blocking probability. The number of measured bands does not increase monotonically with the number of users (see Fig. 3.3a). Due to the fading, the cooperation gain is small for a few cooperating users and it is better to distribute the measurements over multiple bands to increase the chances of measuring enough available bands. Also, for few users, a low blocking probability may not be satisfied for any combination of sensing resources. When the number of users is sufficient, it is possible to reduce the mea-

surement time for maintaining the same number of measured bands. As a general remark, the number of users utilising the spectrum grows much more quickly than the number of measured bands. Based on this fact, we can conclude that low rate services would have potential in the TV spectrum.



(a) Target blocking probability, $Pr_b = 2\%$.



(b) Target blocking probability, $Pr_b = 5\%$.

Figure 3.4. Minimum number of required measured bands, M , with respect to the fraction of available bands, Pr_0 , at the secondary system location. Detection parameters are similar to the ones reported in the caption of Fig. 3.2.

Fig. 3.4 shows the impact of spectrum availability at the location of the secondary network on the required number of measured bands. The results with no detection errors are also included to quantify the impact of fading and noise on the number of measured bands [90]. For areas with high availability, $Pr_0 \geq 0.5$, the required number of measured bands is small. At the same time, the cooperation gain for the network size being considered is sufficient to average out the fading effects. The impact of imperfect sensing is distinct in areas with a low spectrum availability, $Pr_0 < 0.5$, and with a low blocking probability target.

Min & Shin [91] have reported that the number of measured bands can decrease after the node density increases beyond a certain point. At that point, the amount of throughput gained by reducing the sensing time outweighs the corresponding amount of throughput gained by reducing the number of competing users. The secondary throughput at the PHY is the optimization objective in the study by Min & Shin [91]. However, maximising the secondary throughput does not mean that the service requirement is met.

To the best of our knowledge, Publication VIII is the first work that integrates (i) imperfect sensing at the PHY, (ii) a sensing strategy at the MAC layer, (iii) a multi-channel MAC protocol and (iv) a secondary performance evaluation higher than the PHY. The voice service has been considered as an illustrative example, but any constant rate service can be plugged into the analysis. The performance of the voice service in cognitive radio networks has also been studied using more realistic traffic models [92, 93]. However, those studies only consider a perfect sensing accuracy.

3.4 Resource allocation for a known primary traffic model

So far, it has been assumed that the state of the primary system does not change within a given time slot. When a spectrum band is detected to be idle, the primary user does not return during the data transmission time. Also, the states of the primary system between consecutive time slots were assumed to be independent. These assumptions are used when the primary traffic model is not known. They are accurate for relatively static primary systems and for short time slot durations.

For bursty types of traffic and long time slot duration the primary system may be active between two consecutive sensing intervals and the secondary user is not aware that it actually generates interference. In that case, the primary system cannot rely simply on the target misdetection probability for its protection. At the same time, the secondary performance degrades compared with the predictions made using the sensing-throughput trade-off with a static primary traffic model [68].

Various metrics have been proposed in place of misdetection probability for the primary protection. For example, the primary system may impose an upper bound on the time duration that it can tolerate the generated secondary interference no matter when the primary user appears and arrives [94]. Also, the interference ratio, which is defined as the expected

duration of the primary system's active states interrupted by secondary transmissions may be used [95, 96]. An upper bound on the packet collision probability between the primary and secondary user can also be the primary protection constraint [97, 98].

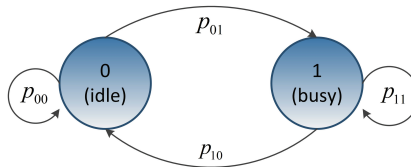


Figure 3.5. Markov channel model and state transition probabilities.

For modelling the impact of the secondary system's generated interference to the primary user, and vice versa, we need a traffic model. The access pattern of the primary system on a single spectrum band is usually modelled using a two-state random process (see Fig. 3.5) with exponentially distributed lengths. The mean durations of the ON and the OFF states are denoted by $1/\mu_{on}$ and $1/\mu_{off}$, respectively. Given the state of the primary system in the current time slot, the probability, p , of observing a particular state after time Δt can be determined from the birth-death rates [99, pp.782]:

$$p_{00}(\Delta t) = \frac{\mu_{on}}{\mu_{on} + \mu_{off}} + \frac{\mu_{off}}{\mu_{on} + \mu_{off}} \cdot \exp(-(\mu_{on} + \mu_{off}) \cdot \Delta t) \quad (3.8i)$$

$$p_{11}(\Delta t) = \frac{\mu_{off}}{\mu_{on} + \mu_{off}} + \frac{\mu_{on}}{\mu_{on} + \mu_{off}} \cdot \exp(-(\mu_{on} + \mu_{off}) \cdot \Delta t) \quad (3.8ii)$$

$$p_{01}(\Delta t) = 1 - p_{00}(\Delta t), \quad p_{10}(\Delta t) = 1 - p_{11}(\Delta t). \quad (3.8iii)$$

As a result, the probability of remaining at the same state in the next time slot can be approximated as $p_{00} \approx 1 - \mu_{off}$ and $p_{11} = 1 - \mu_{on}$. The prior probabilities, Pr_0 and Pr_1 , used for the analysis of secondary systems that are not aware of the primary traffic model can be viewed as the probabilities of observing an idle and busy state, respectively, at any given time instant. They are the fractions of time that the primary system is idle and busy:

$$\text{Pr}_0 = \frac{\mu_{on}}{\mu_{on} + \mu_{off}} \quad (3.9i)$$

$$\text{Pr}_1 = 1 - \text{Pr}_0. \quad (3.9ii)$$

Next, we discuss how the primary user traffic impacts the allocation of sensing resources.

3.4.1 Sensing time and time slot optimization

Unlike unaware secondary systems, where the time slot duration is fixed and the sensing time is optimized, aware secondary systems usually fix the sensing time and optimize the slot duration [96, 97]. The reason for this is that the primary protection depends not only on the quality of the sensing outcome, but also on the primary/secondary collision probability, interference ratio, and so forth. A long time slot increases the transmission time, $T - \tau$, and subsequently the secondary throughput, but unfortunately it increases the collision probability as well [97, 98]. As a general rule of thumb, the slot duration should be less than the average busy and idle times [96].

While it is obvious that high traffic intensity deteriorates the secondary performance, the impact of the primary signal level at the location of the secondary user is not straightforward. If the expected secondary throughput is dominated by the achievable throughput during the primary OFF times, a high signal level will reduce the false alarm rate and favour the secondary system. On the other hand, for high traffic intensity it is beneficial for secondary users to experience a low primary signal level [100].

The sensing-throughput trade-off for aware secondary users becomes more challenging when there are multiple channels with different occupancy statistics. With proactive sensing, the user periodically measures the channels based on the optimal sensing times and time slot durations. The time slot durations maximising the sum throughput are, in general, different for the different channels. Actually, they are also coupled since some of the transmission opportunity for a given channel is lost as a result of sensing some other channel [101].

With reactive sensing, the user has to vacate the channel and perform a channel search as soon as the primary transmitter returns. The relation between the channel search time and the sensing time within a given time slot becomes critical. If the channel search time is set higher than its optimal value, the sensing time within the time slot must increase to minimise false alarms and avoid an unnecessary channel search [102].

3.4.2 Exploration-exploitation trade-off

Let us consider two i.i.d. channels with state transition probabilities of $p_{00} \gg p_{01}, p_{11} \gg p_{10}$ and a user that can sense one channel within a given time slot. We are assuming that there is a perfect sensing accuracy

and that one channel is detected being idle in the first time slot. In the next time slot, the user will transmit with a high degree of probability if it stays on the same channel. If the user switches the channel, it has the opportunity to learn about the state of the other channel, too. Since $p_{00} \gg p_{01}$ and $p_{11} \gg p_{10}$, the user will be able to predict the future state of both channels with a high degree of probability and its reward over some finite time horizon will potentially increase.

The user should select its channel sensing policy to balance the trade-off between an immediate reward and an expected future reward. This is also known as exploitation-exploration trade-off. Mind the difference between the exploration-exploitation trade-off that determines the sensing order between the different time slots and the optimal stopping rule [75] that determines the channel sensing order within a given time slot.

The secondary user explores the spectrum measurements within a given time slot to gain some sort of knowledge about the channel state in the future time slots. The user's knowledge of the primary system state at the beginning of the n -th time slot is summarised on the belief vector, $\Omega(n)$. For independent channels, the belief vector is degenerated to match the user's belief about the availability of each channel:

$$\Omega(n) = [\omega_1(n), \omega_2(n), \dots, \omega_M(n)]. \quad (3.10)$$

A sensing policy maps the belief vector, $\Omega(n)$, onto a channel measured in the n -th time slot so that the secondary throughput over a finite time horizon can be maximised. Deriving the optimal sensing policy has an exponential level of complexity, and because of that, myopic sensing policies have recently become more popular. A myopic policy ignores the impact of the user's action on the future reward and maximises only the immediate reward. According to the myopic strategy, the user measures the channel k^* maximising the conditional throughput:

$$k^*(n) = \max_k \left\{ \mathcal{R}_0^{(k)} \cdot \left(\omega_k(n) p_{00}^{(k)} + (1 - \omega_k(n)) p_{10}^{(k)} \right) \right\}. \quad (3.11)$$

At the end of each slot, the belief vector has to be updated based on the sensing outcome and the user knowledge about the primary traffic model:

$$\omega_k(n+1) = \begin{cases} 1 & k\text{th band detected busy} \\ 0 & k\text{th band detected idle} \\ \omega_k(n) p_{00}^{(k)} + (1 - \omega_k(n)) p_{10}^{(k)} & k\text{th band not measured.} \end{cases} \quad (3.12)$$

The myopic policy is optimal for $M = 2$ i.i.d. channels [103] and can be implemented by using the following simple rule: the user does not switch

channels when the channel in the current slot is busy. Otherwise, the user performs a channel switch. For $M > 2$ channels, the myopic sensing is optimal only if $p_{00} > p_{10}$ [104].

In the presence of sensing errors, the sensing strategy can be separated from the design of the spectrum sensing threshold and spectrum access strategy without losing optimality [105]. This is referred to as the separation principle. The optimal sensor maximises its throughput by always trusting the sensing outcome and setting its decision threshold at the maximum permitted misdetection probability [105]. The sensing time can be set by using the regular sensing-throughput trade-off [68]. After determining the sensing time and the decision threshold, the optimal sensing strategy can be approximated by using myopic sensing policies. The myopic policy for imperfect sensing depends also on the false alarm corresponding to the misdetection probability target [106]. The separation principle also holds true in cases when the user can sense and access multiple channels in a given time slot [107].

3.5 Discussion

The most naive MAC layer sensing schemes would force each user to measure the complete candidate bandwidth and assume a fixed spectrum measurement time. That would require extending single band detection algorithms to include multiband spectrum sensing [108]. In this chapter, we discussed MAC layer sensing schemes that make it possible to use the available sensing resources to optimize the secondary performance and protect the primary system.

We proposed classifying MAC layer sensing protocols based on whether the primary traffic pattern is available at the secondary users or not. This type of classification makes it possible to determine the secondary time slot structure and the metric used to protect the primary system. Also, it helps determine whether the spectrum measurements in different time slots should be considered independent or whether they can be used to predict the idle/busy periods of the primary system in future time slots.

There are two issues related to MAC layer sensing that have not been addressed. The first one has to do with the signalling overhead required to share the measurement information, while the second one has to do with controlling the amount of aggregate interference due to multiple users simultaneously accessing the spectrum. The first problem can be miti-

gated by developing efficient protocols for reporting the sensing information (see, for instance, the studies by Cormio & Chowdhury [109] and Li, Petrova & Mähönen [110] for time-slotted and contention-based reporting protocols, respectively).

The sensing-based control of aggregate interference is still an ongoing problem. According to the current standardisation rules in Europe, secondary spectrum access cannot be based solely on spectrum sensing. In the US, sensing-based spectrum access is allowed only for low-power secondary devices. A centralized entity, also referred to as a geolocation database, which is possibly assisted by distributed spectrum measurements, should be responsible for granting spectrum access requests. Geolocation-controlled secondary spectrum access is the content of the next chapter.

4. Database-based spectrum access

With sensing-based spectrum access, the users decide whether the spectrum is available in an autonomous manner. Due to the hidden node problem, the detection thresholds must be set low enough to protect the primary service. This reduces the amount of recovered spectrum [111] and the economic viability of services based on secondary spectrum access.

At least for secondary spectrum access in TVWS, the standardisation bodies in the US, UK and Europe have already concluded that a centralized approach should be the way forward for commercially feasible secondary services [112, 113, 114]. Based on this conclusion, secondary users are not required to engage in spectrum sensing tasks. Instead, they provide a location estimate to a central entity, often termed a geolocation database. The geolocation database is in charge of handling the spectrum access requests and assigning spectrum to the users.

The protection requirements of TV services are different in different parts of the world. Also, different countries have different regulatory rules for radio devices. In Europe, the device manufacturer is responsible for certifying the equipment, while in the US all radio devices must be certified by the regulator. For these reasons, the secondary spectrum access rules are likely to be different in different countries [115]. For secondary spectrum access using geolocation, the regulatory rules determine the nature of the information provided to the database and returned to the secondary device.

4.1 Information provided to the database and returned to the secondary device

A geolocation database can be broadly understood as a translation mechanism between the primary and the secondary spectrum users [116]. Ini-

tially, the primary spectrum users must be registered in the database. This may include (i) registering how the primary systems perform in the absence of secondary operation as well as (ii) how much generated secondary interference they can tolerate. The secondary users query the database using some other means than the primary spectrum (e.g. the internet or pilot control channels), in order to provide their location estimate, device type and model to the database. The database is responsible for combining the inputs received by the primary system and the secondary users and returning a set of available spectrum bands, if any, along with the permitted transmit power levels (see also Fig. 4.1).

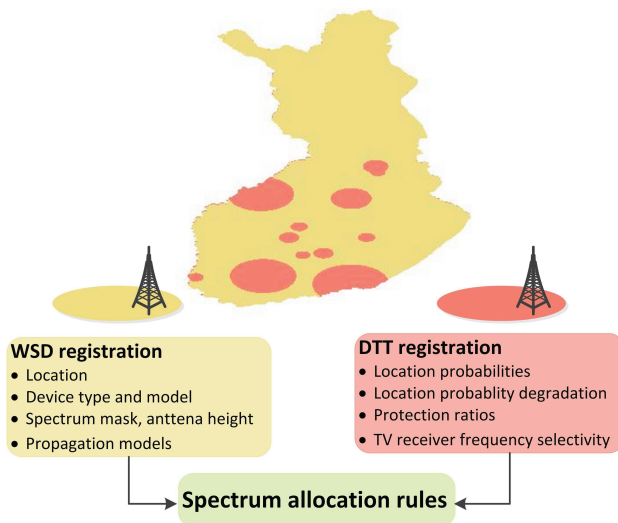


Figure 4.1. Digital terrestrial television (DTT) coverage in Finland for channel 30 along with the required information provided to the geolocation database by the DTT system and the white space device (WSD) according to the ECC rule.

Another key issue when implementing geolocation has to do with how frequently the licensed spectrum use is updated. In the TVWS, the location and the activity pattern of TV broadcasters remain relatively static. Also, the deployment of Programme Making and Special Events (PMSE) is usually planned in advance, and thus, the location and activity of PMSE can also be registered in advance in the database [113]. The channel validity for PMSE is supposed to be checked on an hourly basis [113].

The nature of the information communicated to the database can be different for different regulation rules. For example, the FCC defines fixed transmit power levels for different classes of secondary devices. Also, it defines protection areas around the primary receivers where a secondary operation is prohibited. According to the FCC, a channel is available at

a particular location if that location falls outside the protection areas of the considered channel and its two first adjacent channels [114]. As a result, TV broadcasters in the US can simply register coverage contours in the database. The ECC in Europe and the Office of Communications (OFCOM) in UK follow a more liberal approach, which allows the secondary transmit power to vary based on the device location [112, 117]. The allocated power must not degrade the TV location probability beyond a certain percentage. The TV system may register in the database the location probability across the entire country or over a subset of pixels (test points) more susceptible to the generated secondary interference (see Fig. 4.2).

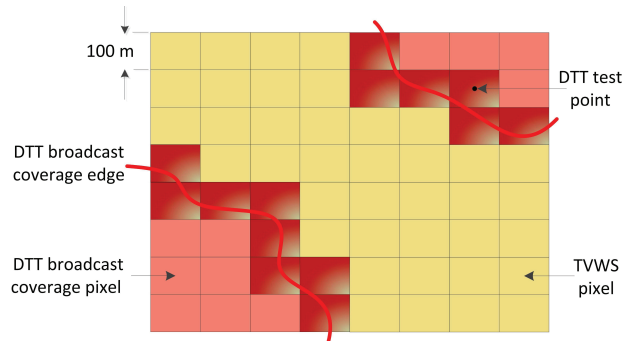


Figure 4.2. Quantisation of the spatial domain and DTT test points where the secondary interference must be controlled.

In Chapter 6, we propose power allocation algorithms for multiple secondary devices in TVWS. Our approach uses a location probability constraint for the TV system at a particular signal-to-interference-and-noise ratio (SINR) target [118, pp.279]. In this sense, our method lies closer to the proposals made by the ECC and OFCOM rather than those made by the FCC. Next, the existing regulatory rules proposed by the ECC are briefly reviewed while a review of world-wide trends in secondary spectrum access in TVWS can be found in a study by Nekovee, Irnich & Karlsson [20].

4.2 Regulatory rules for secondary access in TVWS in Europe

Due to the impact of slow fading, the TV field strength inside each pixel is probabilistic. The location probability is a metric used to assess the quality of the TV reception. It describes the percentage of locations within a square pixel with a 100 m long side where the ratio of the useful TV field strength to the power sum of noise and unwanted interference ex-

ceeds some target value. Let us denote by q_1 the location probability in the presence of TV self-interference and noise. In the presence of secondary transmissions, the location probability is reduced to q_2 . A natural parameter for quantifying the impact of a secondary operation on TV performance is the degradation in location probability $q_1 - q_2$. A typical value is 1%.

The spectrum allocation rule proposed by the ECC precludes secondary spectrum utilisation inside the TV co-channel service area. Outside of the service area, the transmit power level depends on the distance to the nearest pixel belonging to the service area of a co-channel. The operation inside the service area of adjacent TV channels has been approved by the ECC. In that case, the TV receivers and the secondary transmitter can be located inside the same pixel. In order to overcome the location uncertainty, reference coexisting geometries are commonly utilised (see Section 4.2.2).

4.2.1 Power allocation in the co-channel

Let us consider a single secondary transmitter outside of the TV service area. Let us also ignore the TV self-interference and the noise. According to the ECC rule, the allocated transmit power level, P_t , is [119, p.33][120]:

$$P_{t(dB)} = \mu_{TV(dB)} - \mu_{g(dB)} - \gamma_{D/U} - x_q \cdot \sqrt{\sigma_{TV}^2 + \sigma_{SU}^2} - \mathcal{M}\mathcal{I} - \mathcal{S}\mathcal{M}, \quad (4.1)$$

where $\mu_{TV(dB)}$ and σ_{TV} are the mean and standard deviation of the TV signal in dB, σ_{SU} is the standard deviation of the secondary signal in dB, $\mu_{g(dB)}$ is the distance-based pathloss, $\gamma_{D/U}$ is the co-channel protection ratio, x_q is the Gaussian confidence factor, $x_q = Q^{-1}\left(1 - \frac{q_2}{q_1}\right)$, $\mathcal{M}\mathcal{I}$ is a margin used to account for multiple simultaneous secondary transmissions and $\mathcal{S}\mathcal{M}$ is a safety margin incorporating various factors missing from equation (4.1) such as antenna discrimination, gain, and polarization.

Equation (4.1) must be evaluated for all TV test points and the minimum value must then be selected. While the power allocation is straightforward for single transmitter, it becomes more complicated for multiple users transmitting simultaneously. Due to the aggregate interference, the allocated power levels at different locations are coupled. There are multiple combinations of power levels that satisfy the location probability constraint. The ECC has suggested values for the protection margins $\mathcal{M}\mathcal{I}$ and $\mathcal{S}\mathcal{M}$ [112]. Recently, researchers have also proposed evaluating the multiple interference margin based on the number of active transmitters,

$$\mathcal{M}I = 10 \log_{10} N \text{ [119].}$$

One has to keep in mind the following trade-off while setting protection margins. Low margins may result in an unacceptably high transmit power, thus violating the TV performance beyond acceptable limits [121]. After a certain point, higher power levels may not even bring considerable capacity gains in the secondary system due to self-interference. On the other hand, high protection margins may result in less transmit power, thereby requiring secondary network densification for performance enhancement. The regulatory rule should strike a balance between the economic viability of secondary deployment and DTT performance degradation [116].

4.2.2 Power allocation in the adjacent channel

When the secondary transmitter is located outside of the adjacent channel TV service area, the secondary transmit power can be computed in the same way as for the co-channel. Since the protection ratio, $\gamma_{D/U}$, decreases with increasing frequency separation, the permitted power level is expected to be higher in comparison with the co-channel. Computing the transmit power level becomes trickier in cases when the secondary user lies inside the service area of an adjacent DTT channel.

Due to the fact that the precise location of the TV receivers within a pixel is not known, the ECC has suggested using some coexisting reference geometries [112, 119]. There are in total twelve reference coexisting geometries based on the type of secondary user (e.g. fixed or mobile), its height and also on the TV reception mode (e.g. fixed roof-top or portable). One may refer to the ECC report [119, pp.63-71] for the related illustrations. The reference geometry essentially determines the value of the distance-based pathloss term, μ_g , and of the standard deviation, σ_{SU} , in equation (4.1).

The reference geometries proposed by the ECC reflect a worst-case coexistence scenario. The distance separation between the victim TV receiver and the secondary transmitter is set at a conservative level and the permitted transmit power level is underestimated. The reference geometry approach becomes overpessimistic particularly in areas with a low user density [122]. Relaxing the reference geometry rule is a practical method for increasing the cellular capacity in TVWS, at least in rural areas [123].

The protection ratios, $\gamma_{D/U}$, depend on the emission characteristics of the secondary user and the adjacent channel frequency selectivity of the

TV receiver. Digital Video Broadcasting-Terrestrial (DVB-T) performance measurements under secondary interference show that the first eighteen adjacent channels must be considered while setting the transmit power level [124]. This means that at most locations, the allocated power level will be dominated by the adjacent channels.

4.3 Discussion

The transition from analog to digital TV is not harmonised around the world. This has an impact on the pace of development of regulatory rules for secondary spectrum access in the TVWS. Currently, only the FCC has authorised commercial entities (Telcordia in March 2012 and Spectrum Bridge in December 2011) to provide TVWS geolocation database administration.

Geolocation databases will change our view of regulatory rules [125]. So far, a radio device must be recertified to comply with a change in the regulations. With geolocation databases, the certification process will move from the devices to the databases. Not only is it more convenient to certify databases than radio devices, but it also allows for adaptive spectrum access rules. It is expected that there will be different regulatory rules at different locations and times and more frequent updates when the rules do not perform as expected.

In principle, geolocation-based secondary spectrum access makes it possible to pack the secondary transmitters more tightly than with the sensing-based method without violating the TV protection limits. However, even though geolocation databases do not suffer from the uncertainties inherent in spectrum sensing algorithms, they may suffer from errors in propagation pathloss modelling. Actually, the pathloss models used in the database must be approved by the regulator and, ideally, they should be different at different locations to capture the impact of terrain irregularities (see Publication V). Only with accurate propagation models will the database be able to uncover most of the available TVWS without harming the TV system [126].

There are still many unsolved issues pertaining to geolocation database operations. In order to enforce good service standards, it is expected that multiple commercial entities will begin to offer geolocation database functionality [116]. In this case, it is important to arrange the control of aggregate interference towards the TV system. There should be low-complex

methods that make it possible for multiple databases to talk to each other and to jointly decide on secondary spectrum usage (see Publication I).

The current power allocation rules proposed by the ECC and FCC fail to protect TV receivers in all cases because the impact of aggregate interference is not appropriately considered [127, 121]. We need interference models tailored to the primary-secondary system setup. In Chapter 5, we discuss secondary interference models. In Chapter 6, we propose secondary power allocation algorithms without violating the TV protection criteria.

5. Secondary interference models

Aggregate interference models were first developed to describe the performance of cellular systems. Motivated by the Central Limit Theorem, the aggregate interference power in the presence of multiple co-channel interferers had initially been modelled using a Gaussian random variable (RV) [128]. The Gaussian model enjoys analytical tractability, but it is valid only in the absence of dominant interference sources. For instances when the interference deviates from the Gaussian model, stable distributions have been proposed for more accurate performance analysis [129].

With the development of wireless ad hoc networks, the field of interference modelling has evolved to account for the impact of random users' locations, routing and medium access schemes on the generated interference [130]. Elements from the fields of stochastic geometry and spatial statistics [131] have been used to develop probabilistic models for the locations of active transmitters [132].

In this chapter, we do not discuss the statistics of the aggregate interference amplitude (see, for instance, the study by Win, Pinto & Shepp [133]). On the one hand, the amplitude statistics depend on the waveforms that have been employed, which limits the analysis to particular systems. On the other hand, in wireless packet networks the probability of successfully decoding a packet is commonly expressed as a function of the SINR. In order to evaluate the statistics of the SINR, we need a model for the useful signal distribution as well as for the interference power distribution.

The interference power, I_t , at a particular location and time can be broadly written as the sum of the received power levels from the individual interferers

$$I_t = \sum_{k=1}^N \nu_k \cdot P_{tk} \cdot G_k, \quad (5.1)$$

where N is the potential number of interfering sources, ν_k is a binary variable describing whether the k -th interferer is active or not, G_k is the

propagation pathloss and P_{tk} is the transmit power level.

The nature of the components, deterministic vs. probabilistic, also determines the nature of the interference. For example, the propagation pathloss depends on the locations of the interferers, which might be either arbitrary or probabilistic.

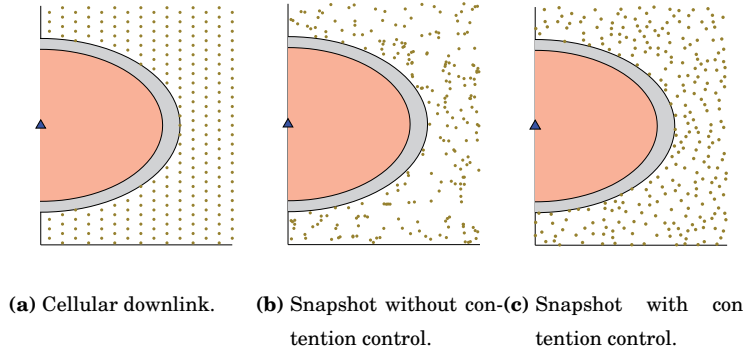


Figure 5.1. Cellular downlink, PPP realisation and Matern type II realisation, all with an equal density of transmitters deployed in the TVWS.

The secondary spectrum access imposes new challenges for interference modelling. The existing interference models are not directly applicable in a primary-secondary system setup. The main reason for this is the existence of borders and protection regions between the two systems.

Two main candidates for secondary spectrum access are the cellular and the WLAN type of systems [134]. These two systems can be distinguished on the basis of the transmitters' locations, i.e. the random locations in a WLAN system vs. the deterministic locations in a cellular downlink system. Snapshots of transmitters' locations for different types of secondary networks are illustrated in Fig. 5.1. In this chapter, we discuss aggregate interference models for secondary networks with fixed locations and random locations and outline how the existence of protection regions impacts the interference modelling.

5.1 Interferers with fixed locations

When the locations of secondary transmitters are fixed and known, there is only randomness at the interference level due to the propagation pathloss. According to equation (5.1), modelling the aggregate interference at the primary receiver degenerates to the point of modelling of the sum of RVs

used to model the fading from each secondary transmitter. For static networks, the effects of small-scale fading can be averaged out and slow fading dominates the generated interference level. Due to the fact that the slow fading is usually modelled by a log-normal RV, modelling the distribution of the sum of log-normal RVs has received considerable attention in relation to geolocation-based secondary spectrum access. The moment-generating function (MGF) of the log-normal distribution does not exist on the positive half axis and so approximations have been widely employed.

Many methods have been proposed for approximating the sum of log-normal RVs using another log-normal RV model. Their difference lies in the way the parameters of the approximating distribution are computed. According to the Fenton-Wilkinson (F-W) method, the first two moments of the sum are matched to the moments of a log-normal RV in the linear domain [135]. The degree of complexity for solving the resulting system of equations is low because the moments of a log-normal RV involve simple expressions.

The Schwartz-Yeh (S-Y) method applies the method of moments to the log-domain [136]. For more than two RVs, the S-Y method needs iterations to converge; as a result, the method becomes more complex. Other approximating methods may involve cumulant matching [137], higher order matching [138] and a Gauss-Hermite approximation of the MGF integral [139].

It is generally acknowledged that the S-Y method achieves better accuracy than the F-W method at the cost of higher implementation complexity. The F-W method degrades as a result of decreasing the mean spread and increasing the standard deviation spread among the RVs [140]. However, it does a better job of tracking the upper tail of the distribution than the S-Y method [137]. Simulations in a primary-secondary system setup illustrate that the F-W method actually tends to slightly overestimate the upper tail [141]. Similarly by using the F-W method for modelling the aggregate secondary interference, the SINR at the primary receiver is underestimated.

In order to model the secondary interference by applying the F-W method, one has to start by computing the first two moments of the aggregate interference. As discussed in Publication IV, the moments of the aggregate interference depend on the fading correlation. To begin with, we consider equal transmit power levels, $P_{tk} = P_t \forall k$, and i.i.d. fading samples [142,

pp.74]:

$$E\{I_C\} = P_t \cdot E\{x\} \cdot \sum_{k=1}^N g_k \quad (5.2)$$

$$E\{I_C^2\} = P_t^2 \cdot \left(E\{x^2\} - E\{x\}^2 \right) \cdot \sum_{k=1}^N g_k^2 + E\{I_C\}^2. \quad (5.3)$$

The summations in the above equations can be approximated by integrals over the secondary deployment area, A :

$$\sum_k g_k = \frac{1}{A_f} \cdot \int_A g_a da, \quad (5.4)$$

where A_f is the area, or footprint, occupied by a single transmitter. No other transmitter can be active inside that area. For the downlink of a cellular system, the footprint becomes equal to the cell size.

The ratio of transmit power, P_t , divided by the footprint, A_f , is the spatial power density, $P_d = P_t/A_f$. For a constant power density over area A , equations (5.2) and (5.3) can be read as follows [142]:

$$E\{I_C\} = P_d \cdot E\{x\} \cdot \int_A g_a da \quad (5.5)$$

$$E\{I_C^2\} = P_d^2 \cdot \left(E\{x^2\} - E\{x\}^2 \right) \cdot A_f \cdot \int_A g_a^2 da + E\{I_C\}^2 \quad (5.6)$$

where g_a is the distance-based propagation pathloss from the integration element of area A to the primary receiver.

Let us consider a power law propagation pathloss model, $g_a \propto r^{-n}$, with n being the pathloss exponent, and a secondary deployment in the infinite plane, $A = (r, \phi) : r \geq R_n, 0 \leq \phi \leq 2\pi$. After carrying out the integration in equation (5.5), it is possible to show that the mean interference at the origin behaves like the interference generated by a single transmitter located at the protection area boundary, $r = R_n$, with a pathloss exponent increased by two $g_a \propto R_n^{-n+2}$ [24, 143]. Based on this remark, one can bound the generated interference at the primary receiver by using a simple expression. However, the integral approximation in equation (5.5) is valid only if the distance between neighbouring interferers is much smaller than the protection distance, R_n [144]. The accuracy of the integral approximations in equations (5.5) and (5.6) is also studied in Publication IV.

The F-W method is a convenient method for identifying the size of the dominant interference region. Counterintuitively, it is not possible to accurately estimate the interference distribution with only a few secondary tiers [145]. The dominant interference region depends on the pathloss exponent and the protection distance [146]. For the pathloss exponent

$n = 3.6$ and an interference region ten times the protection distance, the relative error in the mean becomes less than 3%. Similar results without fading have been reported by Shankar & Cordeiro [147].

5.2 Interferers with random locations

In WLAN type networks, the locations of the active users can often change. The users can be mobile while their activity depends on the traffic and the MAC scheme that are offered. For large networks, the communication signalling overhead for updating the locations of transmitters in the spectrum allocation database will be high. A promising alternative for evaluating their aggregate interference to the primary system with low complexity is to model their locations in a probabilistic manner.

The locations of transmitters in wireless networks with random access are usually modelled using the Poisson point process (PPP) model. A PPP model is characterised by its density, λ_p , which describes the average number of active users in the unit area. The PPP density depends on the user density and the activity factor. According to the PPP model, the number of transmitters at any time instant is drawn from a Poisson RV with a mean that is equal to the PPP density. The locations of the transmitters are modelled using the uniform distribution inside the deployment area A .

For a PPP model the characteristic function (CF) of the aggregate interference can be computed by applying Campell's theorem [148, pp.28]. If the interferers are scattered in the infinite plane and no exclusion region around the primary receiver exists, the CF of the generated interference corresponds to the CF of a skewed-stable RV [133]. The inverse Fourier transform of the CF can be expressed in a closed-form only for a pathloss exponent equal to 4 and it belongs to the family of Lévy distributions [133].

The aggregate interference from the infinite plane can be used to bound the amount of self-interference within a network. In a primary-secondary system setup, there are exclusion areas around every primary receiver. That can make the spatial distribution of interferers non-symmetric.

For finite deployment areas and non-symmetric spatial interference patterns, the CF of the aggregate interference can have a complex form [149]. The standard method for obtaining the PDF of aggregate interference is to integrate numerically the Fourier inverse integral of the CF. Other

alternatives may involve Edgeworth expansion, moment-matching techniques [138, 150] and the heavy-tail approximation theory [151]. Moment-matching is probably the least complex method for modelling aggregate interference but a researcher needs to identify a suitable distribution.

In the absence of fading, the distribution of aggregate interference resembles a Gaussian distribution when the number of dominant interferers is high. This is the case when there are a large number of transmitters and a large exclusion area around the primary receiver [152]. Otherwise, there are few dominant interferers and the interference distribution becomes heavy-tailed. The log-normal distribution [153], or the distribution due to the closest active interferer [154], can provide a better fit.

Fading increases the variance and prolongs the tails of interference distribution [144]. Under log-normal fading, the divergence from the Gaussian model can be high [152]. The log-normal distribution [155], the gamma [156] or the truncated-stable distribution [157] could be used instead. With a suitable distribution at hand, the moments of the aggregate interference still need to be evaluated.

The independence property of the PPP model makes it easier to compute the MGF of the aggregate interference [158]. The conditional MGF is equal to the MGF from one transmitter to the power of the active transmitters. The MGF can be derived by averaging the conditional MGF over the Poisson PDF. The first two moments of the aggregate interference in the linear domain due to a PPP of intensity λ_p are as follows [142, pp.73]:

$$E\{I_P\} = \lambda_p \cdot P_t \cdot E\{x\} \cdot \int_A g_a da \quad (5.7)$$

$$E\{I_P^2\} = \lambda_p \cdot P_t^2 \cdot E\{x^2\} \cdot \int_A g_a^2 da + E\{I_P\}^2. \quad (5.8)$$

After replacing $\lambda_p = N/A$ and $P_t = P_d A_f$ in equation (5.7), one may notice that the mean interference from a PPP becomes equal to the integral representation of the mean interference in equation (5.5). The mean interference levels from a PPP and from a cellular system's downlink are equal if the power density emitted from area A remains the same. On the other hand, the variance in the aggregate interference from a PPP is higher due to the randomness in the locations of the transmitters.

The PPP model may not be accurate when the number of transmitters is small [159]. Conditioned on the number of transmitters, the PPP degenerates to a Binomial Point Process (BPP). Following same approach used in [142, pp.73], the first two moments for a BPP with N users deployed

over finite area A are as follows:

$$E\{I_B\} = \frac{N}{A} \cdot P_t \cdot E\{x\} \cdot \int_A g_a da \quad (5.9)$$

$$E\{I_B^2\} = \frac{N}{A} \cdot P_t^2 \cdot E\{x^2\} \cdot \int_A g_a^2 da + \frac{N-1}{N} \cdot E\{I_B\}^2. \quad (5.10)$$

One can see that if the number of users, N , and the area size, A , increase such that the ratio $\lambda_p = N/A$ remains constant, the moments for the BPP are equivalent to the moments of the PPP.

5.2.1 Interferers with contention control

The PPP model is a convenient tool for assessing the impact of secondary transmissions on primary receivers because the moments of the interference can easily be computed, and in some special cases, the PDF of the aggregate interference is also available [133]. However, the assumptions adopted in the PPP model are valid only for wireless networks employing an ALOHA type of MAC [160].

It is well known that the spatial spectrum reuse can be enhanced by prohibiting users located close to one another from transmitting at the same time [161]. When the secondary MAC protocol employs some minimum separation distance between the transmitters, it is possible to utilise the hardcore point processes [132] for modelling the locations of the active transmitters. The Matern type I and type II processes and the simple sequential inhibition process are typical examples of hardcore processes [153].

According to Slivnyak's theorem, the Palm distribution of a PPP coincides with the distribution of the original PPP [158, pp.41]. This is not the case for a hardcore point process. As a result, the aggregate interference at a particular node of the process and the aggregate interference at an arbitrary point on the plane should be computed using different methods. The self-interference in hardcore wireless networks is computed by using Palm distribution and moment measures [160, pp.199] (see, for instance, the study by Haenggi [162] for the mean interference calculation). On the other hand, some elements from the theory of coverage processes can be borrowed to assess the impact of secondary transmissions on the primary receivers [163].

The Matern type II process associates each transmitter with a random mark. A transmitter is inhibited if there is another transmitter with a lower mark inside a circle with a radius equal to the hardcore distance, δ . The hardcore distance can be viewed as the carrier sensing range in

a wireless network employing Carrier sensing multiple access with collision avoidance (CSMA/CA), while the random mark essentially models the selected backoff window size. Due to its similarity to CSMA/CA, a Matern type II process is commonly employed to model the locations of active transmitters in wireless networks with contention control.

A common practice for computing the aggregate interference at an arbitrary point on the plane is to approximate the Matern process by using a homogeneous equi-dense PPP [164]. For parent density, λ_p , the density of the Matern type II process is as follows [158, pp.164]:

$$\lambda_m = \frac{1 - \exp(-\lambda_p \pi \delta^2)}{\pi \delta^2}. \quad (5.11)$$

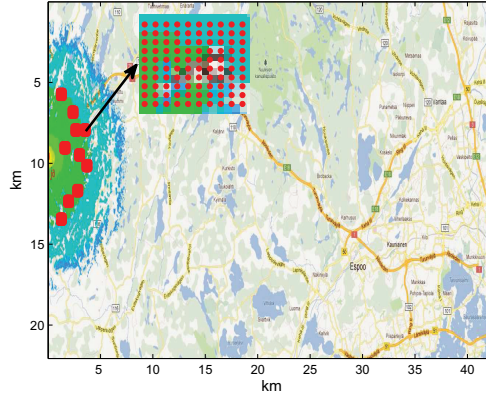
By using the PPP approximation method, the moments of the aggregate interference from a Matern process are computed after replacing λ_p with λ_m in equations (5.7) and (5.8). Unfortunately, this approximation is accurate only for small hardcore distances and low parent densities. The mean interference from a Matern type II process is higher than the mean interference from the equidense PPP due to the existence of borders [164]. Designing the carrier sensing range based on the PPP approximation will violate the protection of the primary receivers. One way to overcome this issue is to bound the mean interference by using a multi-tier PPP [165].

5.3 Impact of terrain morphology on generated interference

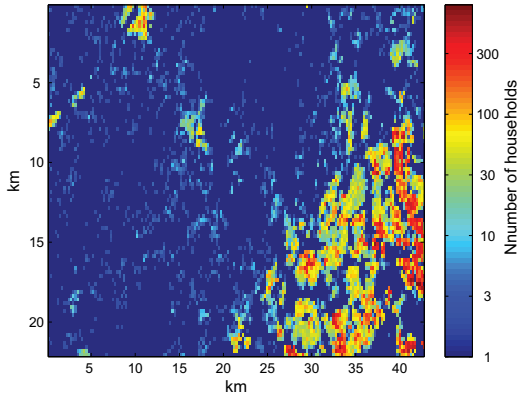
Thus far, it has been assumed that the distance-based pathloss, g_a , from the secondary area to the primary receivers is available. Also, all the transmissions originating from the area, A , are characterised by the same slow fading distribution. These assumptions can be problematic. The irregular terrain morphology may give rise to unequal fading distributions for transmitters located far from each other. Also, the storage requirement in the database can be compromised if a model is used to calculate the pathloss instead of maintaining the values, g_a .

In Publication V, we propose to divide the secondary area into multiple disjoint areas, A_j , and use different parameters to describe the propagation pathloss for each area, $G_j = c_j r^{-n_j} x_j$, where c_j, n_j and x_j are specific to area A_j . In order to estimate the parameters of the pathloss model, we equate the first two moments of the aggregate interference by using the pathloss model, G_j , and also based on the actual pathloss values \mathcal{G} . The actual pathloss values are obtained from the irregular terrain channel

model (ITM) along with the terrain elevation data [166], but they could also have been obtained based on the measurements. When the pathloss model is used, the aggregate interference is approximated using the log-normal distribution.



(a) Terrain and TV coverage area.



(b) Density of households.

Figure 5.2. The system setup used for the modelling. Real terrain and user density maps from Helsinki area.

After matching the first two moments of aggregate interference, we obtain the following system of equations:

$$c_j \cdot e^{\frac{\sigma_j^2}{2\xi^2}} \sum_k r_{km}^{-n} = \frac{1}{L_p} \sum_k \sum_\ell \mathcal{G}_{km\ell} \quad (5.12)$$

$$c_j^2 \cdot e^{\frac{\sigma_j^2}{\xi^2}} \cdot (e^{\frac{\sigma_j^2}{\xi^2}} - 1) \cdot \sum_k r_{km}^{-2n} = \frac{1}{L_p} \sum_\ell \sum_{k_1} \sum_{k_2} \mathcal{G}_{k_1 m \ell} \mathcal{G}_{k_2 m \ell} - \left(\frac{1}{L_p} \sum_k \sum_\ell \mathcal{G}_{km\ell} \right)^2, \quad (5.13)$$

where $\xi = 10/\log(10)$ is a scaling constant, the indexes k, k_1 and k_2 span all pixels belonging to the area, A_j , L_p is the number of test points used to model the slow fading and \mathcal{G}_{km_ℓ} represents the pathloss when using terrain-based propagation between the k -th pixel and the m_ℓ -th primary test point (see Fig. 5.2a).

Since there are three unknown parameters and only two equations, we decided to fix the value for the pathloss attenuation exponent, $n_j = n$. In order to compute the slow fading standard deviation, σ_j , we square equation (5.12) and divide it by using equation (5.13):

$$\sigma_j^2 = \xi^2 \log \left(1 + \frac{\left(\sum_k r_{km}^{-n} \right)^2}{\sum_k r_{km}^{-2n}} \left(L_p \frac{\sum_\ell \sum_{k_1} \sum_{k_2} \mathcal{G}_{k_1 m_\ell} \mathcal{G}_{k_2 m_\ell}}{\left(\sum_\ell \sum_k \mathcal{G}_{km_\ell} \right)^2} - 1 \right) \right). \quad (5.14)$$

The attenuation constant c_j is computed after replacing the standard deviation σ_j in equation (5.12) and solving for c_j . In the most extreme case, each secondary pixel can be considered as an area, A_j . In that case, the attenuation constant, c_j , and the standard deviation, σ_j , are computed based on equations (5.12) and (5.13) after eliminating the summations in terms of k . The results are depicted in Fig. 5.3. One can see that the transmissions originating from neighbouring pixels can have a high degree of correlation.

5.3.1 Impact of user density on generated interference

According to the PPP model, the active transmitters are distributed uniformly inside the area. However, this might not reflect reality, since the users tend to form clusters (see for instance the density of households in Fig. 5.2b). In Publication V, we model the interference from each area, A_j , by using a PPP model. We assume that by increasing the number of areas, we will be able to capture better the irregular propagation and non-uniform user density.

Since the areas are disjoint, the moments of the aggregate interference can be computed as a sum of the moments over the disjoint areas:

$$E \{ I_P \} = P_t \cdot \sum_j \lambda_{p,j} \cdot e^{\frac{\sigma_j^2}{2\xi^2}} \cdot \int_{A_j} g_a da \quad (5.15)$$

$$E \{ I_P^2 \} = P_t^2 \cdot \sum_j \lambda_{p,j} \cdot e^{\frac{2\sigma_j^2}{\xi^2}} \cdot \int_{A_j} g_a^2 da + E \{ I_P \}^2, \quad (5.16)$$

where $\lambda_{p,j}$ is the PPP density inside the area, A_j .

In Fig. 5.4, the interference distribution is expressed as the histogram of interference levels for all test points. All of the approximating distri-

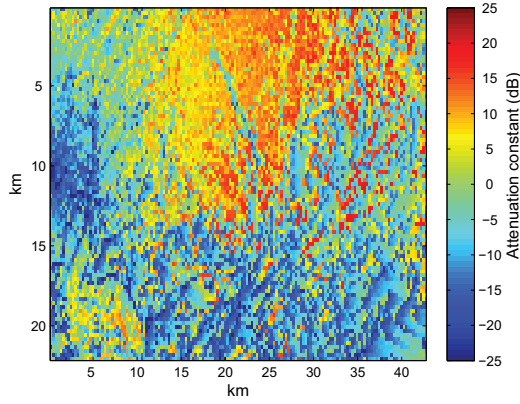
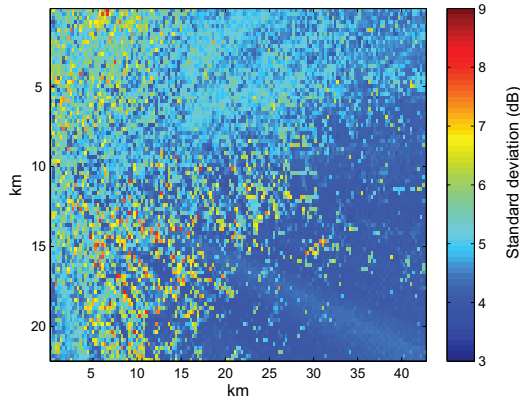
(a) Attenuation constant, $10 \log_{10}(c_j)$.(b) Standard deviation, σ_j .

Figure 5.3. Pathloss attenuation constant and standard deviation for each pixel. The pathloss attenuation exponent is fixed at $n = 3.5$.

butions are log-normals with the parameters calculated based on the F-W method and with the linear moments calculated using equations (5.15) and (5.16). Since the moments in equations (5.15) and (5.16) have been matched to the moments using ITM, the particular choice of pathloss exponent values η_j while solving the system of equations (5.12) and (5.13) does not impact the quality of the approximation. In Fig. 5.4 one can see that the assumption of a uniform distribution of users overestimates the interference level by 8 dB. Surprisingly, it is possible to obtain a good approximation of aggregate interference using only a few areas, A_j . Fortunately, the proposed method overestimates the interference distribution in the upper tail.

If there is user mobility and due to that changes in the user density, the

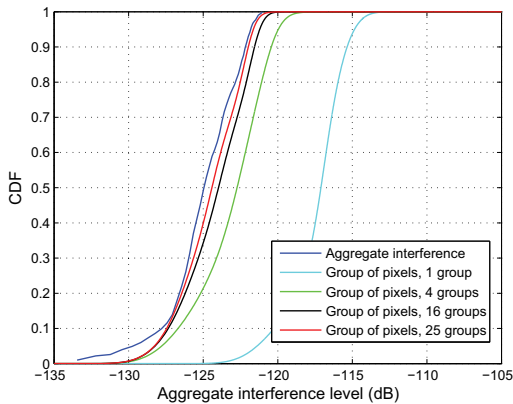


Figure 5.4. Approximation of the aggregate interference distribution at the TV test points using the modified PPP model.

database can still use the calculated pathloss models to identify whether the generated secondary interference disturbs the DTT receivers. The database just needs to update the PPP intensities λ_j in the equations (5.15) and (5.16). Only if there are significant changes in the user density it might be optimal in terms of approximation accuracy to use a different set of clusters.

Also, the impact of indoor-to-outdoor propagation has not been considered into the proposed model. In the simplest case, indoor-to-outdoor propagation is modelled by a constant attenuation due to the wall penetration loss and the proposed model is still valid. However, it is a matter of future research to identify whether the log-normal distribution can provide a good fit for indoor-to-outdoor propagation measurements.

5.4 Impact of shadowing correlation on generated interference

Measurements indicate that the radio signals arriving from the same angular direction are correlated. There are various models describing the slow fading correlation as a function of the signal arrival angle and the relative distance between the interfering transmitters and the victim receiver [167, 168]. In order to incorporate a log-normal fading correlation into the aggregate interference modelling, we need a method that can describe the distribution of the sum of correlated log-normal RVs.

For a constant and positive correlation coefficient, $0 < \rho \leq 1$, between all pairs of log-normals RVs, their sum asymptotically converges with another log-normal RV [169]. The log-normal approximation shows good

accuracy as the slow fading standard deviation decreases and the number of RVs increases. The extension of the F-W, S-Y and cumulant matching methods for the correlated log-normal RVs can be found in a study by Abu-Dayya & Beaulieu [170]. The F-W method still enjoys the lowest complexity, and actually its accuracy improves when the correlation coefficient increases [140].

In Publication IV we show that for secondary transmitters with fixed locations, the correlation does not impact the mean (in the linear domain) but it increases the variance of the aggregate interference distribution. The second moment is as follows:

$$\begin{aligned} E\{I_C^2\} &= P_t^2 \sum_m \sum_n g_m g_n E\{x_m x_n\} \\ &= P_t^2 \sum_m g_m^2 E\{x_m^2\} + P_t^2 \sum_m \sum_{n \neq m} g_m g_n E\{x_n x_m\}. \end{aligned} \quad (5.17)$$

Starting from the MGF of the bivariate normal distribution [99, pp.217], the cross-correlation between two zero-mean log-normal RVs with standard deviations σ_n and σ_m and a correlation coefficient ρ_{nm} is

$$E\{x_n x_m\} = e^{\frac{\sigma_n^2 + \sigma_m^2 + 2\rho_{nm}\sigma_n\sigma_m}{2\xi^2}}. \quad (5.18)$$

Based on the assumption of equal standard deviations, $\sigma_n = \sigma_m = \sigma$, and an equal correlation coefficient, ρ , for all transmission pairs, Publication IV shows that equation (5.17) can be simplified to

$$E\{I_C^2\} = P_t^2 \left(e^{\frac{2\sigma^2}{\xi^2}} - e^{\frac{\sigma^2(1+\rho)}{\xi^2}} \right) \sum_m g_m^2 + P_t^2 e^{\frac{\sigma^2(1+\rho)}{\xi^2}} \sum_m \sum_n g_m g_n. \quad (5.19)$$

Fig. 5.5 shows the interference distribution for uncorrelated, $\rho = 0$, fully correlated, $\rho = 1$, and equally correlated, $\rho = 0.7$ transmissions, using the F-W method. The correlation models [167, 168] are also simulated. One can see that a constant correlation coefficient approximates well the upper tail of the interference distribution obtained using the correlation models.

Even if the correlation between the transmission pairs can be estimated, the constant correlation coefficient approximation is still useful because it reduces the amount of computations and storage requirements in the database. The correlation coefficient, ρ , can be set by equating equation (5.17) with equation (5.19):

$$\rho = \frac{\xi^2}{\sigma^2} \cdot \log \left(\frac{\sum_m \sum_{n \neq m} g_m \cdot g_n \cdot e^{\rho_{mn}\sigma^2/\xi^2}}{\sum_m \sum_{n \neq m} g_m \cdot g_n} \right), \quad (5.20)$$

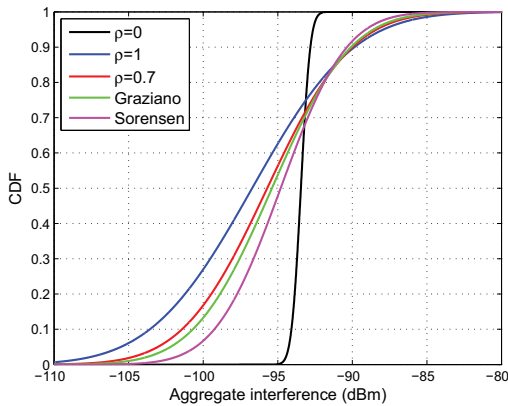


Figure 5.5. Aggregate secondary interference distribution at the TV cell border with shadowing correlation models. The secondary transmitters are located in the TVWS and they are placed on a cellular lattice.

where the ρ_{mn} has to be evaluated for each pair of secondary transmitters based either on the correlation model or on the measurements. In Fig. 5.6, one can see that the constant correlation model achieves good accuracy for a smaller slow fading standard deviation and a higher number of secondary transmitters.

Similar to what we found in Publication IV for a PPP, the parameters of the approximating log-normal distribution for the generated interference due to a BPP depend on the density of the transmitters, the correlation model and the slow fading standard deviation [171]. Both studies show that the log-normal distribution, with a careful selection of its parameters, is able to capture the statistics of the aggregate interference.

5.5 Discussion

In this chapter, we focused on aggregate interference modelling for the geolocation-controlled secondary spectrum access. We did not address the issue of interference generated by secondary devices with sensing capabilities, see, for instance, the studies by Win, Pinto & Shepp and Ghasemi & Sousa [133, 138].

The existing models for computing the aggregate interference within a system are not directly applicable for a primary-secondary system setup. The primary receivers are spatially separated from the secondary transmitters with protection distances that can be in the order of a few kilometers. When the distance between secondary transmitters is much smaller

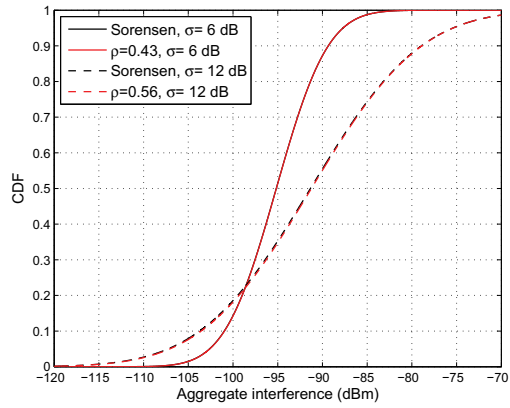
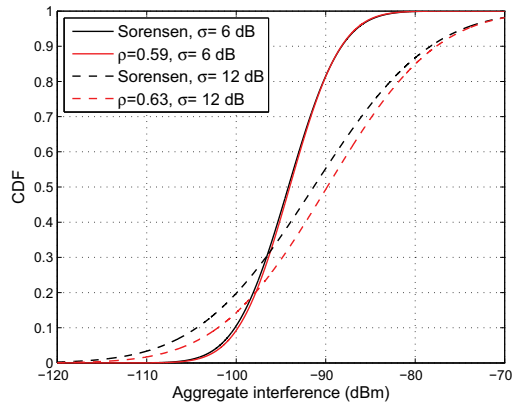
(a) Cell radius, $d = 1$ km.(b) Cell radius, $d = 4$ km.

Figure 5.6. Aggregate interference distribution at a TV test point due to the transmissions from a secondary cellular downlink deployed in the TVWS. For constant correlation coefficient model, the correlation coefficient ρ is calculated based on equation (5.20). For different secondary cell sizes, the transmit power levels are scaled so that the power density emitted from the secondary area remains the same.

than the primary-secondary distance separation, the interference levels produced by different secondary transmitters can be correlated with one another. As demonstrated in Publication IV, the correlation should be carefully considered because it impacts the distribution of the generated interference.

For random access wireless networks, the spatial separation between the primary and secondary system makes the spatial interference pattern non-uniform. In Publication V, we show how to compute the generated interference from finite area wireless networks with a possibly non-uniform

user density. Also, in wireless networks with contention control the existence of borders between the primary and secondary systems impacts the active user density close to the border and, subsequently, the generated interference.

It is expected that regulators will impose constraints on the amount of generated secondary interference that is permitted. A spectrum allocation database can control the generated interference by adjusting some operational parameters of the secondary network. In this chapter, we discussed three different types of secondary networks. The generated interference from different types of systems can be controlled by adjusting the different parameters.

The generated interference from a cellular system can be reduced by increasing the reuse distance. For random access wireless networks, a smaller activity factor results in a lower amount of interference. For wireless networks with contention control, decreasing the carrier sensing threshold increases the carrier sensing range and, subsequently, reduces the density of active users.

6. Secondary power allocation

A good model for measuring the amount of generated secondary interference to the primary system is needed for describing accurately the primary performance degradation in the presence of secondary transmissions. With a good model at hand, we can look for methods to allocate the transmit power level to secondary users. A power allocation algorithm for secondary spectrum access must meet the regulatory spectrum access constraints on the one hand and optimize the secondary performance on the other.

Transmit power control (TPC) algorithms have been already proposed since early 1960s [172]. To operate in an energy efficient manner, the total power assigned to a group of transmitters can be minimised while a target SINR is maintained for all transmission pairs [172]. TPC has been used for interference management since the advent of 2G wireless networks. For a summary of TPC algorithms in 2G/3G/4G cellular networks, see, for instance, [173] and the references therein. The existing TPC algorithms can be tailored to a single system.

Current standardisation rules for secondary power allocation in Europe and the US do not provide any secondary system performance guarantees. In addition, they are not able to protect the primary system service in all cases. The power allocation algorithms proposed by the academic research community usually assume a common power level for all secondary transmitters [24, 143, 147]. While they are able to maintain satisfactory quality for the primary service, they are inadequate for transmitters located far from the primary coverage area.

In this chapter, we adopt the concept of interference margin for describing the amount of permitted generated interference at the primary system. We discuss how the interference margin can be used to introduce simple constraints while allocating power levels to secondary users. Also,

we propose a joint rate and power allocation scheme that maintains a fixed SINR target on the side of the secondary system.

6.1 Interference margin

For satisfactory operation of wireless packet services, a target SINR, γ_t , must be satisfied at a certain outage probability target, O_t . For example, the TV reception is satisfactory if the following condition holds true [118, pp.279]:

$$\Pr(\gamma_i \leq \gamma_t) \leq O_t, \quad (6.1)$$

where γ_i is the SINR at the i -th TV pixel and γ_t is the TV SINR target.

Equation (6.1) is a chance type of constraint, which is in general difficult to handle. Starting from inequality (6.1), one can obtain the maximum mean generated secondary interference [174]. This quantity is commonly referred to as the interference margin, I_Δ . In [174], the authors derive the interference margin assuming a log-normal fading both for the TV signal and the secondary user signal. The F-W method is used to compute the parameters of the approximating distribution of the aggregate interference (see Chapter 5). Based on these assumptions, the chance constraint (6.1) becomes

$$E\{I_t\} \leq e^{\frac{1}{2\xi}} \left(I_{\Delta(dB)} + \frac{1}{2\xi} \text{var}\{I_{t(dB)}\} \right) = I_\Delta. \quad (6.2)$$

The interference margin depends on the secondary system parameters, i.e. the link gains to the primary test point and the transmit power levels through the variance of the aggregate interference, $\text{var}\{I_{t(dB)}\}$. The constraint (6.2), is a non-linear function of the transmit power levels. However, it is important to notice that the aggregate interference level is an order of magnitude less than the useful TV signal level. This property provides the approximation tightness for the lower bound of the interference margin, $I_{\Delta l} \leq I_\Delta$, which was first established in [174] and later verified in Publication I. The lower bound depends only on the primary system parameters and the noise level

$$I_{\Delta l} = 10^{\frac{\mu_{TV(dB)} - \gamma_{t(dB)} + \sigma_{TV} \cdot Q^{-1}(1-O_t)}{10}} - P_N. \quad (6.3)$$

By using the lower bound of the interference margin, one essentially turns the probabilistic constraint (6.1), into a linear constraint, $E\{I_t\} \leq I_{\Delta l}$, which is easier to handle. The necessary condition for interference

control at the i -th TV test pixel can be read as

$$E \left\{ \sum_{j=1}^N G_{ij} \cdot P_{tj} \right\} \leq I_{\Delta l, i}. \quad (6.4)$$

If we group together the secondary transmitters with similar propagation properties, and if we assume that each group emits a uniform power density, then the above equation becomes

$$\sum_j E\{x_j\} \cdot P_{dj} \int_{A_j} g_{ai} da \leq I_{\Delta l, i}, \quad (6.5)$$

where g_{ai} describes distance-based pathloss and $E\{x_j\}$ the mean of the slow fading for the group, A_j . The integral approximation, equation (5.4), has been used to turn the summation in inequality (6.4) into an integration.

6.1.1 Hierarchical interference control

Inequality (6.5) indicates that the interference margin can be treated as an available resource. Each transmitter, or each group of transmitters, can take up a fraction of the available resource. Allocating the interference margin to different transmitters becomes a resource sharing problem. For protecting the primary system, the necessary condition is as follows:

$$\sum_j I_{\Delta l, j} \leq I_{\Delta l}, \quad (6.6)$$

where $I_{\Delta l, j}$ is the margin allocated to the j -th group.

After sharing the interference margin among the groups of transmitters, the transmit power allocation within a group can be treated as an independent process. In Publication I, we assume the uniform power density within each group. In that case, the allocated margin can be taken either from a few high-power transmitters or from many low-power transmitters, thus maintaining the same power density in both cases.

Geolocation databases can also trade the interference margin between each other. A database can manage multiple groups of secondary transmitters; each group would have its own power density, channel model and footprint. Instead of exchanging the deployment contours, A_j , channel models, $E\{x_j\}$, g_a , transmission footprint, A_f , and power densities, P_{dj} , for interference control, the databases can first agree on their share of the interference margin. Then, the databases can allocate transmit power levels independent of one another without violating the primary interference constraint. In this way, the communication signalling overhead between

databases is reduced. The idea for a hierarchical power allocation has been communicated to the ECC through the draft contribution [21].

In Publication I, we consider N_S cellular secondary networks deployed in the TVWS. Also, we define N_P test points along the TV coverage contour. The allocation of an interference margin among the different systems is not arbitrary. We assume a uniform power density within each system and maximise the sum power density for all the systems:

$$\text{Maximise : } \mathbf{w}^T \cdot \mathbf{P}_d, \quad (6.7i)$$

$$\mathbf{P}_d \succeq 0$$

$$\text{Subject to: } \mathbf{G}' \cdot \mathbf{P}_d \leq \mathbf{I}_{\Delta l}, \quad (6.7ii)$$

where the symbol \succeq represents the vector inequality, or $P_{dj} \geq 0 \forall j$, and \mathbf{P}_d and $\mathbf{I}_{\Delta l}$ are column vectors with N_S and N_P elements, respectively; the weights, \mathbf{w} , can be selected to favour the different systems and \mathbf{G}' is a link gain matrix with $N_P \times N_S$ elements. For the i -th test point and the j -th secondary system, the $[ij]$ -th element of the link gain matrix is

$$G'_{ij} = E\{x_j\} \cdot \int_{A_j} g_{aid} da. \quad (6.8)$$

For $\mathbf{I}_{\Delta l} > 0$, the optimization problem (6.7), is bounded and consistent. In Fig. 6.1a, all of the systems take an equal margin share due to the symmetric network topology. In Fig. 6.1b, one of the systems is favoured and the rest had to adapt their power densities to maintain sufficient TV protection.

Given the allocated interference margin for a group of transmitters, hereafter $I_{\Delta l, j} = I_{\Delta l}$ for simplicity, different utilities, $f_u(\cdot)$, can be optimized:

$$\text{Maximise : } f_u(\mathbf{P}_t), \quad (6.9i)$$

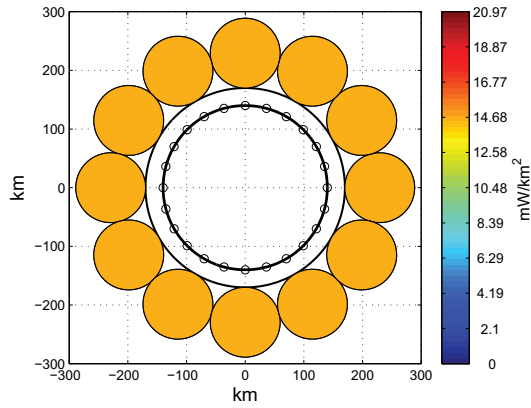
$$\mathbf{P}_t \succeq 0$$

$$\text{Subject to: } \mathbf{G} \cdot \mathbf{P}_t \leq \mathbf{I}_{\Delta l}, \quad (6.9ii)$$

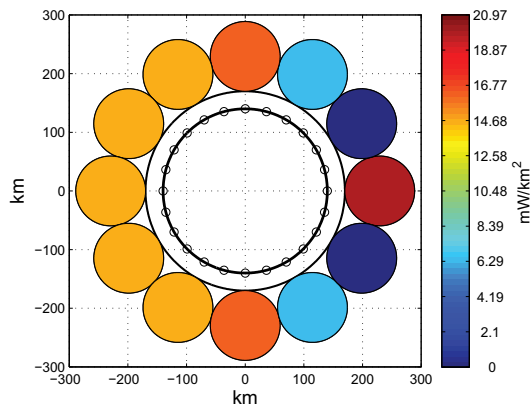
where $\mathbf{P}_t, \mathbf{I}_{\Delta l}$ are column vectors with N and N_P elements, respectively, and \mathbf{G} is an $N_P \times N$ matrix of the mean link gains, including slow fading.

6.2 Optimization of secondary transmit power

The ECC standardisation rule allocates the maximum permitted transmit power to a single secondary user, equation (4.1). For multiple users transmitting simultaneously, the ECC rule scales down their transmit power levels by using protection margins. The ECC rule does not define a quantity similar to the interference margin for protecting the TV service. Also,



(a) Uniform power density.



(b) Non-uniform power density.

Figure 6.1. Power density allocated to cellular secondary systems possibly controlled by different geolocation databases. Each coloured circle corresponds to a cellular system having multiple cells. Available interference margin I_{Δ} at each test point is -115 dBm and the noise power level P_N is -106 dBm. HATA model for secondary propagation pathloss has been used.

it does not suggest an algorithm for setting the protection margins unless there are up to four secondary transmitters. Using the same protection margins in all cases would violate the TV protection limits [121]. Next, we review the power allocation algorithms proposed in the literature.

In general, a higher transmit power level results in higher capacity. For multiple secondary transmitters, a natural utility function to use is the sum-power, $f_u = \mathbf{1}^T \cdot \mathbf{P}_t$. Secondary transmitters located far from the primary system can contribute more to the sum because their link gains are smaller. In an extreme case, the transmitter with the smallest link gain takes most of the interference margin and the transmit power levels

for the rest become nearly zero. The linear utility function is highly unfair. To remedy this problem, a logarithmic utility could be used instead [175]. With logarithmic utility, the optimization problem (6.9) becomes

$$\text{Maximise : } \mathbf{1}^T \cdot \log \mathbf{P}_t, \quad (6.10i)$$

$$\mathbf{P}_t \geq 0$$

$$\text{Subject to: } \mathbf{G} \cdot \mathbf{P}_t \leq \mathbf{I}_{\Delta l}. \quad (6.10ii)$$

A proportional fair (PF) power allocation scheme introduces fairness but also a high degree of implementation complexity. The complexity grows with the number of transmitters and primary test points. On the other hand, the geolocation database should operate with low complexity algorithms in order to handle frequent spectrum access requests in real time. In order to reduce the complexity of the PF power allocation scheme, we propose a simplified proportional fair (SPF) algorithm in Publication II. A schematic illustration of SPF and PF schemes is presented in Fig. 6.2.

According to the SPF scheme, we associate each secondary transmitter with the primary test point where its generated interference is maximised. We perform PF power allocation for secondary transmitters dominated by the same test point. The parameter, p_0 , in Fig. 6.2b describes the mean interference each transmitter generates at its dominating test point:

$$p_0 = \min_{i \in \mathcal{D}} \left\{ I_{\Delta l, i} \cdot \left(|\mathcal{J}_i| + \sum_{k \neq i} \sum_{j \in \mathcal{J}_k} \frac{g_{ij}}{g_{kj}} \cdot e^{\frac{\sigma_{ij}^2 - \sigma_{kj}^2}{2\xi^2}} \right)^{-1} \right\}, \quad (6.11)$$

where \mathcal{D} is the set of dominating primary test points, \mathcal{J}_i is the set containing secondary transmitters dominated by the i -th test point and σ_{ij} is the slow fading standard deviation from the j -th secondary transmitter to the i -th test point.

In Fig. 6.3b, we compare the linear and the logarithmic utility for the system setup illustrated in Fig. 6.3a. With linear utility, a single transmitter is essentially favoured. With a logarithmic utility, the power levels are allocated so that each transmitter generates equal interference at the binding points; test points where the constraint (6.10ii), holds true with the equality. Also, the SPF scheme is nearly optimal; it favours the transmitters located far from the test points slightly more compared with the PF scheme.

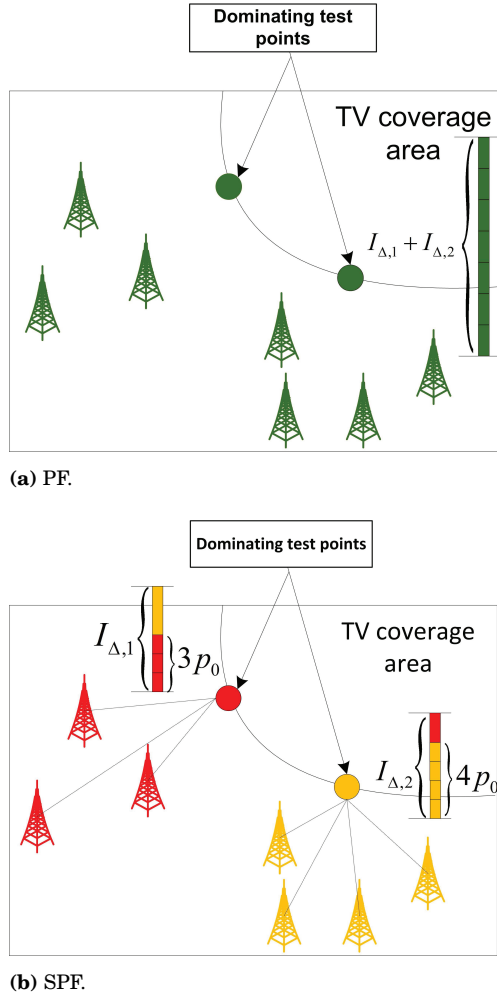
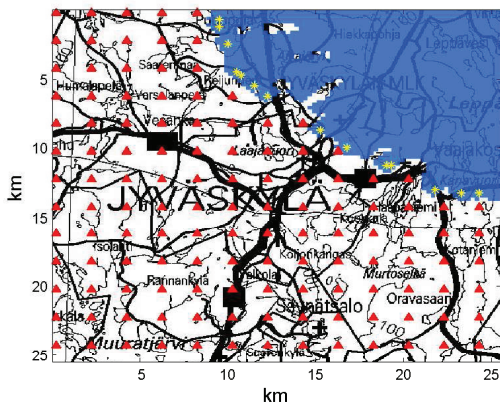


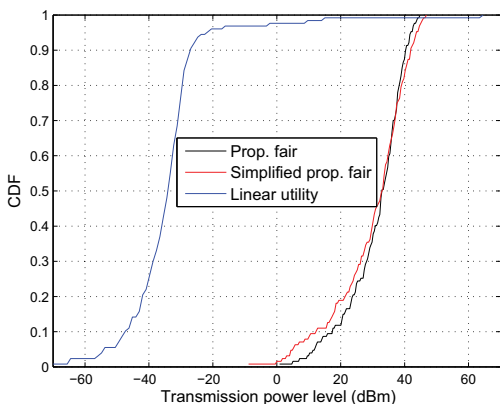
Figure 6.2. Schematic representation of proportional fair and simplified proportional fair power allocation schemes.

6.3 Optimization of secondary rate

For a single secondary transmitter, the power allocation maximising the secondary ergodic and outage capacity has been investigated under average/peak interference power constraints by Musavian & Aissa [176] and under primary outage constraint by Kang et al. [177]. The common assumption is that the secondary user is able to adapt its transmission power level based on the channel state. More transmit power is allocated when either the link gain to the primary system decreases or the link gain to the secondary receiver increases. This implies that fading in the secondary-to-primary link can be beneficial from the perspective of secondary rate.



(a) System setup.



(b) Transmit power distribution.

Figure 6.3. TV protection area (blue-shaded area), secondary transmitters (red triangles) and dominating TV test points (yellow stars). Distribution of secondary transmit power level using PF, SPF and linear power allocation algorithms. HATA model for secondary propagation pathloss has been used.

In single user OFDM, the sum-rate subject to transmit power constraint is maximised by using the water-filling algorithm. For OFDM-based secondary users, the primary systems impose additional transmit power constraints on each subchannel, making water-filling nonoptimal. The secondary user should consider not only the channel state but also the available interference margin of each subchannel. An optimal algorithm based on iterative water-filling has been proposed by Wang et al. [178]. In another study [179], Wang et al. extended the algorithm to incorporate the effect of subcarrier sidelobes on adjacent channel interference.

6.3.1 Multiple secondary transmission pairs

With multiple secondary transmission pairs, a natural utility to maximise is the sum-rate. Given the interference margin at the primary test points, the optimization problem in equation (6.9), becomes [180]

$$\text{Maximise : } \sum_{\mathbf{P}_t \succeq 0} \sum_{i=1}^N w_i \cdot \log_2(1 + \Gamma_i(\mathbf{P}_t)). \quad (6.12i)$$

$$\text{Subject to: } \mathbf{G} \cdot \mathbf{P}_t \leq \mathbf{I}_{\Delta l}, \quad (6.12ii)$$

where $\Gamma_i(\mathbf{P}_t)$ is the SINR at the i -th secondary test point.

An explicit constraint on the minimum permitted secondary SINR introduces fairness. In Publication III, we illustrate the difference in power allocation with and without secondary constraints for a cellular secondary system in TVWS. With TV constraints only, the secondary downlink sum rate is maximised in a similar way as with the PF power allocation scheme (see Fig. 6.4b). The less the link gain to the TV test points, the higher the allocated transmission power. The power allocation trend changes if secondary SINR constraints are also considered:

$$\Pr(\Gamma_i \leq \Gamma_t) \leq O_t^{(SU)}, \quad (6.13)$$

where Γ_t and $O_t^{(SU)}$ are the secondary SINR target and the secondary outage probability target, respectively.

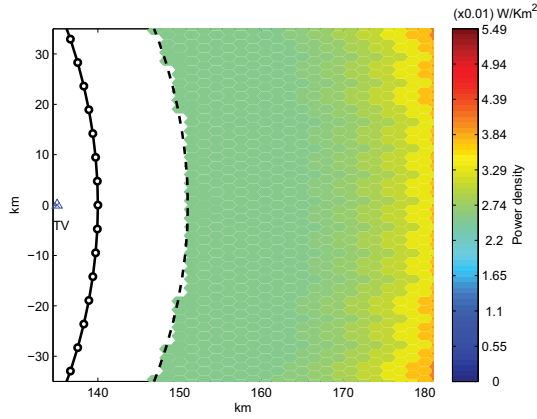
Secondary cells located close to the primary system suffer more from the generated primary interference and they have to utilise higher transmit power levels to meet their own SINR constraints. As a result, less of a TV interference margin is allocated to secondary cells located further away and the power allocation looks almost uniform (see Fig. 6.4a). In Publication III, the optimization problem in equation (6.9), subject to secondary self-interference constraints is formulated as follows as:

$$\text{Maximise : } \sum_{\mathbf{P}_t \succeq 0} \sum_{i=1}^N \log_2(1 + \Gamma_i(\mathbf{P}_t)). \quad (6.14i)$$

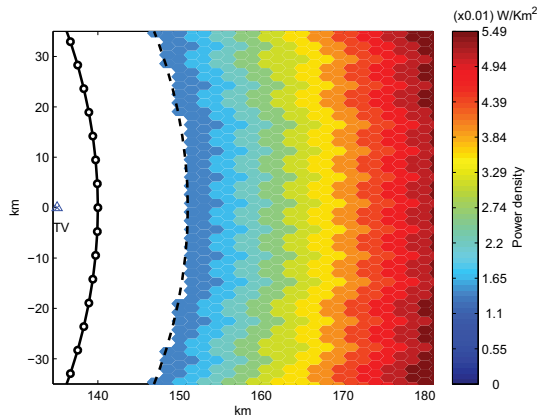
$$\text{Subject to: } \mathbf{G} \cdot \mathbf{P}_t \leq \mathbf{I}_{\Delta l} \quad (6.14ii)$$

$$\mathbf{G}_2 \cdot \mathbf{P}_t \leq \mathbf{I}_{\Delta l}^{(SU)}, \quad (6.14iii)$$

where $\mathbf{I}_{\Delta l}^{(SU)}$ is the vector of interference margins available at the secondary test points calculated by following steps similar to the ones used for equations (6.2) and (6.3), and \mathbf{G}_2 is the matrix of mean link gains, including slow fading, from the secondary interfering transmitters to the secondary test points.



(a) TV and secondary protection constraints.



(b) TV protection constraints.

Figure 6.4. Spatial power density emitted from the secondary deployment area. Secondary transmitters are placed on a cellular lattice with reuse 3. TV SINR target is 17.1 dB and secondary SINR target is -3.5 dB. Target outage probability for TV and secondary system is 10 %. HATA model for secondary propagation pathloss has been used.

The optimization problem in equation (6.14), can be formulated as a difference-convex programming problem [181]. For this class of optimization problems, the global optimal solution can be identified only for small problem instances. The results in Publication III were derived using sub-optimal methods, which made it possible, however, to capture the general behaviour of the power allocation. Based on Fig. 6.4a, one can deduce that the FCC rule captures the general trend better than the ECC rule, since it suggests the use of constant power. However, the transmit power level must not be set equal to 4 W, as proposed by the FCC rule [114], but according to the interference margin available at the primary and secondary

test points.

Power allocation algorithms for sum rate maximisation problems have also been studied for the secondary multiple access channel: multiple secondary transmitters communicating simultaneously with a single secondary receiver [182, 183]. In that case, successive interference cancellation should be used for enhancing the uplink capacity. The power allocation maximising the uplink sum-rate has been derived by Zhang et al. [182] subject to the interference power constraint at the primary receiver and the transmit power constraints at the secondary transmitters. If the secondary receiver is able to decode the primary signal, it can cancel it off from the received signal. Based on this assumption, the sum-rate maximisation problem has been studied for different channel conditions between the primary transmitter and secondary receiver subject to an outage probability constraint for the primary system [183].

In addition to the the sum-rate, the secondary transmit power levels can be allocated by optimizing some other utility function. For example, an alternative method for capturing the impact of secondary self-interference on the power allocation scheme is the following cost function [184]:

$$\min \left\{ \sum_{i=1}^N (\Gamma_i - \Gamma_t)^2 \right\}. \quad (6.15)$$

According to the cost function (6.15), the secondary transmit power levels are allocated so that most secondary transmission pairs experience SINR close to the SINR target. If a user selfishly increases its own power, the SINR of the other pairs will be reduced due to the self-interference and the cost function (6.15) will increase. Another way to introduce fairness is to maximise the minimum secondary SINR. The max-min fairness can be formulated as a geometric programming problem with linear constraints on the secondary interference generated to the primary system [185]. Finally, the PF allocation of the secondary SINR can be achieved by allocating power levels maximising the following utility [186]:

$$\sum_{i=1}^N \log (\Gamma_i(\mathbf{P}_t) - \Gamma_t). \quad (6.16)$$

6.4 Joint power and channel allocation

Within a single spectrum band, the secondary performance targets might not be satisfied for all transmission pairs due to the combined impact

of primary and secondary generated interference. The power allocation problem becomes more challenging when there are multiple spectrum band candidates and the geolocation database has to allocate the users among these candidates. Joint channel allocation and TPC schemes for wireless ad hoc networks (see, for instance, [187]) are not directly applicable to secondary spectrum access because they do not consider interference constraints on the candidate channels.

Channel allocation algorithms that maximise the secondary spectrum utilisation were first proposed using the protocol interference model [188]. Their applicability is rather limited because the protocol model may not correctly capture the co-channel interference on the secondary system side. Also, these algorithms overlook the impact of aggregate secondary interference to the primary test points.

Joint spectrum and power allocation algorithms that include secondary SINR constraints and primary interference constraint have been proposed by Hoang & Liang [189]. The objective is to maximise secondary spectrum usage, or, equivalently, to maximise the number of secondary users that are served. Without primary constraints, a power assignment on a given channel is feasible if the spectral radius of the link gain matrix is less than one [190]. With the primary-secondary system setup, the Pareto optimal transmit power vector can be used only if the primary interference constraints are also met.

Joint spectrum and power allocation algorithms are usually characterised by a high degree of complexity. Two possible ways to reduce the amount of computations in the database are to (i) allocate a single secondary transmitter on each channel [191, 192, 193] or to (ii) apply a two-phase approach where channel allocation is followed by user allocation [193].

When there is a single secondary transmitter on each channel, the secondary transmit power levels stop being coupled. In that case, identifying nearly optimal solutions for the secondary sum-rate maximisation problem [191] and outage probability minimisation problem [192] subject to primary interference constraints becomes possible. However, exclusive secondary spectrum usage can be problematic in areas with low spectrum availability, and also it is unfair to use it when the transmission quality of the different channels is different. When spectrum allocation and power control are carried out independent of each other, it is possible to first allocate the channels to the users so that a minimum secondary rate requirement is met. The transmission power allocation per channel can

be optimized by using, for instance, constrained water-filling [178, 193].

For secondary spectrum access in TVWS, the power allocation in the co-channel and the adjacent channel can be jointly optimized. The optimization criterion can be the maximum secondary capacity subject to interference constraints at the TV test points. For large secondary cells, the cellular system can operate with interference limited mode only in the adjacent channel. In that case, it is better to only allocate the available power in the adjacent channel [174]. Some of the power budget can be spent on the co-channel only if the secondary cell size is small.

6.5 Discussion

In this chapter, we discussed secondary power allocation algorithms for secondary spectrum access using geolocation. Distributed TPC algorithms can be found in studies by Setoodeh et al. and Nadkar et al. [194, 195], while secondary sensing-based TPC is discussed by Zhou et al. [196].

To protect the primary service, we first calculate the available interference margin at the primary test points [174]. The interference margin describes the amount of permitted secondary interference; hence, the concept is similar to that of interference temperature [27]. By using the concept of interference margin, the coordination of secondary interference becomes a hierarchical process. Different groups of secondary transmitters can trade an interference margin between each other. Based on their allocated fraction of margin, the transmit power allocation can be treated independently between the groups without violating the protection limits of the primary system. A hierarchical interference control reduces the complexity of power allocation in the geolocation database.

The current power allocation rules proposed by the standardisation bodies in the US and Europe for secondary spectrum access in TVWS do not protect the TV service in all cases [127, 121]. The power allocation algorithms proposed in Publication II and Publication I maintain the aggregate secondary interference under the value indicated by the available interference margin. At the same time, we need power allocation algorithms with a low degree of complexity to enable real-time computations in the geolocation database. Publication II proposes a simplified proportional fair power allocation scheme that can also support mobile secondary users, while Publication I proposes allocating the transmit power levels by maintaining a uniform power density. Both schemes are charac-

terised by a low signalling overhead between the secondary users and the databases.

Power allocation algorithms for secondary spectrum access have been applied in TVWS to study whether spatial spectrum holes correspond to real secondary transmission opportunities. In a recent study, a spectrum opportunity at a particular location was assumed to exist, only if the spectral efficiency was at least 25% of the spectral efficiency required in the dedicated spectrum [197]. The study concluded that a significant amount of TVWS is lost even when there are only moderate requirements for secondary system performance.

In Publication III, we propose a low-complexity power allocation algorithm for cellular systems in TVWS. The algorithm incorporates secondary self-interference constraints and has been used to assess the amount of available TVWS capacity in Finland. Our results agree with the findings presented by Dudda & Irnich [197]. For reuse one, the secondary SINR constraints are not satisfied in most of the TV spectrum bands. Reducing the cell size does not provide any significant capacity enhancement, either. We had to increase the cellular reuse factor to obtain realistic secondary capacity values.

7. Summary and future work

7.1 Summary and conclusions

In this thesis, we studied methods for detecting secondary transmission opportunities in white spaces based on the requirement to protect the primary spectrum using system. Currently, two types of detection methods exist: one is based on spectrum sensing and the other on geolocation database access.

The sensing-based spectrum access usually boils down to a signal detection problem. Cooperative detection algorithms can be used to resolve the hidden node problem and maintain a low false alarm rate without violating the misdetection probability target. In this thesis, we illustrated that the traditional signal detection framework is not appropriate for discovering secondary transmission opportunities in the spatial domain because it does not capture the primary signal level distribution under the null hypothesis. To remedy the problem, we approximated the distribution of the primary signal level under the null hypothesis using the uniform distribution. Also, we proposed to utilise the percentage of recovered TVWS as a metric for assessing the detection performance.

A good detector does not provide much insight into the secondary performance at higher network layers. The MAC layer arranges the allocation of the sensing resources by taking into account the performance targets. In this thesis, we proposed a MAC layer sensing algorithm for energy efficient wideband spectrum sensing. The allocation of sensing resources depends on the fading channel and the cost of engaging users in the spectrum measurements. It is not always optimal to involve all users in spectrum sensing or to measure the complete candidate bandwidth. Also, we proposed a sensing strategy based on the capacity demand of

the secondary service. We studied the trade-off between the service requirement and the demand in the measured spectrum and illustrated the potential for secondary services in TVWS. At least for low rate services, the amount of users getting the service grows much quicker in comparison with the number of required measured spectrum bands.

While the primary signal level at the location of the secondary user can be used to infer the distance to the primary transmitter, little can be deduced about the location of the primary receivers. In order to bypass the location uncertainty, the secondary user can access the spectrum only if it is located sufficiently far away from the primary transmitters. As a result, even with perfect detectors, a tight spectrum reuse cannot be achieved by using spectrum sensing [198]. Also, the bottleneck of secondary spectrum usage is the aggregate interference generated at the primary system. It is difficult to assess the aggregate interference level based on the local spectrum measurements at each secondary transmitter. All of these factors contribute to high protection margins, which reduce the number of recovered spectrum opportunities for sensing-only secondary devices.

In the US, sensing-only devices must use low transmission power and low decision levels and obey strict rules regarding the channel vacate time [20]. At this moment, geolocation is considered the way forward for secondary spectrum access in a primary/secondary system setup. The main issue is the set of rules and algorithms that should govern the operation of the database. The existing standardisation rules for secondary access in TVWS fail to protect the TV system in all cases. Also, the rule proposed by the ECC would suffer from a high signalling overhead between mobile secondary transmitters and the geolocation database. In this thesis, we proposed low-complex secondary interference models and power allocation algorithms that guarantee the protection of the TV services.

In order to reduce the amount of computations in the database, secondary users with similar propagation characteristics can be grouped together. Their combined effect on the primary system can be approximated based on the integral of the power density emitted from the secondary deployment area. In this thesis, we showed how to incorporate the slow fading correlation while computing the integral-based moments of the aggregate interference. We proposed a constant correlation coefficient model based on the average correlation over all the transmission pairs. The proposed model has a low degree of complexity and matched well with the

method that sums the interference from each transmitter.

For random access networks, the impact of the non-uniform user density on the generated interference was captured by dividing the secondary deployment area into multiple areas. A PPP was used to model the generated interference from each area. Different areas can be characterised by different power densities and different propagation characteristics due to terrain irregularities.

To protect the primary system service in all cases, we calculated the available interference margin at the primary system's test points. The interference margin was treated as an available resource. Based on its share of the margin, a database can allocate transmit power levels independently of other databases. This strategy reduces the amount of communication signalling overhead among geolocation databases. The secondary power allocation algorithm was viewed as a constrained optimization problem. Given the available margin, the secondary sum power, the sum power in log-domain and the sum-rate utilities were maximised.

In order to assess the real-life benefits of secondary spectrum access, we considered a cellular system deployed in the TVWS. Under secondary coverage constraints, we illustrated that the optimal power density allocation tends to be uniform. The uniform approximation reduces the amount of computations, making it possible to assess cellular capacity on a national level. To meet the secondary coverage constraints, the secondary self-interference should be controlled by careful frequency planning. This suggests that the joint channel and power allocation in TVWS is a good possible topic for future research.

7.2 Future work

Sensing-based and database-based algorithms for secondary spectrum access proposed in this thesis could be extended in many possible directions. An interesting idea could be to devise a hybrid method combining geolocation and sensing techniques. As mentioned in Chapter 4, the registration of coverage contours in the database can be inaccurate due to errors in propagation pathloss modelling. A WSD with sensing capabilities could measure the TV field strength and decide whether it is located inside or outside the TV coverage contour. An open research question in this system setup is the way to combine the outcomes received from the database and obtained from spectrum sensing.

There is also a clear direction to extend the results of Publication V related to the approximation of aggregate interference distribution in environments with correlated fading and user deployment. In Publication V, the secondary area has been divided into equally-sized smaller areas in an arbitrary manner. Obviously, too few areas do not describe the distribution of aggregate interference accurately, while on the other hand, too many areas necessitate high computational and storage overheads. A potential topic for future research could be to devise an algorithm that strikes a balance between implementation complexity and model accuracy. The Akaike information criterion that penalizes the model accuracy with the number of model parameters could for instance be used.

Bibliography

- [1] W. Webb. A license to do (almost) anything you want. *IET Communications Engineer*, pp. 12-16, Dec. 2006. (Cited on pages 1 and 4.)
- [2] J. Louis. International radio spectrum management beyond spectrum harmonisation. In *Proc. International Conference on Emerging Trends in Engineering and Technology*, pp. 116-120, Nov. 2011. (Cited on page 1.)
- [3] K. Harrison, M. Mishra and A. Sahai. How much white space is there? In *Proc. IEEE International Symposium on New Frontiers in Dynamic Spectrum Access Networks (DySPAN)*, pp. 1-10, Apr. 2010. (Cited on page 1.)
- [4] V. Valenta, K. Challapali and M. Ghosh. Cognitive PHY and MAC layers for dynamic spectrum access and sharing of TV bands. In *Proc. IEEE Radio and Wireless Symposium*, pp. 352-355, Jan. 2009. (Cited on page 1.)
- [5] Cisco visual networking index: Global mobile data traffic forecast update 2012-2017. (Cited on page 1.)
- [6] ITU Digital dividend: Insights for spectrum decisions, pp. 1-72, Aug. 2012. (Cited on page 2.)
- [7] European Commission. Communication from the commission to the European parliament, the council, the European economic and social committee and the committee of the regions. Promoting the shared use of radio spectrum resources in the internal market. COM(2012) 478. (Cited on page 2.)
- [8] ITU-R Recommendation SF.1486. Sharing methodology between fixed wireless access systems in the fixed service and very small

- aperture terminals in the fixed-satellite service in the 3400-3700 MHz band. (Cited on page 2.)
- [9] E.A. Jorswieck *et al.* Resource sharing improves the network efficiency for network operators. WWRWF27-WG4-10. (Cited on page 2.)
- [10] ECC Report 24: Technical considerations regarding harmonisation options for the digital dividend. A preliminary assessment of the feasibility of fitting new/future applications/services into non-harmonised spectrum of the digital dividend. Jun. 2008. <http://www.ero.dk>. (Cited on page 2.)
- [11] ECC Report 132: Light licensing, license-exempt and commons. Jun. 2009. <http://www.ero.dk>. (Cited on page 2.)
- [12] S. Kawade and M. Nekovee. Is wireless broadband provision to rural communities in TV whitespaces viable? A UK case study and analysis. In *Proc. IEEE International Symposium on New Frontiers in Dynamic Spectrum Access Networks (DySPAN)*, pp. 438-443, Oct. 2012. (Cited on page 3.)
- [13] M. Fitch, M. Nekovee, S. Kawade, K. Briggs and R. MacKenzie. Wireless service provision in TV white space with cognitive radio technology: A telecom operator's perspective and experience. *IEEE Communications Magazine*, pp. 64-73, Mar. 2011. (Cited on page 3.)
- [14] M. Song, C. Xin, Y. Zhao and X. Cheng. Dynamic spectrum access: From cognitive radio to network radio. *IEEE Wireless Communications*, pp. 23-29, Feb. 2012. (Cited on pages 3 and 4.)
- [15] Y. Selen, R. Baldemair and J. Sachs. A short feasibility study of a cognitive TV black space transmission. In *Proc. IEEE International Symposium on Personal Indoor and Mobile Radio Communications (PIMRC)*, pp. 520-524, Sept. 2011. (Cited on page 3.)
- [16] A. Goldsmith, S.A. Jafar, I. Marić and S. Srinivasa. Breaking spectrum gridlock with cognitive radios: An information theoretic perspective. *Proceedings IEEE*, vol. 97, no. 5, pp. 894-914, May. 2009. (Cited on pages 3 and 4.)
- [17] Qualcomm presentation at Radio spectrum policy group. ASA-a novel spectrum policy vision. Available at http://ipsc.jrc.ec.europa.eu/fileadmin/repository/sta/corsa/docs/SDR_ASA.pdf (Cited on page 4.)

- [18] Radio spectrum policy group report on collective use of spectrum and other spectrum sharing approaches, RSPG11-392. Nov. 2011. (Cited on page 4.)
- [19] V. Goncalves and S. Pollin. The value of sensing for TV white spaces. In *Proc. IEEE International Symposium on New Frontiers in Dynamic Spectrum Access Networks (DySPAN)*, pp. 231-241, May 2011. (Cited on page 5.)
- [20] M. Nekovee, T. Irnich and J. Karlsson. Current trends in worldwide regulation of secondary access to white spaces using cognitive radio. *IEEE Wireless Communications Magazine*, pp. 32-40, Aug. 2012. (Cited on pages 6, 47, and 84.)
- [21] Aalto University and BT Research. Draft proposal SE43(11)23. Control of aggregated interference from WSDs. Jul. 2011, <http://www.ero.dk>. (Cited on pages 6 and 72.)
- [22] Aalto University and BT Research. Draft proposal SE43(11)97. Control of aggregated interference from WSDs. Dec. 2011, <http://www.ero.dk>. (Cited on page 6.)
- [23] Aalto University and BT Research. Draft proposal SE43(12)12. Control of aggregated interference from WSDs. Dec. 2012, <http://www.ero.dk>. (Cited on page 6.)
- [24] N. Hoven, and A. Sahai. Power scaling for cognitive radio. In *Proc. IEEE International Conference Wireless Networks, Communications and mobile Computing (WiCOM)*, pp. 250-255, Jun. 2005. (Cited on pages 11, 56, and 69.)
- [25] H.V. Trees. Detection, estimation, and modulation theory, Part I. John Wiley & Sons, 2001. (Cited on pages 11 and 22.)
- [26] P.K. Varshney. Distributed detection and data fusion. Springer, Dec. 1996. (Cited on pages 12 and 17.)
- [27] S. Haykin. Brain-empowered wireless communications. *IEEE Journal on Selected Areas in Communications*, vol 23, no. 2, pp. 201-220, Feb. 2005. (Cited on pages 13 and 81.)
- [28] R. Tenney and N. Sandell. Detection with distributed sensors. *IEEE Transactions on Aerospace and Electronic Systems*, vol. AES 17, no. 4, pp. 501-510, 1981. (Cited on page 13.)

- [29] R. Viswanathan and P. Varshney. Distributed detection with multiple sensors: Part I-Fundamentals. *Proceedings IEEE*, vol. 85, no. 1, pp. 54-63, Jan. 1997. (Cited on page 13.)
- [30] R. Viswanathan and B. Ahsant. A review of sensing and distributed detection algorithms for cognitive radio networks. *Journal on Smart Sensing and Intelligent Systems*, vol. 5, no. 1, pp. 177-190, Mar. 2012. (Cited on page 13.)
- [31] S. Thomopoulos, R. Viswanathan and P. Bougoulas. Optimal decision fusion in multiple sensor systems. *IEEE Transactions on Aerospace and Electronic Systems*, vol. AES-23, pp. 644-653, 1987. (Cited on pages 15, 16, 17, and 23.)
- [32] J. Ma, G. Zhao and Y. Li. Soft combination and detection for cooperative spectrum sensing in cognitive radio networks. *IEEE Transactions on Wireless Communications*, vol. 7, no. 11, pp. 4502-4507, Nov. 2008. (Cited on pages 15 and 19.)
- [33] A.R. Reibman and L.W. Nolte. Optimal detection and performance of distributed sensor systems. *IEEE Transactions on Aerospace and Electronic Systems*, vol. AES-23, pp. 24-30, 1987. (Cited on pages 15 and 17.)
- [34] Z. Chair and P.K. Varshney. Optimal data fusion in multiple sensor detection systems. *IEEE Transactions on Aerospace and Electronic Systems*, vol. AES 22, no. 1, pp. 98-101, Jan. 1986. (Cited on pages 16 and 17.)
- [35] S. Stearns. Optimum detection using multiple sensors. In *Proc. of Carnahan Conference on Security Technology*, 1983. (Cited on page 16.)
- [36] A. Aziz, M. Tummala and R. Cristi. Optimal data fusion strategies using multiple-sensor detection systems. In *Proc. of Asilomar Conference on Signals, Systems and Computers*, pp. 941-945, Nov. 1997. (Cited on page 16.)
- [37] J Tsitsiklis. Decentralized detection with a large number of sensors. *Mathematical Control, Signals Systems*, vol. 1, pp. 167-182, 1988. (Cited on page 17.)

- [38] E. Drakopoulos and C. Lee. Optimum fusion of correlated local decisions. In *Proc. IEEE Decision and Control*, pp. 2489-2494, Dec. 1988. (Cited on page 17.)
- [39] M. Kam, Q. Zhu and W. Gray. Optimal data fusion of correlated local decisions in multiple sensor detection systems. *IEEE Transactions on Aerospace and Electronic Systems*, vol. 28, no. 3, pp. 916-920, 1992. (Cited on page 17.)
- [40] E. Visotsky, S. Kuffner and R. Peterson. On collaborative detection of TV transmissions in support of dynamic spectrum sharing. In *Proc. IEEE Symposium New Frontiers Dynamic Spectrum Access Networks (DySPAN)*, pp. 338-345, Nov. 2005. (Cited on pages 17 and 18.)
- [41] A. Ghasemi and E. Sousa. Asymptotic performance of collaborative spectrum sensing under correlated log-normal shadowing. *IEEE Communications Letters*, vol. 11, no. 1, pp. 34-36, Jan. 2008. (Cited on page 17.)
- [42] J. Shen, Y. Liu, S. Liu, G. Xie, J. Gao and C. Chi. Correlation between local sensors in hard cooperative spectrum sensing: beneficial or detrimental? In *Proc. IEEE Global Communications Conference (GlobeCom)*, pp. 1-5, Dec. 2008. (Cited on page 17.)
- [43] S. Chaudhari, J. Lunden and V. Koivunen. BEP walls for collaborative spectrum sensing. In *Proc. IEEE International Conference on Acoustics, Speech and Signal Processing (ICASSP)*, pp. 2984-2987, May 2011. (Cited on page 17.)
- [44] Z. Quan, S. Cui and A. Sayed. Optimal linear cooperation for spectrum sensing in cognitive radios networks. *IEEE Journal on Selected topics in Signal Processing*, vol. 2, no. 1, pp. 28-40, Feb. 2008. (Cited on page 17.)
- [45] M. Madishetty, V. Kanchumarthy, R. Viswanathan and C. Gowda. Distributed detection with channel errors. In *Proc. Southeastern Symposium on System Theory*, pp. 302-306. Mar. 2005. (Cited on page 17.)
- [46] S. Chaudhari, J. Lunden, V. Koivunen and H. Poor. Cooperative sensing with imperfect reporting channels: Hard decisions or soft

- decisions? *IEEE Transactions on Signal Processing*, vol. 60, no. 1, pp. 18-28, Jan. 2012. (Cited on page 17.)
- [47] B. Chen, R. Jiang, T. Kasetkasem and P. Varshney. Channel aware decision fusion in wireless sensor networks. *IEEE Transactions on Signal Processing*, vol. 52, no. 12, pp. 3454-3458, Dec. 2004. (Cited on page 17.)
- [48] C. Cordeiro, K. Challapali, D. Birru and S. Shankar. IEEE 802.22: The first worldwide wireless standard based on cognitive radios. In *Proc. IEEE Symposium New Frontiers Dynamic Spectrum Access Networks (DySPAN)*, pp. 130-138, Nov. 2005. (Cited on page 18.)
- [49] A. Ghasemi and E.S. Sousa. Collaborative spectrum sensing for opportunistic access in fading environments. In *Proc. IEEE Symposium New Frontiers Dynamic Spectrum Access Networks (DySPAN)*, pp. 130-138, Nov. 2005. (Cited on page 18.)
- [50] K. Ruttik, K. Koufos and R. Jäntti. Distributed power detection in shadowing environment and with communication constraint. In *Proc. IEEE International Symposium on Personal Indoor and Mobile Radio Communications (PIMRC)*, pp. 1-5, Sept. 2007. (Cited on page 18.)
- [51] W. Zhang, R. Mallik and K. Letaief. Optimization of cooperative spectrum sensing with energy detection in cognitive radio networks. *IEEE Transactions on Wireless Communications*, vol. 8, no. 12, pp. 5761-5766, Dec. 2009. (Cited on page 19.)
- [52] F. Digham, M. Alouini and M. Simon. On the energy detection of unknown signals over fading channels. *IEEE Transactions on Communications*, vol. 55, no. 1, pp. 21-24, Jan. 2007. (Cited on page 19.)
- [53] A. Ghasemi and E.S. Sousa. Opportunistic spectrum access in fading channels through collaborative sensing. *Journal on Communications*, vol. 2, no. 2, pp. 71-82, Mar. 2007. (Cited on page 19.)
- [54] S. Mishra, A. Sahai and R. Brodersen. Cooperative sensing among cognitive radios. In *Proc. IEEE International Conference on Communications (ICC)*, pp. 1658-1663, Jun. 2006. (Cited on page 19.)
- [55] A. Sonnenschein and P. Fishman. Radiometric detection of spread-spectrum signals in noise of uncertain power. *IEEE Transactions on*

Aerospace and Electronic Systems, vol. 28, pp. 654-660, Jul. 1986.
(Cited on page 19.)

- [56] R. Tandra and A. Sahai. Fundamental limits on detection in low SNR under noise uncertainty. In *Proc. IEEE International Conference on Wireless Networks, Communications and Mobile Computing*, vol. 1, pp. 464-469. (Cited on page 19.)
- [57] R. Tandra, S.M. Mishra, and A. Sahai. What is a spectrum hole and what does it take to recognize one? *Proceedings IEEE*, vol. 97, no. 5, pp. 824-848, May 2009. (Cited on pages 21 and 24.)
- [58] R. Tandra, A. Sahai and V. Veeravalli. Space time metrics for spectrum sharing. In *Proc. IEEE International Symposium on New Frontiers in Dynamic Spectrum Access Networks (DySPAN)*, pp. 1-12, Apr. 2010. (Cited on page 24.)
- [59] R. Tandra, A. Sahai and V. Veeravalli. Unified space-time metrics to evaluate spectrum sensing. *IEEE Communications Magazine*, vol. 49, no. 3, pp. 54-61, Mar. 2011. (Cited on page 24.)
- [60] K. Ruttik, K. Koufos and R. Jäntti. Spectrum reuse at the border of a primary user cell. *IEEE Transactions on Wireless Communications*, vol. 57, no. 12, pp. 3836-3846, Dec. 2009. (Cited on page 24.)
- [61] K. Koufos, K. Ruttik and R. Jäntti. Signal model for OFDM sensing in cognitive radio. In *Proc. IEEE International Symposium on Personal Indoor and Mobile Radio Communications (PIMRC)*, pp. 1672-1676, Sept. 2009. (Cited on pages 24 and 25.)
- [62] Y. Chen. Analytical performance of collaborative spectrum sensing using censored energy detection. *IEEE Transactions on Wireless Communications*, vol. 9, no. 12, pp. 3856-3865, Dec. 2010. (Cited on page 25.)
- [63] C. Sun, W. Zhang and K. Letaief. Cluster-based cooperative spectrum sensing in cognitive radio systems. In *Proc. IEEE International Conference on Communications (ICC)*, pp. 2511-2515, Jun. 2007. (Cited on page 25.)
- [64] W. Zhang and K. Letaief. Cooperative spectrum sensing with transmit and relay diversity in cognitive radio networks. *IEEE Transactions on Wireless Communications*, vol. 7, no. 12, pp. 4761-4766, Dec. 2008. (Cited on page 25.)

- [65] I. Katzela and M. Naghshineh. Channel assignment schemes for cellular mobile telecommunication systems: A comprehensive survey. *IEEE Personal Communications*, vol. 3, no. 3, pp. 10-31, Jun. 1996. (Cited on page 27.)
- [66] Y. Akaiwa and H. Andoh. Channel segregation—A self-organised dynamic channel allocation method: Application to TDMA/FDMA microcellular system. *IEEE Journal on Selected Areas in Communications*, vol. 11, no. 6, pp. 949-954, Aug. 1993. (Cited on page 27.)
- [67] E.C. Peh, Y.C. Liang, Y.L. Guan and Y. Zeng. Cooperative spectrum sensing in cognitive radio networks with weighted decision fusion schemes. *IEEE Transactions on Wireless Communications*, vol. 9, no. 12, pp. 3838-3847, Dec. 2010. (Cited on page 30.)
- [68] Y.C. Liang, Y. Zeng, E.C. Peh and A.T. Hoang. Sensing-throughput tradeoff for cognitive radio networks. *IEEE Transactions on Wireless Communications*, vol. 7, no. 4, pp. 1326-1337, Apr. 2008. (Cited on pages 30, 38, and 42.)
- [69] M.C. Juarez and M. Ghogho. Spectrum sensing and throughput trade-off in cognitive radio under outage constraints over Nakagami fading. *IEEE Communications letters*, vol. 15, no. 10, pp. 1110-1113, Oct. 2011. (Cited on page 30.)
- [70] E.C. Peh, Y.C. Liang, Y.L. Guan and Y. Zeng. Optimization of cooperative sensing in cognitive radio networks: a sensing throughput tradeoff view. *IEEE Transactions on Vehicular Technology*, vol. 58, no. 9, pp. 5294-5299, Nov. 2009. (Cited on page 30.)
- [71] S. Althunibat, R. Palacios and F. Granelli. Performance optimization of soft and hard spectrum sensing schemes in cognitive radio. *IEEE Communications letters*, vol. 16, no. 7, pp. 998-1000, Jul. 2012. (Cited on page 30.)
- [72] Y. Pei, Y.C. Liang, K.C. Teh and K.H. Li. Sensing-throughput tradeoff for cognitive radio networks: A multiple-channel scenario. In *Proc. IEEE International Symposium on Personal Indoor and Mobile Radio Communications (PIMRC)*, pp. 1-5, Sept. 2010. (Cited on page 30.)
- [73] Y. Pei, Y.C. Liang, K.C. Teh and K.H. Li. How much time is needed for wideband spectrum sensing? *IEEE Transactions on Wireless*

- Communications*, vol. 8, no. 11, pp. 5466-5471, Nov. 2009. (Cited on page 30.)
- [74] R. Fan and H. Jiang. Optimal multi-channel cooperative sensing in cognitive radio networks. *IEEE Transactions on Wireless Communications*, vol. 9, no. 3, pp. 1128-1138, Mar. 2010. (Cited on page 30.)
- [75] H. Jiang, L. Lai, R. Fan and H.V. Poor. Optimal selection of channel sensing order in cognitive radio. *IEEE Transactions on Wireless Communications*, no. 8, no. 1, pp. 297-307, Jan. 2009. (Cited on pages 31 and 41.)
- [76] R. Fan and H. Jiang. Channel sensing-order setting in cognitive radio networks: A two-user case. *IEEE Transactions on Vehicular Technology*, vol. 58, no. 9, pp. 4997-5008, Nov. 2009. (Cited on page 31.)
- [77] H.T. Cheng and W. Zhuang. Simple channel sensing order in cognitive radio networks. *IEEE Journal on Selected Areas in Communications*, vol. 29, no. 4, pp. 676-688, Apr. 2011. (Cited on page 31.)
- [78] S. Stotas and A. Nallanathan. On the throughput and spectrum sensing enhancement of opportunistic spectrum access cognitive radio networks. *IEEE Transactions on Wireless Communications*, vol. 11, no. 1, pp. 97-107, Jan. 2012. (Cited on page 31.)
- [79] Y. Zou, Y.D. Yao and B. Zheng. Outage probability analysis of cognitive transmissions: Impact of spectrum sensing overhead. *IEEE Transactions on Wireless Communications*, vol. 9, no. 8, pp. 2676-2688, Aug. 2010. (Cited on page 31.)
- [80] P. Kaligineedi and V.K. Bhargava. Sensor allocation and quantization schemes for multi-band cognitive radio cooperative sensing system. *IEEE Transactions on Wireless Communications*, vol. 10, no. 1, pp. 284-293, Jan. 2011. (Cited on page 32.)
- [81] J. Khan, J. Lehtomäki, K. Umembayashi and J. Vartiainen. On the selection of the best performance sensors for cognitive radio networks. *IEEE Signal Processing letters*, nol. 17, no. 4, pp. 359-362, Apr. 2010. (Cited on page 32.)
- [82] Y. Chen. Optimum number of secondary users in collaborative spectrum sensing considering resources usage efficiency. *IEEE Commu-*

- nications letters*, vol. 12, no. 12, pp. 877-879, Dec. 2008. (Cited on page 32.)
- [83] S. Wu, M. Zhao and J. Zhu. Optimal number of secondary users through maximizing utility in cooperative spectrum sensing. In *Proc. IEEE Vehicular Technology Conference (VTC)*, pp. 1-5, Sept. 2009. (Cited on page 32.)
- [84] D. Pisinger. Algorithms for knapsack problems. Ph.D. dissertation, Department of Computer Science, University of Copenhagen, Feb. 1995. (Cited on page 33.)
- [85] D. Pisinger. A minimal algorithm for the multiple-choice knapsack problem. *European Journal Operational Research*, vol. 83, no. 2, pp. 394-410, 1995. (Cited on page 33.)
- [86] Y.J. Choi, W. Pak, Y. Xin and S. Rangarajan. Throughput analysis of cooperative spectrum sensing in Rayleigh-faded cognitive radio systems. *IET Communications*, vol. 6, no. 9, pp. 1104-1110, 2012. (Cited on page 33.)
- [87] G. Bianchi. Performance analysis of the IEEE 802.11 distributed coordination function. *IEEE Journal on Selected Areas in Communications*, vol. 18, no. 3, pp. 535-547, Mar. 2000. (Cited on page 34.)
- [88] Y. Chen, K. Yang and B. Zhao. Collaborative user number selection based on saturation throughput and sensing performance. *IEEE Transactions on Vehicular Technology*, vol. 60, no. 8, pp. 4019-4023, Oct. 2011. (Cited on page 34.)
- [89] T.V. Nguyen, H. Shin, T. Quek and M.Z. Win. Sensing and probing cardinalities for active cognitive radios. *IEEE Transactions on Signal Processing*, vol. 60, no. 4, pp. 1833-1845, Apr. 2012. (Cited on page 34.)
- [90] K. Koufos, K. Ruttik and R. Jäntti. Feasibility of voice service in cognitive networks over the TV spectrum. In *Proc. IEEE International Conference Cognitive Radio Oriented Wireless Networks and Communications (CrownCom)*, pp. 1-5, Jun. 2010. (Cited on page 37.)
- [91] A.W. Min and K.G. Shin. On sensing-access tradeoff in cognitive radio networks. In *Proc. IEEE International Symposium on New Frontiers in Dynamic Spectrum Access Networks (DySPAN)*, pp. 1-12, Apr. 2010. (Cited on page 38.)

- [92] H. Lee and D. Cho. VoIP capacity analysis in cognitive radio system. *IEEE Communications letters*, vol. 13, no. 6, pp. 393-395, Jun. 2009. (Cited on page 38.)
- [93] P. Wang, D. Niyato and H. Jiang. Voice service support over cognitive radio networks. In *Proc. IEEE International Conference on Communications (ICC)*, pp. 1-5, Jun. 2009. (Cited on page 38.)
- [94] J.K. Choi and S.J. Yoo. Sensing parameter optimization using a new detection probability in cognitive radio networks. In *Proc. IEEE International Conference on Computing, Networking and Communications (ICNC)*, pp. 386-391, Jan. 2012. (Cited on page 38.)
- [95] W.Y. Lee and I. Akyildiz. Optimal spectrum sensing framework for cognitive radio networks. *IEEE Transactions Wireless Communications*, vol. 7, no. 10, pp. 3845-3857, Oct. 2008. (Cited on page 39.)
- [96] X. Zhou, Y.G. Li, Y.H. Woon and A.C.K. Soong. Detection timing and channel selection for periodic spectrum sensing in cognitive radio. In *Proc. IEEE Global Communications Conference (GlobeCom)*, pp. 1-5, Dec. 2008. (Cited on pages 39 and 40.)
- [97] Y. Pei, A.T. Hoang and Y.C. Liang. Sensing-throughput tradeoff in cognitive radio networks: How frequently should spectrum sensing be carried out? In *Proc. IEEE International Symposium on Personal Indoor and Mobile Radio Communications (PIMRC)*, pp. 1-5, Sept. 2007. (Cited on pages 39 and 40.)
- [98] X. Liu, B. Krishnamachari and H. Liu. Channel selection in multi-channel opportunistic spectrum access networks with perfect sensing. In *Proc. IEEE International Symposium on New Frontiers in Dynamic Spectrum Access Networks (DySPAN)*, pp. 1-8 Apr. 2010. (Cited on pages 39 and 40.)
- [99] A. Papoulis and S.U. Pillai. Probability, random variables and stochastic processes. 4th Edition, Mc Graw-Hill, 2002. (Cited on pages 39 and 65.)
- [100] L. Tang, Y. Chen, E.L. Hines and M.S. Alouini. Effect of primary user traffic on sensing-throughput tradeoff for cognitive radios. *IEEE Transactions on Wireless Communications*, vol. 10, no. 4, pp. 1063-1068, Apr. 2011. (Cited on page 40.)

- [101] H. Kim and K.G. Shin. Efficient discovery of spectrum opportunities with MAC-layer sensing in cognitive radio networks. *IEEE Transactions on Mobile Computing*, vol. 7, no. 5, pp. 533-545, May 2008. (Cited on page 40.)
- [102] A. Ghasemi and E.S. Sousa. Optimization of spectrum sensing for opportunistic spectrum access in cognitive radio networks. In *Proc. IEEE Consumer Communications and Networking Conference (CCNC)*, pp. 1022-1026, Jan. 2007. (Cited on page 40.)
- [103] Q. Zhao and B. Krishnamachari. Structure and optimality of myopic sensing for opportunistic spectrum access. In *Proc. IEEE International Conference on Communications (ICC)*, pp. 6476-6481, Jun. 2007. (Cited on page 41.)
- [104] S. Ahmad, M. Liu, T. Javidi, Q. Zhao and B. Krishnamachari. Optimality of myopic sensing in multichannel opportunistic access. *IEEE Transactions on Information Theory*, vol. 55, no. 9, pp. 4040-4050, Sept. 2009. (Cited on page 42.)
- [105] Y. Chen, Q. Zhao and A. Swami. Joint design and separation principle for opportunistic spectrum access. In *Proc. IEEE Asilomar Conference on Signals, Systems and Computers (ACSSC)*, pp. 696-700, Oct. 2006. (Cited on page 42.)
- [106] Q. Zhao, L. Tong, A. Swami and Y. Chen. Decentralized cognitive MAC for opportunistic spectrum access in ad hoc networks: A POMDP framework. *IEEE Journal on Selected Areas in Communications*, vol 25, no. 3, pp. 589-600, Apr. 2007. (Cited on page 42.)
- [107] Y. Chen, Q. Zhao and A. Swami. Joint design and separation principle for opportunistic spectrum access in the presence of sensing errors. *IEEE Transactions on Information Theory*, vol. 54, no. 5, pp. 2053-2071, May 2008. (Cited on page 42.)
- [108] Z. Quan, S. Cui, A.H. Sayed and H.V. Poor. Optimal multiband joint detection for spectrum sensing in cognitive radio networks. *IEEE Transactions Signal Processing*, vol. 57, no. 3, pp. 1128-1140, Mar. 2009. (Cited on page 42.)
- [109] C. Cormio and K.R. Chowdhury. A survey on MAC protocols for cognitive radio networks. *Ad Hoc Networks*, vol. 7, pp. 1315-1329, Sept. 2009. (Cited on page 43.)

- [110] X. Li, M. Petrova and P. Mähönen. FCSS: CSMA/CA based fast cooperative spectrum sensing over multiband cognitive networks. In *Proc. IEEE International Symposium on Personal Indoor and Mobile Radio Communications (PIMRC)*, pp. 1-5, Sept. 2012. (Cited on page 43.)
- [111] S.M. Mishra and A. Sahai. How much white space is there? *Elect. Eng. and Comput. Sci. Dept., Univ. California, Berkeley. Tech. Rep. No. UCB/EECS-2009-3*, Jan. 2009. (Cited on page 45.)
- [112] ECC Report 159: Technical and operational requirements for the possible operation of cognitive radio systems in the white spaces of the frequency band 470-790 MHz, Jan. 2011. <http://www.ero.dk>. (Cited on pages 45, 47, 48, and 49.)
- [113] Ofcom. Digital dividend: geolocation for cognitive access. A discussion on using geolocation to enable license-exempt access to the interleaved spectrum. Nov. 2009, <http://stakeholders.ofcom.org.uk/binaries/consultations/cogaccess/summary/cogaccess.pdf> (Cited on pages 45 and 46.)
- [114] In the matter of unlicensed operation in the TV broadcast bands: Third memorandum opinion and order, Federal Communications Commission, FCC 12-36A1, Aug. 2012, http://hraunfoss.fcc.gov/edocs/_public/attachmatch/FCC-12-36-A1.pdf. (Cited on pages 45, 47, and 78.)
- [115] Radio spectrum policy group report on cognitive technologies, RSPG10-306. Feb. 2010. (Cited on page 45.)
- [116] W. Webb. White space databases: A guidance note for regulators and others. Jan. 2012, <http://www.weightless.org>. (Cited on pages 45, 49, and 50.)
- [117] Ofcom. Implementing geolocation. Nov. 2010, <http://stakeholders.ofcom.org.uk/binaries/consultations/geolocation/summary/geolocation.pdf>. (Cited on page 47.)
- [118] U. Reimers, DVB-the family of international standards for digital video broadcasting, Springer, 2nd edition, 2005. (Cited on pages 47 and 70.)

- [119] ECC Report 186: Technical and operational requirements for the operation of white space devices under geo-location approach. Jan. 2013, <http://www.ero.dk>. (Cited on pages 48 and 49.)
- [120] L. Shi, K.W. Sung and J. Zander. On the permissible transmit power for secondary user in TV white spaces. In *Proc. IEEE International Conference Cognitive Radio Oriented Wireless Networks and Communications (CrownCom)*, pp. 13-17, Jun. 2012. (Cited on page 48.)
- [121] R. Jäntti, J. Kerttula, K. Koufos, and K. Ruttik. Aggregate interference with FCC and ECC white space usage rules: Case study in Finland. In *Proc. IEEE International Symposium on New Frontiers in Dynamic Spectrum Access Networks (DySPAN)*, pp. 599-602, May 2011. (Cited on pages 49, 51, 73, and 81.)
- [122] L. Shi, K.W. Sung and J. Zander. Controlling aggregate interference under adjacent channel interference constraint in TV white space. In *Proc. IEEE International Conference Cognitive Radio Oriented Wireless Networks and Communications (CrownCom)*, pp. 1-6, Jun. 2012. (Cited on page 49.)
- [123] J. Kerttula, K. Ruttik and R. Jäntti. Dimensioning of secondary cellular system in TVWS. In *Proc. IEEE International Conference Cognitive Radio Oriented Wireless Networks and Communications (CrownCom)*, pp. 1-5, Jun. 2012. (Cited on page 49.)
- [124] J. Kerttula and R. Jäntti. DVB-T receiver performance measurements under secondary system interference. In *Proc. International Conference on Advances in Cognitive Radio (COCORA)*, pp. 1-5, Apr. 2011. (Cited on page 50.)
- [125] K. Harisson and A. Sahai. Seeing the bigger picture: context-aware regulations. In *Proc. IEEE International Symposium on New Frontiers in Dynamic Spectrum Access Networks (DySPAN)*, pp. 1-12, Oct. 2012. (Cited on page 50.)
- [126] R. Murty, R. Chandra, T. Moscibroda and P. Bahl. SenseLess: A database-driven white spaces network. In *Proc. IEEE International Symposium on New Frontiers in Dynamic Spectrum Access Networks (DySPAN)*, pp. 10-21, May. 2011. (Cited on page 50.)
- [127] K. Harrison and A. Sahai. Potential collapse of whitespaces and the prospect for a universal power rule. In *Proc. IEEE Interna-*

- tional Symposium on New Frontiers in Dynamic Spectrum Access Networks (DySPAN)*, pp. 316-327, May 2011. (Cited on pages 51 and 81.)
- [128] E.S. Sousa. Interference modeling in a direct-sequence spread-spectrum packet radio network. *IEEE Transactions on Communications*, vol. 38, no. 9, pp. 1475-1482, Sept. 1990. (Cited on page 53.)
- [129] M. Shao and C. Nikias. Signal processing with fractional lower order moments: Stable processes and their applications. *Proceedings IEEE*, vol. 81, no. 7, pp. 986-1010, Jul. 1993. (Cited on page 53.)
- [130] P. Cardieri. Modeling interference in wireless ad hoc networks. *IEEE Communications Surveys and Tutorials*, vol. 12, no. 4, pp. 551-572, 2010. (Cited on page 53.)
- [131] N. Cressie. Statistics for spatial data. Revised edition, Wiley Series in Probability and Mathematical Statistics, 1993. (Cited on page 53.)
- [132] G. Andrews, R.K. Ganti, M. Haenggi, N. Jindal and S. Weber. A primer on spatial modeling and analysis in wireless networks. *IEEE Communications Magazine*, vol. 48, no. 11, pp. 156-163, Nov. 2010. (Cited on pages 53 and 59.)
- [133] M.Z. Win, P.C. Pinto and L.A. Shepp. A mathematical theory of network interference and its applications. *Proceedings IEEE*, vol. 97, no. 2, pp. 205-230, Feb. 2009. (Cited on pages 53, 57, 59, and 66.)
- [134] J. Zander, J. Kronander, A. Achtzehn, M. Nekovee, K.W. Sung and S.L. Kim. QUASAR scenarios for white space assessments and exploitation. In *Proc. International union of Radio Science (URSI EMC Europe*, Sept. 2010. (Cited on page 54.)
- [135] L.F. Fenton. The sum of lognormal probability distributions in scatter transmission systems. *IRE Transactions on Communications Systems*, vol. 8, pp. 57-67, 1960. (Cited on page 55.)
- [136] S. Schwartz and Y. Yeh. On the distribution function and moments of power sums with lognormal components. *Bell System Technical Journal*, vol. 61, pp. 1441-1462, 1982. (Cited on page 55.)
- [137] N.C. Beaulieu, A.A. Abu-Dayya and P.J. McLane. Estimating the distribution of a sum of independent lognormal random variables.

- IEEE Transactions on Communications*, vol. 43, no. 12, pp. 2869-2873, Dec. 1995. (Cited on page 55.)
- [138] A. Ghasemi and E. Sousa. Interference aggregation in spectrum-sensing cognitive wireless networks. *IEEE Journal on Selected topics in Signal Processing* vol. 2, no. 1, pp. 41-56, Feb. 2008. (Cited on pages 55, 58, and 66.)
- [139] J. Wu, N.B. Mehta and J. Zhang. A flexible log-normal sum approximation method. In *Proc. IEEE Global Communications Conference (GlobeCom)*, pp. 3413-3417, Nov. 2005. (Cited on page 55.)
- [140] P. Cardieri and T. Rappaport. Statistical analysis of co-channel interference in wireless communications systems. *Wireless Communications Mobile Computing*, vol. 1, no. 1, pp. 111-121, Jan. 2001. (Cited on pages 55 and 65.)
- [141] Y. Selen and J. Kronander. Optimizing power limits for white space devices under a probability constraint on aggregated interference. In *Proc. IEEE International Symposium on New Frontiers in Dynamic Spectrum Access Networks (DySPAN)*, Oct. 2012. (Cited on page 55.)
- [142] K. Ruttik. Secondary spectrum usage in TV white space. Doctoral dissertation, Aalto university, Dec. 2011. (Cited on pages 55, 56, and 58.)
- [143] M. Vu, N. Devroye, and V. Tarokh. On the primary exclusive regions in cognitive networks. *IEEE Transactions on Wireless Communications*, vol. 8, no. 7, pp. 3380-3385, Jul. 2009. (Cited on pages 56 and 69.)
- [144] K. Woyach, P. Grover and A. Sahai. Near vs far field: Interference aggregation in TV whitespaces. Extended Edition. In *Proc. IEEE Global Communications Conference (GlobeCom)*, pp. 1-5, Dec. 2011. (Cited on pages 56 and 58.)
- [145] K. Ruttik, K. Koufos and R. Jäntti. Computation of aggregate interference from multiple secondary transmitters. *IEEE Communications letters*, vol 15, no. 4, pp. 437-439, Apr. 2011. (Cited on page 56.)
- [146] M. Aljuaid and H. Yanikomeroglu. Identifying boundaries of dominant regions dictating spectrum sharing opportunities for large sec-

- ondary networks. In *Proc. IEEE International Symposium on Personal Indoor and Mobile Radio Communications (PIMRC)*, pp. 1-5, Sept. 2010. (Cited on page 56.)
- [147] S. Shankar, and C. Cordeiro. Analysis of aggregated interference at DTV receivers in TV band. In *Proc. IEEE International Conference Cognitive Radio Oriented Wireless Networks and Communications (CrownCom)*, pp. 1-6, May 2008. (Cited on pages 57 and 69.)
- [148] J. Kingman. *Poisson Processes*. Oxford University Press, 1993. (Cited on page 57.)
- [149] L. Vijayandran, P. Dharmawansa, T. Ekman and C. Tellambura. Analysis of aggregate interference and primary system performance in finite area cognitive radio networks. *IEEE Transactions on Communications*, vol. 60, no. 7, pp. 1811-1822, Jul. 2012. (Cited on page 57.)
- [150] R. Dahama, K.W. Sowerby and G.B. Rowe. Outage probability estimation for licensed systems in the presence of cognitive radio interference. In *Proc. IEEE Vehicular Technology Conference (VTC)*, pp. 1-5, Apr. 2009. (Cited on page 58.)
- [151] Y. Wen, S. Loyka and A. Yongacoglu. Asymptotic analysis of interference in cognitive radio networks. *IEEE Journal on Selected Areas in Communications*, vol. 30, no. 10, pp. 2040-2052, Nov. 2012. (Cited on page 58.)
- [152] M. Aljuaid and H. Yanikomeroglu. Investigating the Gaussian convergence of the distribution of the aggregate interference power in large wireless networks. *IEEE Transactions on Vehicular Technology*, vol. 59, no. 9, pp. 4418-4424, Nov. 2010. (Cited on page 58.)
- [153] A. Busson, G. Chelius and J.M. Gorce. Interference modeling in CSMA multi-hop wireless networks. Technical Report, INRIA, Feb. 2009. (Cited on pages 58 and 59.)
- [154] S. Kusaladharma and C. Tellambura. On approximating the cognitive radio aggregate interference. *IEEE Wireless communications letters*, vol. 2, no. 1, pp. 58-61, Feb. 2013. (Cited on page 58.)
- [155] X. Hong, C.X. Wang and J. Thompson. Interference modeling of cognitive radio networks. In *Proc. IEEE Vehicular Technology Conference (VTC)*, pp. 1851-1855, May 2008. (Cited on page 58.)

- [156] S. Kusaladharma and C. Tellambura. Aggregate interference analysis for underlay cognitive radio networks. *IEEE Wireless communications letters*, vol. 1, no. 6, pp. 641-644, Dec. 2012. (Cited on page 58.)
- [157] A. Rabbachin, T.Q. Quek, H. Shin, and M.Z. Win. Cognitive network interference. *IEEE Journal on Selected Areas in Communications*, vol. 29, no. 2, pp. 480-493, Feb. 2011. (Cited on page 58.)
- [158] D. Stoyan, W. Kendall and J. Mecke. Stochastic geometry and its applications. 2nd Edition, John Wiley and Sons, 1996. (Cited on pages 58, 59, and 60.)
- [159] S. Srinivasa and M. Haenggi. Modeling interference in finite uniformly random networks. In *Proc. International Workshop on Information Theory for Sensor Networks (WITS 2007)*, Jun. 2007. (Cited on page 58.)
- [160] M. Haenggi and R. K. Ganti. Interference in large wireless networks. *Foundations and Trends in Networking*, vol. 3, no. 2, pp. 127-248, 2009. (Cited on page 59.)
- [161] A. Hasan and J.G. Andrews. The guard zone in wireless ad hoc networks. *IEEE Transactions on Wireless Communications*, vol. 6, no. 3, pp. 897-906, Mar. 2007. (Cited on page 59.)
- [162] M. Haenggi. Mean interference in hard-core wireless networks. *IEEE Communications letters*, vol. 15, no. 8, pp. 792-794, Aug. 2011. (Cited on page 59.)
- [163] P. Hall. Introduction to the theory of coverage processes (Wiley Series in Probability and Statistics). Oct. 1998. (Cited on page 59.)
- [164] Z. Chen *et al.* Aggregate interference modeling in cognitive radio networks with power and contention control. *IEEE Transaction on Communications*, vol. 60, no. 2, pp. 456-468, Feb. 2012. (Cited on page 60.)
- [165] B. Cho, K. Koufos and R. Jäntti. Interference control in cognitive wireless networks by tuning the carrier sensing threshold. *IEEE International Conference Cognitive Radio Oriented Wireless Networks and Communications (CrownCom)*, pp. 1-6, Jul. 2013. (Cited on page 60.)

- [166] G.A. Hufford, A.G. Longley, and W.A. Kissick. A guide to the use of the irregular terrain model in the area prediction mode. Technical Report 82-100, NTIA, 1982. (Cited on page 61.)
- [167] V. Graziano. Propagation correlations at 900 MHz. *IEEE Transactions Vehicular Technology*, vol. 27, pp. 182-189, Nov. 1999. (Cited on pages 64 and 65.)
- [168] T.B. Sorensen. Slow fading cross-correlation against azimuth separation of base stations. *IEE Electronic letters*, vol. 35, no. 2, Jan. 1999. (Cited on pages 64 and 65.)
- [169] S.S. Szyszkowicz and H. Yanikomeroglu. Limit theorem on the sum of identically distributed equally and positively correlated joint lognormals. *IEEE Transactions on Communications*, vol. 57, no. 12, Dec. 2009. (Cited on page 64.)
- [170] A.A. Abu-Dayya and N.C. Beaulieu. Outage probabilities in the presence of correlated lognormal interferers. *IEEE Transactions on Vehicular Technology*, vol. 43, no. 1, pp. 164-173, Feb. 1994. (Cited on page 65.)
- [171] S.S. Szyszkowicz and H. Yanikomeroglu. Analysis of interference from large clusters as modeled by the sum of many correlated lognormals. In *Proc. IEEE Wireless Communications and Networking Conference (WCNC)*, pp. 741-745, Apr. 2008. (Cited on page 66.)
- [172] F. Bock and B. Ebstein. Assignment of transmitter powers by linear programming. *IEEE Transactions on Electromagnetic Compatibility*, vol. 6, pp. 36-44, Jul. 1964. (Cited on page 69.)
- [173] M. Chiang, P. Hande, T. Lan and C.W. Tan. Power control in wireless cellular networks. Foundations and trends in networking, NOW Publishers, 2008. (Cited on page 69.)
- [174] K. Ruttik, K. Koufos and R. Jäntti. Modeling of the secondary system's generated interference and studying of its impact on the secondary system design. *Journal Radio Engineering*, vol. 19, no. 4, pp. 488-493, Dec. 2010. (Cited on pages 70 and 81.)
- [175] D. Li and J. Gross. Distributed TV spectrum allocation for cognitive cellular network under game theoretical framework. In *Proc. IEEE International Symposium on New Frontiers in Dynamic Spectrum Access Networks (DySPAN)*, Oct. 2012. (Cited on page 74.)

- [176] L. Musavian and S. Aissa. Capacity and power allocation for spectrum-sharing communications in fading channels. *IEEE Transactions on Wireless Communications*, vol. 8, no. 1, pp. 148-156, Jan. 2009. (Cited on page 75.)
- [177] X Kang, R. Zhang, Y.C. Liang and H.K. Garg. Optimal power allocation strategies for fading cognitive radio channels with primary user outage constraint. *IEEE Journal on Selected Areas in Communications*, vol 29, no. 2, pp. 374-383, Feb. 2011. (Cited on page 75.)
- [178] P. Wang, M. Zhao, L. Xiao, S. Zhou and J. Wang. Power allocation in OFDM-based cognitive radio systems. In *Proc. IEEE Global Communications Conference (GlobeCom)*, pp. 4061-4065, Nov. 2007. (Cited on pages 76 and 81.)
- [179] P. Wang, X. Zhong, L. Xiao, S. Zhou and J. Wang. A general power allocation algorithm for OFDM-based cognitive radio systems. In *Proc. IEEE International Conference on Communications (ICC)*, pp. 1-5, Jun. 2009. (Cited on page 76.)
- [180] E.D. Anese, S.J. Kim, G.B. Giannakis and S. Pupolin. Power allocation for cognitive radio networks under channel uncertainty. In *Proc. IEEE International Conference on Communications (ICC)*, pp. 1-6, Jun. 2011. (Cited on page 77.)
- [181] R. Horst and N. V. Thoai. DC programming: Overview. *Journal of Optimization Theory and Applications*, vol. 103, no. 1, pp. 1-43, Oct. 1999. (Cited on page 78.)
- [182] L. Zhang, Y. Xin, Y.C. Liang and H.V. Poor. Cognitive multiple access channels: Optimal power allocation for weighted sum rate maximization. *IEEE Transactions on Communications*, vol. 57, no. 9, pp. 2754-2762, Sept. 2009. (Cited on page 79.)
- [183] B. Maham, P. Popovski, X. Zhou and A. Hjørungnes. Cognitive multiple access network with outage margin in the primary system. *IEEE Transactions on Wireless Communications*, vol. 10, no. 10, pp. 3343-3353, Oct. 2011. (Cited on page 79.)
- [184] O. Biggelaar, J.M. Dricot, P.D. Doncker and F. Horlin. Power allocation in cognitive radio networks using distributed machine learning. In *Proc. IEEE International Symposium on Personal In-*

- door and Mobile Radio Communications (PIMRC)*, pp. 826-831, Sept. 2012. (Cited on page 79.)
- [185] L. Tang, H. Wang and Q. Chen. Power allocation with max-min fairness for cognitive radio networks. In *Proc. Global Mobile Congress (GMC)*, pp. 1-5, Oct. 2010. (Cited on page 79.)
- [186] C.G. Yang, J.D. Li and Z. Tian. Optimal power control for cognitive radio networks under coupled interference constraints: A cooperative game-theoretic perspective. *IEEE Transactions on Vehicular Technology*, vol. 59, no. 4, pp. 1696-1706, May 2010. (Cited on page 79.)
- [187] G. Kulkarni, S. Adlakha, and M. Srivastava. Subcarrier allocation and bit loading algorithms for OFDMA-based wireless networks. *IEEE Transactions on Mobile Computing*, vol. 4, no. 6, pp. 652-662, Dec. 2005. (Cited on page 80.)
- [188] W. Wang and X. Liu. List-coloring based channel allocation for open spectrum wireless networks. In *Proc. IEEE Vehicular Technology Conference (VTC)*, pp. 1-5, Sept. 2005. (Cited on page 80.)
- [189] A.T. Hoang and Y.C. Liang. Downlink channel assignment and power control for cognitive radio networks. *IEEE Transactions on Wireless Communications*, vol. 7, no. 8, pp. 3106-3117, Aug. 2008. (Cited on page 80.)
- [190] J. Zander and S.L. Kim. Radio resource management for wireless networks. Artech House, Inc. Norwood, MA, US, 2001. (Cited on page 80.)
- [191] F.F. Digham. Joint power and channel allocation in cognitive radios. In *Proc. IEEE Wireless Communications and Networking Conference (WCNC)*, pp. 1-5, Apr. 2008. (Cited on page 80.)
- [192] D. Xu, Z.Y. Feng, Y. Liu and P. Zhang. Outage probability minimizing joint channel and power allocation for cognitive radio networks. *Electronics Letters*, vol. 47, no. 25, pp. 1402-1404, Dec. 2011. (Cited on page 80.)
- [193] M. Shaat and F. Bader. Efficient resource allocation algorithm for uplink multicarrier-based cognitive radio networks with fairness consideration. *IET Communications*, vol. 5, no. 16, pp. 2328-2338, 2011. (Cited on pages 80 and 81.)

- [194] P. Setoodeh and S. Haykin. Robust transmit power control for cognitive radio. *Proceedings IEEE*, vol. 97, no. 5, pp. 939, May 2009. (Cited on page 81.)
- [195] T. Nadkar, V. Thumar, G.P. Tej, S.N. Merchant and U.B. Desai. Distributed power allocation for secondary users in a cognitive radio scenario. *IEEE Transactions on Wireless Communications*, vol. 11, no. 4, pp. 1576-1586, Apr. 2012. (Cited on page 81.)
- [196] X. Zhou, G.Y. Li, D. Li, D. Wang and A.C. Soong. Probabilistic resource allocation for opportunistic spectrum access. *IEEE Transactions on Wireless Communications*, vol. 9, no. 9, pp. 2870-2879, Sept. 2009. (Cited on page 81.)
- [197] T. Dudda and T. Irnich. Capacity of cellular networks deployed in TV white space. In *Proc. IEEE International Symposium on New Frontiers in Dynamic Spectrum Access Networks (DySPAN)*, pp. 254-265, Oct. 2012. (Cited on page 82.)
- [198] J. Zander and K.W. Sung. Opportunistic secondary spectrum access: Opportunities and limitations. *Radio Science Bulletin*, no. 340, pp. 29-33, Mar. 2012. (Cited on page 84.)



ISBN 978-952-60-5454-4
ISBN 978-952-60-5455-1 (pdf)
ISSN-L 1799-4934
ISSN 1799-4934
ISSN 1799-4942 (pdf)

Aalto University
School of Electrical Engineering
Department of Communications and Networking
www.aalto.fi

**BUSINESS +
ECONOMY**

**ART +
DESIGN +
ARCHITECTURE**

**SCIENCE +
TECHNOLOGY**

CROSSOVER

**DOCTORAL
DISSERTATIONS**